Micro and Nanoscale Imaging of Leaf Surfaces

Shaun Carl Walker, BSc (Hons) MSc

A thesis submitted to the University of Nottingham for the Degree of Doctor of Philosophy

February 2017

Contents

Abstract

The plant cuticle is located on most surfaces of the plant from seeds to leaves from stem to petal, this is to allow a direct interface between the plant and its environment. These cuticles act as a barrier to prevent waters loss from the plant to the environment and penetration of compounds through the cuticle, like agrochemicals and formulations. The leaf cuticle provides an ideal surface to try to penetrate agrochemicals through. The leaf surface has a larger surface area then most surfaces of the plant allowing ease of application of formulation via spraying. This makes the study of the leaf and its cuticle important, with the interaction of the formulation and the cuticle an area of interest.

The main purpose of this thesis is to investigate the applications of a relatively new imaging technique called scanning ion conductance microscopy (SICM). This new technique is utilised to image live cells with the intention to characterise the living processors on the surface. SICM has not been used to image leaf surface before, but its non-contact nature and large z axis range makes it ideal for surface analysis. The first part of this thesis is to describe the comparison of SICM with other conventional techniques used to image leaf surfaces. For example, atomic force microscopy (AFM) and scanning electron microscopy (SEM) and asses the strengths and weaknesses of the technique for leaf imaging. This was achieved by imaging various leaf surfaces and surface features like epicuticular wax (EW) crystals and stomata. Also the possible research routes for the SICM were identified and experiments conducted to ascertain the abilities to perform them. This resulted in wetting being imaged and imaging the drying of a formulation.

The other purpose of this thesis is to investigate the possibility of live leaf imaging and characterisation, and the implications of adjuvants on live leaves. This was achieved by thermal characterisation of different leaf surfaces in two states, them being live and intact (but dried). This allowed the understanding of the impact water has on the cuticle and the importance of studying live leaves. This shows that water has a plasticizing effect on the cuticle waxes, and also effects the structure of the cuticle.

AFM with scanning thermal microscope (SThM) with local thermal analysis (LTA) were also utilised to investigate the impact of two adjuvants on the surface of live leaf cuticle. These were Brij 98 and Tris (2-ethylhexyl) phosphate (TEHP), Brij 98 in a non-ionic ethoxylated surfactant, while TEHP is a phosphoric acid ester known for its properties has a plasticizer. Both AFM and LTA showed that both resulted in the plasticizing of the cuticle with the area affected showing depression in melting transition compared with that of the native leaf surface. The thesis also shows that it is possible to characterise the impact of adjuvants on live leaf cuticles.

This thesis has shown the importance of new techniques being used to image and characterise the leaf surface, showing that image wetting as a possible research route for SICM. The new techniques have resulted in new experiments being performed that provide insight into the interactions of the cuticle with formulations and components of formulations. Also the importance of water in understanding the structure of the cuticle

Abbreviations

AFM - Atomic Force Microscopy

CM - Cuticular Membrane

CL – Cuticularized Layer

CM-AFM - Contact Mode Atomic Force Microscopy

CSEM - Conventional Scanning Electron Microscopy

DSC – Differential Scanning Calorimetry

ESEM - Environmental Scanning Electron Microscopy

EW - Epicuticular Wax

IW – Intracuticular Wax

LTA - Local Thermal Analysis

PBS – Phosphate Buffer Solution

PEG – Poly ethylene Glycol

PP – Poly Propylene

SEM - Scanning Electron Microscopy

SICM - Scanning Ion Conductance Microscopy

SPM - Scanning Probe Microscope

SThM - Scanning Thermal Microscopy

TEHP - Tris (2-ethylhexyl) phosphate

Tm – Melting Transition Temperature

TM-AFM - Tapping Mode Atomic Force Microscopy

VP-SEM - Variable Pressure Scanning Electron Microscopy

List of Figures

List of Tables

Chapter 1

Introduction

1.1 General Introduction

The development of new herbicide and pesticide compounds is expensive and challenging. This is partly because of government legislation and processes for approving new chemicals which are often time consuming (Green and Beestman, 2007). For this reason, companies are actively researching the development of improved formulations to increase efficacy of existing approved herbicides and pesticides. This approach has been successful, with improvements for existing active compounds by improving formulations to increase uptake activity efficacy and other factors while reducing the overall active concentration needed (Pimentel, 1995, Wang and Liu, 2007, Nair et al., 2010, Tsuji, 2001). Such a strategy based in improvement in formulation performance is hence an effective way of improving the applicability and commercial life of agrochemical actives.

Glyphosate is an ideal example of an active being formulated to improve efficacy. Glyphosate is a broad spectrum herbicide that is one of the largest selling agrochemical product on the market (Woodburn, 2000). A common adjuvant added to a formulation is a surfactant. A group of surfactants called polyoxyethylene chain surfactants of varying lengths, have been shown to improve the activity of glyphosate, both the salt and acid form (Baylis, 2000), . Since glyphosate was developed in 1970s a number of patents for diffing formulations have been submitted (Voegler and Euler, 2004, Li et al., 2013, Baylis, 2000).

The relative lack of new actives and a need for improved performance is not the only reason for developing novel formulations, there is also a need to increase safety, for example, preventing leaf target absorption from leeching to the environment (Doublet et al., 2009). This requires an understanding of the interactions of formulations with foliate surfaces, not just interactions of classical formulations but also new types such as those based on nanoparticles (Nair et al., 2010). It is estimated that when applying a pesticide formulation to

the leaf surface only less than 0.1% will reach the targeted site (Pimentel, 1995). To reduce the amount of fungicide or insecticide lost the efficacy of the overall formulation hence needs to be improved (Wang and Liu, 2007).

To improve formulations there needs to be an understanding of the processes and the interactions involved between the leaf surface and the formulation. The work of this thesis in part addresses this issue, as well as introducing a new tool to study foliar surfaces, the Scanning Ion Conductance Microscope (SICM).

1.2 Leaf surfaces structure and chemistry

1.2.1 The cuticularized and cutinized layers of the cuticle.

Plant leaves are specialized organs that are adapted in capturing light and carbon dioxide, which ensures the plants growth (Sinha, 1999). The leaves size, morphology, surface topology and other factors are different for different kingdoms of plants (McLellan, 2005), with water transport capacity and water availability during leaf expansion being linked to these factors (Zwieniecki et al., 2004, Sack and Holbrook, 2006).

The cuticle is crucial to leaf survival, by offering a protective barrier for the biosphere from the atmosphere. The cuticle is a multi-functional protective surface for the plant tissue, which aids in survival of different plants in different environments. The cuticle is located on the adaxial and abaxial surface of the leaf covering the stomata, free epidermal cell surfaces, sub stomatal and free intercellular spaces.

The majority of the leaf is covered with the cuticle, which is between 0.1 and 15 µm (Gouret et al., 1993) and is thickest above the anticlinal epidermal cell walls. The cuticle is made of two layers, and is generalised to include the EW (Holloway, 1993). These are split into two areas; these consist of the top layer, called the cuticularized layer (CL) (Jeffree, 1996), and the bottom layer, called the cutinized layer (Holloway, 1993) and, when generalised the EW (Koch and Ensikat, 2008). There exists different terminologies for both layers in literature; the cuticularized layer can also be called the cuticle proper or primary cuticle. The cutinized layer can also be called the cutinised layer or the secondary cuticle, as shown in figure 1.1.

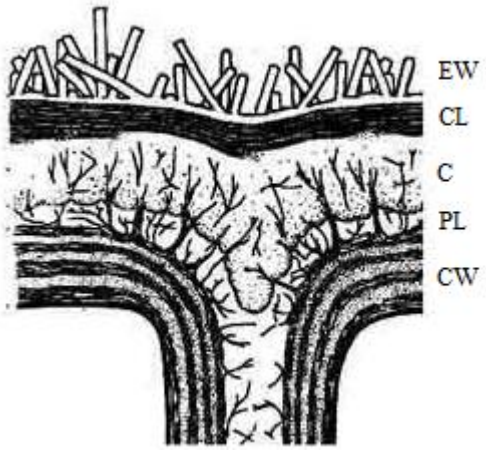

Figure 1.1 - A general schematic of the plant cuticle. EW - Epicuticular Wax, CL – Cuticularized layer, C – Cutinized layer with polysaccharide and pectin fibrillae, PL – Pectinaceous layer and CW Cell wall (Buchholz, 2006)

The two layers are composed of the polymer cutin and/or a cutan matrix with waxes inside the matrix. These waxes are termed intracuticular wax (IW) if in the cuticle and epicuticular wax (EW), if on the surface (Pollard et al., 2008, Kolattukudy, 1981). The waxes are mainly composed of long chain fatty acids and their derivatives, which are hydrophobic compounds. Also other compounds are present including triterpenoids and phenylpropanoids (Jetter et al., 2006, Nawrath, 2006).The cuticle is connected to the epidermis cell wall by a projection of branched polysaccharides and pectin, call the fibrillae, which anchor the cuticle to the cell wall (Jeffree, 2006). Cutin and cutan both provide a protective physical barrier against microbes and water loss, cutan also increases the hydrophobic nature of the cuticle and is found in drought resistant plants (Boom et al., 2005, Deshmukh et al., 2005, Shechter et al., 2010).

Cutin is a polymer that is composed of hydroxyl fatty acid and epoxy fatty acid monomers, which can be grouped into two families, having a carbon chain-lengths of 16 and 18 (Holloway, 1993, Heredia, 2003), as shown in figure 1.2. Cutin is composed mainly of 10, 16 - 8, 16- and 9, 16-dihydroxyhexadecanoic acids (Deshmukh et al., 2005, Jeffree, 2006,

Shechter and Chefetz, 2008). This composition varies for different species of plant and also changes with the age of the leaf (Jeffree, 1996).

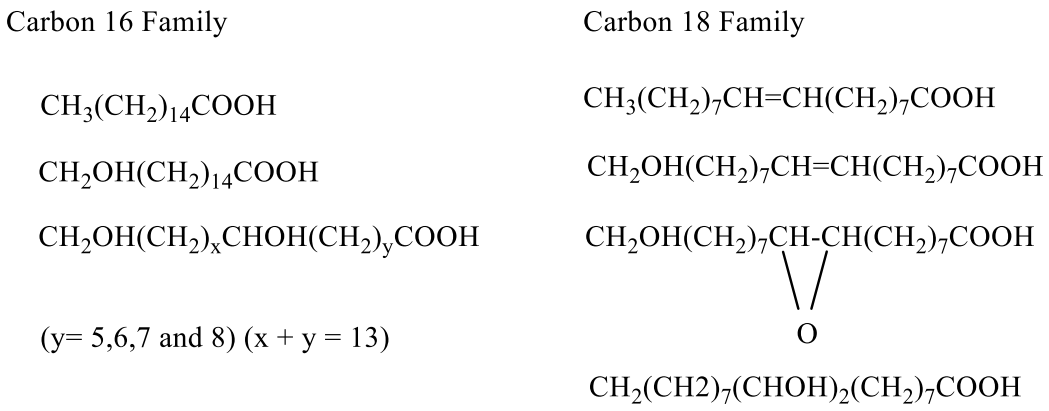

Figure 1.2 - The two groups of the cutin monomers

Cutan chemical composition and structure has recently been revealed, though the structure of the polymer is not fully understood. The polymer is crossed linked, constructed from aromatic compounds linked by ester groups, reacted from carboxylic and hydroxyl functional groups (McKinney et al., 1996). The monomers are shown in figure 1.3.

The IW that fills the spaces between the polymer backbone also have structure, consisting of amorphous and crystalline areas. The crystalline areas are made of alkane crystals and have an orthorhombic crystal structure (Perkins et al., 2005a, Merk et al., 1998).

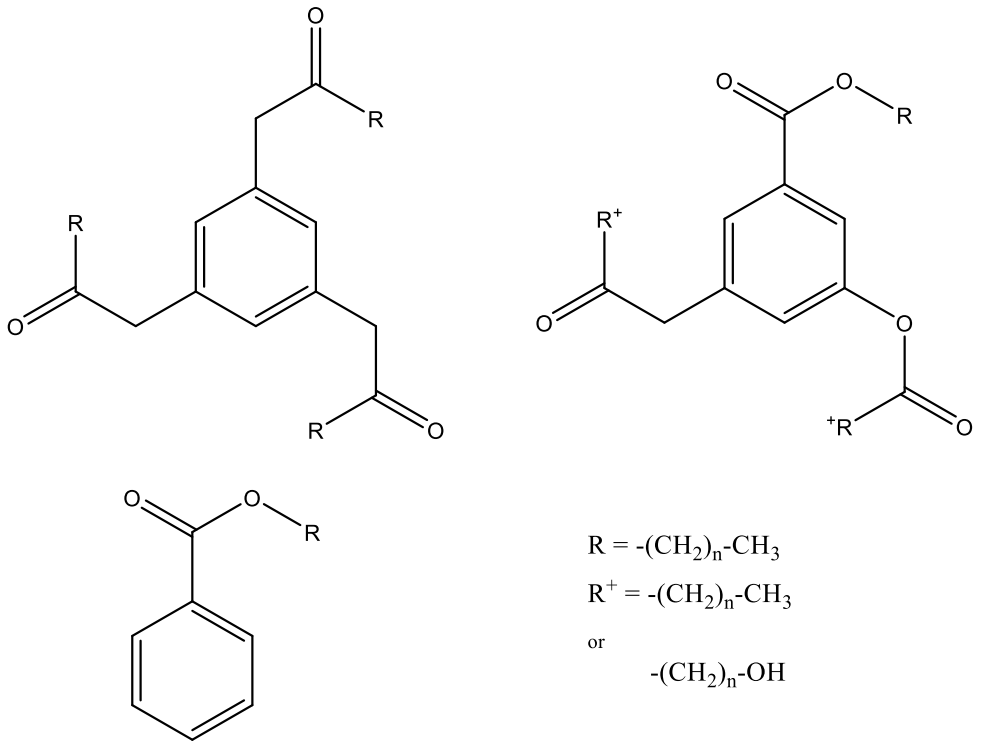

Figure 1.3 - The proposed monomers that make the cutan polymer

1.2.2 The epicuticular wax.

EW is defined by the position on the top leaf surface (Jeffree, 2006). The EW is located above the cuticle and changes according to the chemical content and species of the plant. EWs have been isolated and their properties, structure and chemistries been studied (Jeffree, 2006, Koch et al., 2008, Barthlott et al., 1998, Koch and Barthlott, 2009). EW structures are categorised in six main groups (Jeffree, 2006). The most common wax morphologies are thin films and three dimensional structures, these include massive crusts, filaments, rods, tubules, plates and platelets. These wax structures range from 0.2 to 100 µm in size (Koch and Ensikat, 2008) each with certain properties associated with the chemistry

and structures. For example, the EW of the lotus leaf can cause the leaf to be super hydrophobic and have self-cleaning properties (Koch et al., 2008).

Differences between the EW and IW have been shown to be chemical as well. Studies on *Prunus laurocerasus* (English Laurel) showed the IW to have concentrations of triterpenoid acids, while the EW did not (Jetter et al., 2000), while the EW was composed of aliphatic compounds. Another, more in depth, study on *Rosa canina* (Dog Rose) showed the difference between more compounds of the IW and EW (Buschhaus et al., 2007). Again the presence of triterpenoids to be higher in the IW than the EW. Alkanes were present in larger quantities in the EW than the IW. The study also showed secondary alcohols were present in the EW while absent from the IW and alkyl esters were present in higher quantities in the EW.

The species of plant has an impact on the differences observed for overall weights of EW and IW combined, with these also showing different percentages of total wax weight within the species (Buschhaus and Jetter, 2011). From IW this ranges from 1 – 30 μg cm^{-2}(10 – 80 % of total wax) in some leaf surfaces and, by association, to EW 5 – 30 μg cm^{-2} (20 – 90 % of total wax) in others (Buschhaus and Jetter, 2011). This is shown in the literature with *Pisum sativum* (Pea) to have an IW to EW ratio of 1:9 and *Ligustrum vulgare* (Privet) to have a ratio of 4:1 (Gniwotta et al., 2005).

EW structures have been associated with certain chemicals, and groups of chemicals. For example the platelet structures of *Pisum sativum* are made from hexacosanol (Macey and Barber, 1970), while other platelet structures are made with hentriacontan-16-one (Rhee et al., 1998). The structures are not only limited to aliphatic compounds but also aromatic compounds, for example the feature threads are built from β-amryrin (Markstadter et al., 2000) and β-amryrin acetate (Manheim and Mulroy, 1978), with chemical structures shown

in figure 1.4. The characterization of both IW and EW is important to gain understanding of the properties of the two regions of the cuticle. The EW being the region where majority of the contact from the environment, from interaction with water, insect or agrochemicals. Allowing for certain properties, hydrophobicity and anti-fungal properties to be described. While the IW is the significant barrier to movement of chemicals, both into the leaf and towards the environment.

Hexacosanol $CH_3(CH_2)_{24}CH_2OH$

Hentriacontan-16-one $CH_3(CH_2)_{14}C(=O)(CH2)_{14}CH_3$

Beta-amyrin

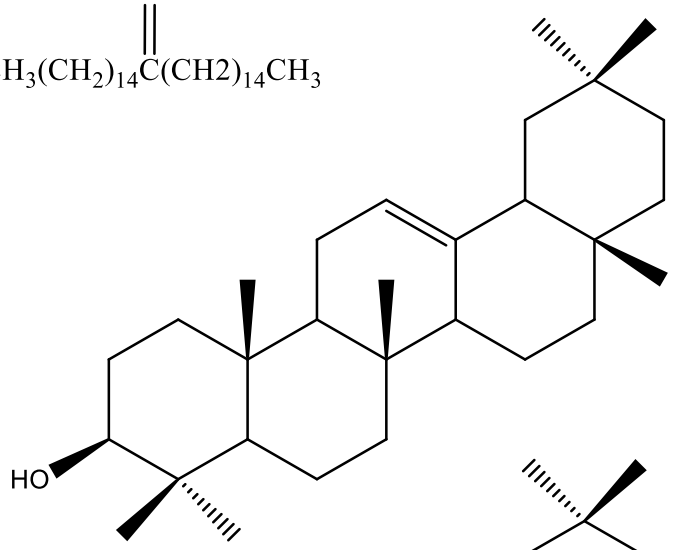

Beta-amyrin acetate

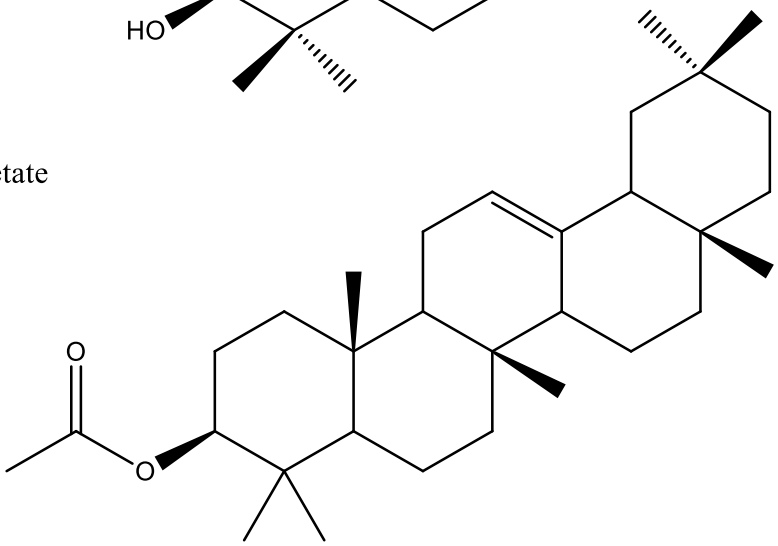

Figure 1.4 – Significant compounds, which have been identified to self-assembly to form EW crystals and morphology. Constructing important structure like platelets and tubules giving leaf surfaces certain properties.

1.3 Leaf surface properties

1.3.1 Barrier properties

The cuticle is used to aid in the survival of the leaf and the plant via its surface properties. One of the main roles of the cuticle is the regulation and prevention of water loss from the leaf surface (Riederer and Schreiber, 2001). Another is that it acts as a protective barrier for the leaf and plant. A list of protective properties of the cuticle are shown in Table 1.1.

Table 1.1.1 - List of the protective properties of the cuticle (Riederer and Schreiber, 2001)

Protecting function	**Cuticle process**
Water loss	Prevents transpiration by trapping the water inside the leaf.
Infection	Acts as a mechanical barrier that prevents fungal hyphae and insect mouthpart penetration
Leaching	Prevents water retention on the epidermal cells, that would remove substances from leaf
Foliar penetration	Prevents pollutants and adjuvants from entering the leaf

Some of the cuticle properties come from the EW and some from the other cuticle layers including the CL and cutinised layer with properties resulting from the structure and the chemistry of these surfaces (Bargel et al., 2006). For the EW there are many properties that arise from the combination of these factors including self-cleaning (Marmur, 2004), water adhesion (Feng et al., 2008) and others (Koch et al., 2008), as shown in figure 1.5.

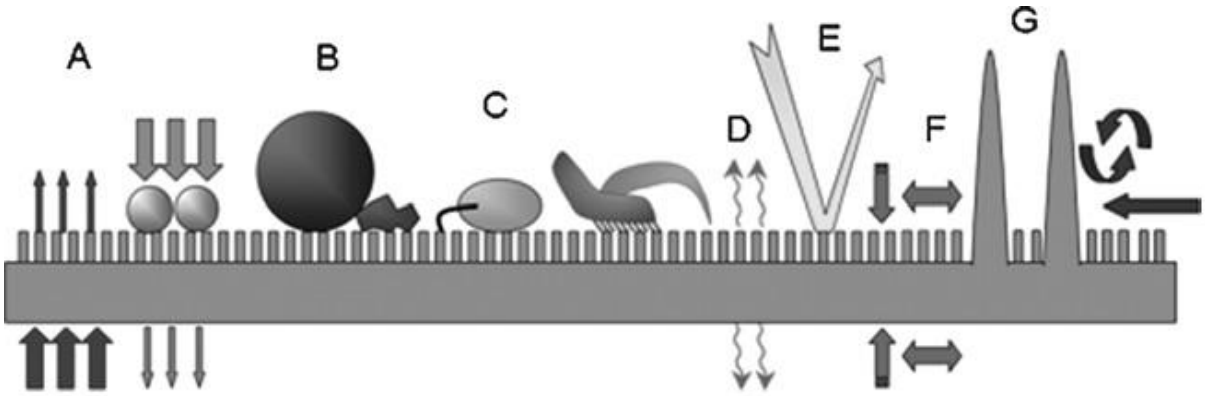

Figure 1.5 - Diagram of properties related to the surface of the hydrophobic cuticle. A) Transport barrier; B) Wetting; C) self-cleaning; D) signalling; E) UV protection; F) resistance to mechanical stress and G) temperature control. (Koch et al., 2008)

Most studies of leaf surface properties to date have been on wetting including on lotus self-cleaning (Marmur, 2004), salvinia (Barthlott et al., 2010) and petal effect (Feng et al., 2008). The salvinia effect is when a complex surface can hold an air film underwater, this is to provide insulation and gases for respiration. The petal effect is when a surface possesses super hydrophobic and high adhesive properties, for droplets to maintain a static spherical shape on the leaf (Feng et al., 2008).

The ability to resist wetting is the first barrier for agrochemical foliar penetration. If a formulation droplet cannot be retained or fully wet a surface then the efficacy of the formulation is reduced (Holloway, 1969). To aid in wetting the droplet surface tension needs to be reduced, this can be done by the use of surfactants and wetting agents.

The regions of amorphous and crystalline wax materials in the plant has an effect on the uptake pathway of actives. An x-ray diffraction study has shown that the lower the crystalline content of the extracted waxes the faster the uptake of an active (Schreiber and Riederer, 1996). This implies that faster transport is occurring in via the disordered amorphous regions of the wax. This is because a chemically moving through the cuticle cannot move through the crystalline structures, and so would move within the amorphous regions.

1.3.2 Transportation of molecules through the cuticle

The cuticle is a wax structure that is proposed to have separate transportation paths for lipophilic non-electrolytes and hydrated ionic compounds. These are called the lipophilic pathway and the polar pathway (Buchholz, 2006, Eichert and Goldbach, 2008).

The lipophilic pathway is actively area of study with investigations into how actives of a formulation can penetrate and permeate the cuticle (Kirkwood, 1999, Wang and Liu, 2007). This is because early experiments and literature showed the lipophilic pathway was associated with the cutin and cuticle waxes, while the polar pathway mechanism remained unknown (Foy, 1964). Also the cuticle was assumed to be a homogenous membrane for a significant period of time up to the late 1990 to the early 2000 (Niederl et al., 1998, Schreiber, 2002).

The lipophilic pathway is an experimentally established model of permeability of the plant cuticle for lipophilic compounds (Schonherr and Riederer, 1989). Transport through the lipophilic pathway happens in three stages, (1) sorption into the cuticle, (2) diffusion and (3) desorption from the cuticle (Riederer, 1995). The uptake of compounds is a diffusion process,

with permeability being dependent on two factors. These are solubility, partition coefficient (P), and mobility, diffusion coefficient (K). For a homogeneous surface permeability, as the permeability coefficient, is proportional to the partition coefficient (K) and the diffusion coefficient and inversely proportional to surface thickness (λ). This is shown in the equation (1), partition coefficient, and (2) (Riederer, 1995, Schreiber and Riederer, 1996).

$$K = \frac{C_{lipid}}{C_{Water}} \quad (1)$$

$$P = \frac{D\,x\,K}{\lambda} \quad (2)$$

Due to the cuticle not being homogenous, permeability isn't inversely proportional to cuticle thickness; this is due to the crystal/amorphous composition of the cuticle. Any compound penetrating through the cuticle would have a pathway through the amorphous regions. Nevertheless, the equation is a useful gauge for understanding the permeability properties of the cuticle (Baur et al., 1996, Baur et al., 1999a).

Factors that affect the diffusion coefficient include the molecular weight of the lipophilic compound and the temperature. For example, the cuticle amorphous regions are areas of relatively high molecular motion (Schonherr and Riederer, 1989, Baur et al., 1997a). When the cuticle is subjected to increased temperatures, penetration of lipophilic compounds is increased (Buchholz and Schonherr, 2000). It has been shown that if the molecular weight of the lipophilic compounds is increased by a factor of 4 then the mobility of the molecule is decreased by a factor more than a 1000 (Baur et al., 1997a).

The polar pathway is the route by which charged and polar molecules cross the cuticle; this is achieved by using aqueous pores (Schreiber, 2005). This is thought to be the

case because charged and polar molecules have a shell of hydration around the molecule and are not soluble in the wax of the cuticle. As a result, compounds must diffuse by a different pathway to that of the lipophilic molecules (Schonherr, 2006). These aqueous pores have not been directly observed (Eichert and Goldbach, 2008) so the hypothesis relies on five indirect observations. These are that penetration of ions is independent of temperature, plasticizers and only weakly affected by wax (Schreiber, 2005). Also the effect of humidity and size selectivity on the rate of penetration, compared to the lipophilic pathway.

Studies using plasticizers such as tributyl phosphate and diethyl suberate did not show a significant increase in penetration rate of Ca^{2+} (Buchholz and Schonherr, 2000). Although a study with a different hydrophilic compound, a glyphosate anion, with diethyl suberate showed an increase in penetration by 35 % (Schonherr, 2002). Since the size of the Ca^{2+} ion is relatively smaller, compared to glyphosate, the ability to penetrate the cuticle would be easier for the Ca^{2+} than the glyphosate. This would result in the penetration of the Ca^{2+} being unaffected by the plasticizer.

Although the proposed aqueous pores have not been visually proven there are studies that show the movement of polar compounds through the cuticle. The area of polar penetration has been shown to be located near the anticlinal walls and on the cuticular ledges of the stomata guard cells (Eichert and Burkhardt, 2001). Also the aqueous pore size has a radius ranging from 0.3nm (Popp et al., 2005) to 2.4 nm (Eichert et al., 2008, Eichert and Goldbach, 2008) making them challenging to observe in practice.

The size of the pore is estimated using the size selectivity of the pore relating to the uptake of ^{15}N-labelled urea and ^{13}C-labelled sucrose across the cuticle, using the equation (3) (Eichert and Goldbach, 2008). Where r_p is the radius of the pore, r_n is the hydrodynamic radii of the nitrogen containing compound, r_c is the hydrodynamic radii of sucrose, D_c is the

diffusion coefficient of sucrose and D_n is the diffusion coefficient of the nitrogen containing compound. Parameter K is determined by observations of the correlations between cumulative urea and sucrose uptake across the cuticle (Eichert and Goldbach, 2008).

$$r_p = \frac{r_n - r_c \sqrt[4]{k\frac{D_c}{D_n}}}{1 - \sqrt[4]{k\frac{D_c}{D_n}}} \quad (3)$$

Water moving through the cuticle needs to be considered since it is one of the major transported molecules via cuticular transpiration (Schönherr, 1982). Water moves through the cuticle by both the lipophilic and the polar pathways (Kerstiens, 2006). Movement of water through the lipophilic pathway is still governed by the solubility and mobility within the amorphous regions (Buchholz, 2006). Evidence for the movement of water by the lipophilic pathway comes from studies that correlate water cuticle permeability with the permeability of a range of lipophilic compounds with a range of isolated cuticles (Niederl et al., 1998, Schreiber, 2002), as shown in figure 1.6. The graph correlates the permeability of ^{3}H water with that of ^{14}C benzoic acid, showing water move through the cuticle by the same pathway as the organic acid, that being the lipophilic pathway. The studies main assumption is that the cuticle is a homogenous membrane, which it is not, and there needs to be consideration of the polar pathway.

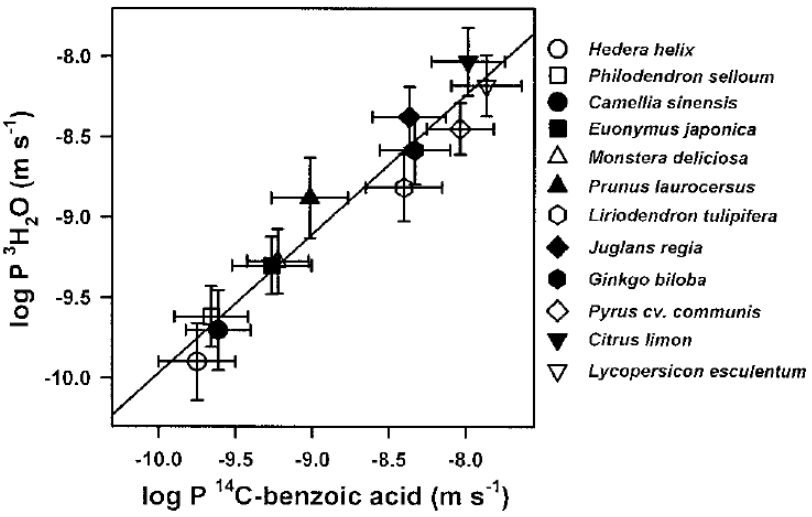

Figure 1.6 - Logarithmic plot showing the simultaneous penetration of $^{3}H_2O$ and ^{14}C Benzoic acid through a number of isolated cuticles. Error bars represent 95% confidence intervals (Niederl et al., 1998).

Movement of water through the aqueous pores restricted in the same way as the lipophilic pathway, in the sense of a solution-diffusion membrane, with water moving through the pore still governed by the solubility and mobility within the pores (Wijmans and Baker, 1995). A study that shows the importance of the polar pathway for cuticular transpiration, preventing movement of water by blocking the aqueous pores (Schreiber et al., 2006). This was achieved using NaCl and AgNO3 penetrating the cuticle from different sides of the cuticle, allowing the formation of AgCl precipitates within the aqueous pores. This precipitate blocked the pores and prevented the movement of water through the hydrophilic pathway, as shown in figure 1.7. Figure 1.7, shows the result of the precipitate within the aqueous pores, with the permeability of water being coming significantly lower by a factor of 2.8 before treatment.

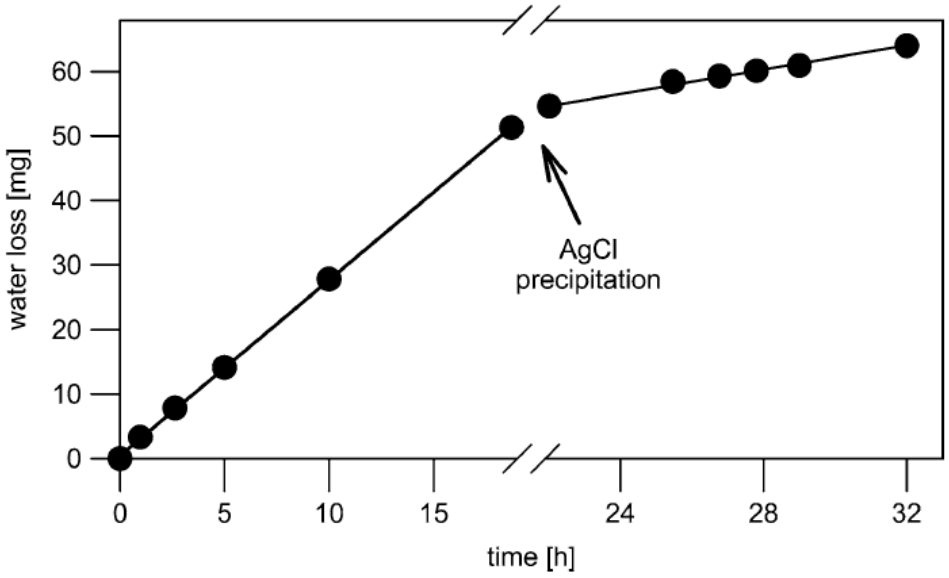

Figure 1.7 - Typical transpiration kinetic plot of isolated Populus canescens before and after AgCl precipitation (Schreiber et al., 2006).

The AgCl study also showed that two different isolated cuticles, that of *Hedera helix* and *Nerium olender*, didn't have statistically significant reductions in water permeability (Schreiber et al., 2006). These exceptions can be the result of no aqueous pores being present in the cuticles, suggesting many more cuticles might have no polar pathway. Though the pore size for *Hedera helix* is 0.3 nm (Popp et al., 2005) and could be considered that the pore size could restrict sufficient flow of Ag and Cl ions and prevent blocking.

1.3.2 How formulations aid uptake

The enhancing of the transportation of actives is a fundamental area in increasing the usefulness of actives. Though, there might never be a unifying mechanism/formulation approach due to different adjuvants, surfactants and agrochemicals having varying effects on different target species (Stock and Holloway, 1993).

The cuticular properties of permeability are a changing dynamic structure which is influenced by the environment, humidity and temperature, and by the addition of certain chemicals. To increase the transportation of compounds through the cuticle a common approach is to increase the solubility or mobility or both. There are an ever growing number of chemicals that can increase mobility (diffusion coefficient) in the plant cuticle. These can be grouped non-ionic surfactants and oils/solvents (Riederer and Friedmann, 2006a), with further chemical groups shown in table 1.2.

Table 1.2 General chemical group of non-ionic surfactants and oils (Hamilton, 1993, Castro et al., 2014).

Non-ionic surfactants	**Oils**
Alcohol Ethyoxylate	Triglyceride
Alkyl Phenol Ethoxylate	Fatty Acid Methyl Esters
Alkyl Polyglucoside	Naphthenic Oils
Alkyl Ethoxylate	Terpene Oils

Surfactants have been studied to a great extent and their use is now well defined in the agrochemical industry. For example, alkyl ethoxylate surfactants with a lower degree of ethoxylation have been shown to influence the penetration of lipophilic, while a higher degree of ethoxylation improves the penetration of hydrophilic compounds, across the lipophilic pathway (Riederer and Friedmann, 2006b). This is due to the high ethoxylated surfactants have humectant property allowing the active to remain liquid for longer,

suggesting an increase in water content of the leaf cuticle (Stevens and Bukovac, 1987, Gaskin and Holloway, 1992). Allowing more hydrophilic actives to penetrate the cuticle, while low ethoxylated surfactants wouldn't increase water content of the cuticle and allow more lipophilic actives to penetrate.

Another way a formulation can aid an actives penetration is by lowering of activation energy of diffusion (Baur et al., 1999b). For example, alcohol ethoxylates and tributyl phosphate surfactants were able to decrease the activation energy of diffusion by 50 to 275 times of observed mobilities at 15^{o}C (Baur et al., 1999b). This was achieved by monitoring the rate of desorption of actives over a range of temperatures, with and without surfactants. Lowering the activation energy of diffusion influences the rate of cuticular penetration by changing the driving force, of the active, and diffusivity, within the cuticle. Affecting the actives partition coefficient and its mobility (Baur et al., 1999b).

1.4 Leaf topology with different techniques

1.4.1 Optical microscopy and the leaf surface

The utility of optical microscopy for imaging the leaf surface is limited due to the resolution of the technique. Though it isn't used to image the EW, it can image the overall topology of the leaf surface. A study by Burton and Bhushan used optical height mapping to image the surface of hydrophobic, as shown in figure 1.8 and 1.9 (Burton and Bhushan, 2006). The study investigated the impact of surface roughness on the adhesion and friction properties and their impact on hydrophobicity.

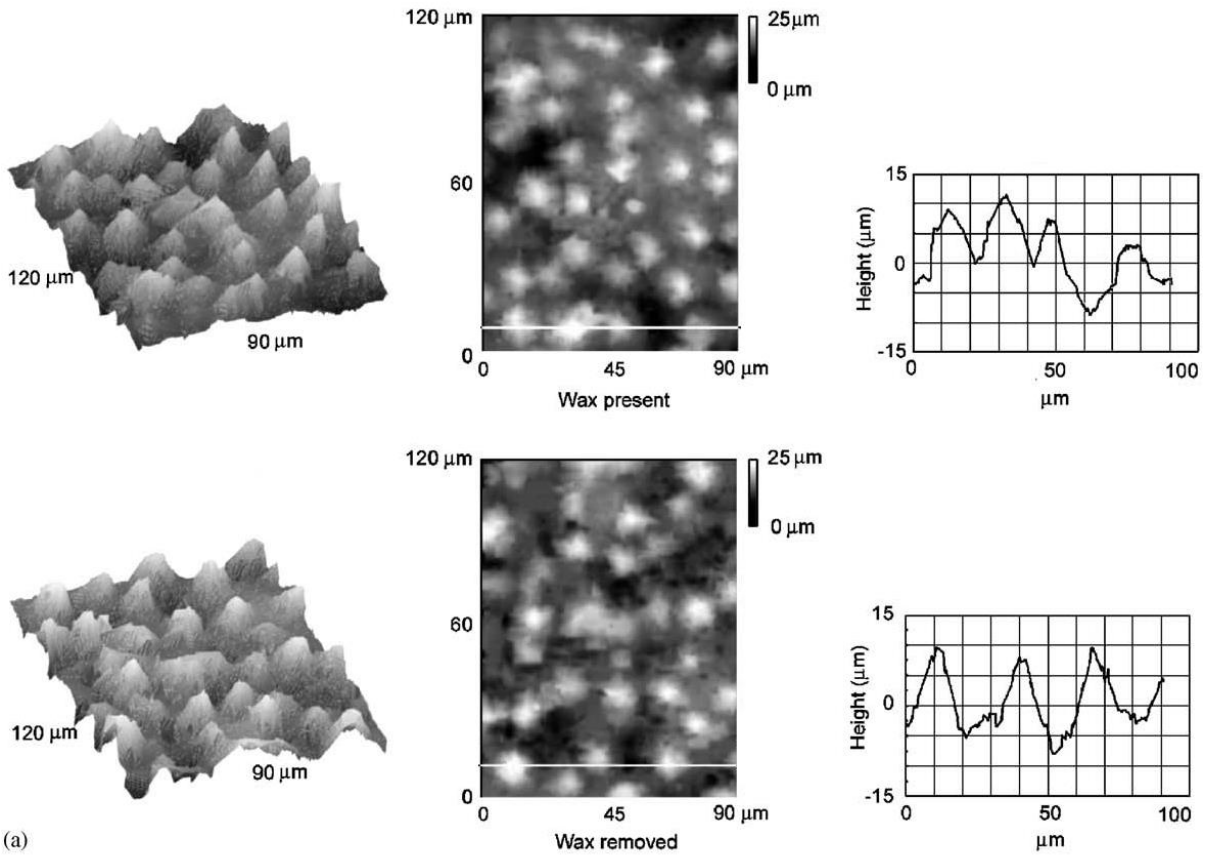

Figure 1.8 – Optical height mapping of fresh and removed Lotus wax structures, with line trace showing variations in height due to these features (Burton and Bhushan, 2006)

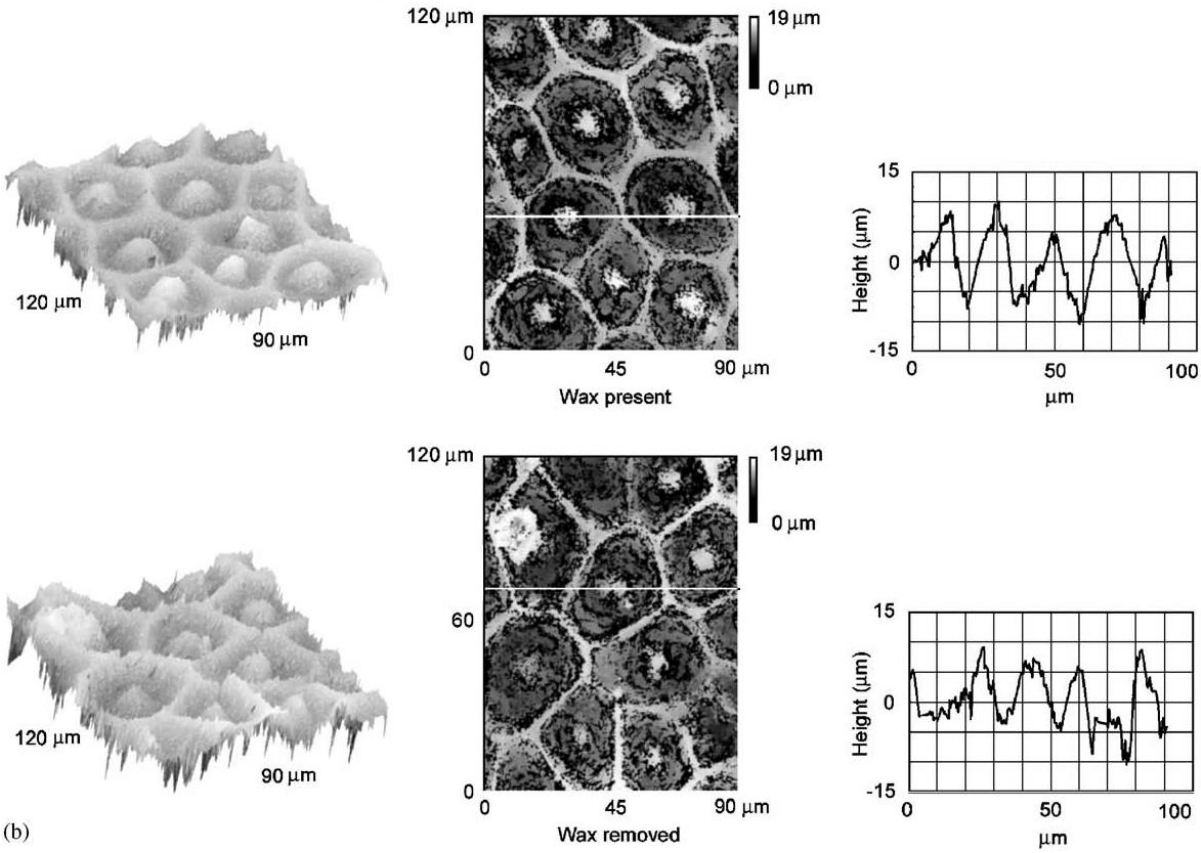

Figure 1.9 - Optical height mapping of fresh and removed Colocasia wax structures, with line trace showing variations in height due to these features (Burton and Bhushan, 2006)

The optical images show the overall topology of the two leaves and the variations in height, gaining the important information in height variation. Though, the technique misses the added variation of height that EW crystals contribute to roughness, requiring the use of other techniques like SEM and SPM (Burton and Bhushan, 2006)

1.4.2 The use of SEM in imaging leaf topology and morphology

Since the development of scanning electron microscopy (SEM) it has been the main imaging technique used to image leaf surfaces. This is due to the higher resolutions of SEM, its ability to image the crystalline structures of the EW and the field of view to image large sections of the leaf surface.

The improved resolution has aided in the improvement of nomenclature of the different EW structures. The epicuticular wax is located on the surface of the cuticle; the epicuticular waxes have many different structures, with these structures changing according to the chemical content and species of the leaf. These are categorised in six main groups (Jeffree, 2006), these are shown in figure 1.10. The most common wax morphologies are thin films and several three-dimensional structures, these include massive crusts (a), filaments (b) rods (c) tubules (d) plates (e) and platelets (f). Figure 1.10, shows the SEM ability to image the EW structures clearly, with these structures ranging from 0.2 to 100 μm (Koch and Ensikat, 2008).

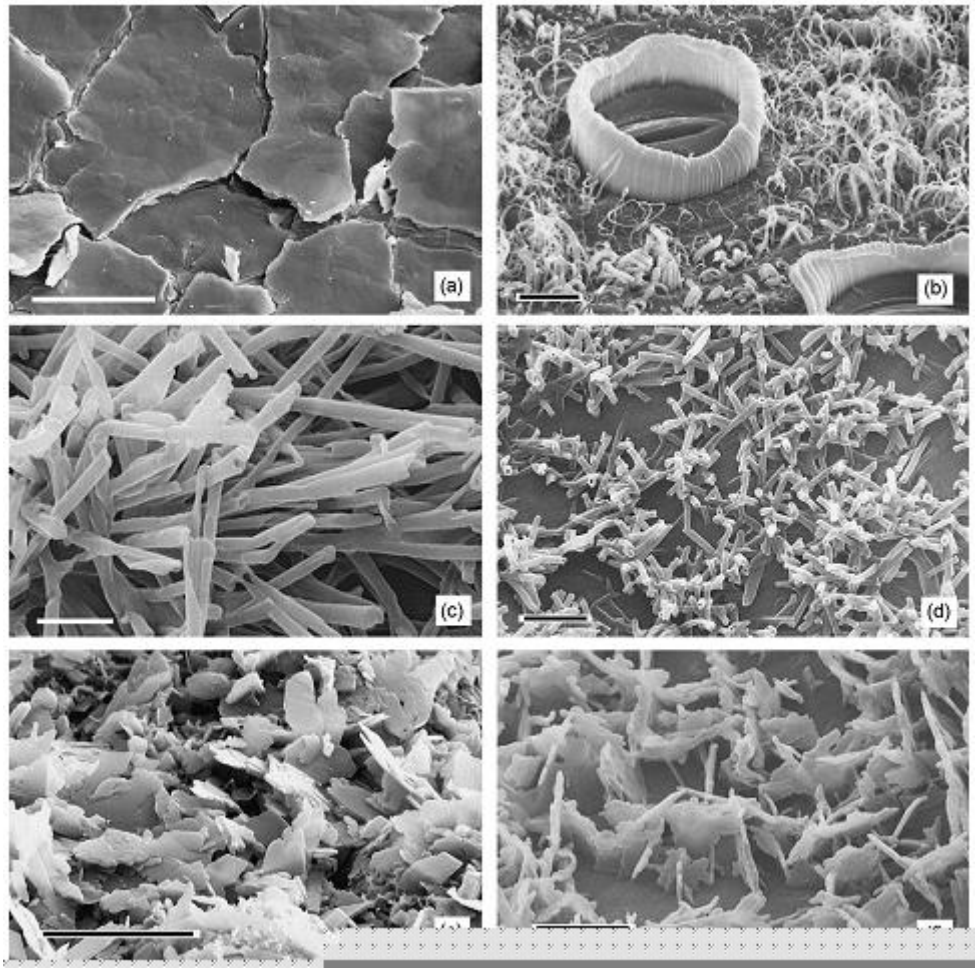

Figure 1.10 - SEM images of the six main categories of epicuticular structures, (a) crusts, (b) filaments, (c) rods, (d) tubules, (e) plates and (f) platelets (Koch and Ensikat, 2008).Scale Bar; (a) = 100µm, (b) = 100µm, (c) = 1µm, (d) = 1µm, (e) 10µm & (f) = 1µm

SEM is also used to image the topology of the leaf surface, showing the variations in the height of the cuticle from cuticle folding or the under laying epidermal cells. This combined with the superimposed nano structures of the EW allows the SEM to view the double structure of the cuticle. SEM image in figure 11.1a and 11.1b, shows the convex cells and the EW crystals of *Euphorbia mysinites* and *Oryza sativa*, respectively (Koch et al., 2008).

Figure 1.11 – Epicuticular wax crystals of (A) Euphorbia mysinites and (B) Oryza sativa (Koch et al., 2008)

The ability of SEM to image the double structure provides more detail than optical height mapping. Providing, the added detail of both the topology of the micro and nano structures of the cuticle. Though, there are disadvantages of SEM, including the possibility of surface damage from the technique and sample preparation, and precluding live leaf studying.

1.4.3 Use of AFM to image leaf surfaces

Atomic force microscopy is used to image leaf surfaces because of the improved nanoscale imaging capacity over than SEM and the ability to image in ambient conditions. AFM also generates 3D information and images, allowing more details to be analysed.

The higher resolution combined with the ambient conditions allows dynamic events to be imaged at the nanoscale. For example, a study by Koch et al shows AFM images the self assemble of nonacosan-10-ol into tubules at different time points (figure 1.12) (Koch et al., 2009b). The consecutive imaging shows the tubules I and II forming circles during the early stages of self-assembly and form the tube at later stages. The self-assembly is

controlled by the evaporation of chloroform; AFM could image the tubule growth because it was done in ambient conditions.

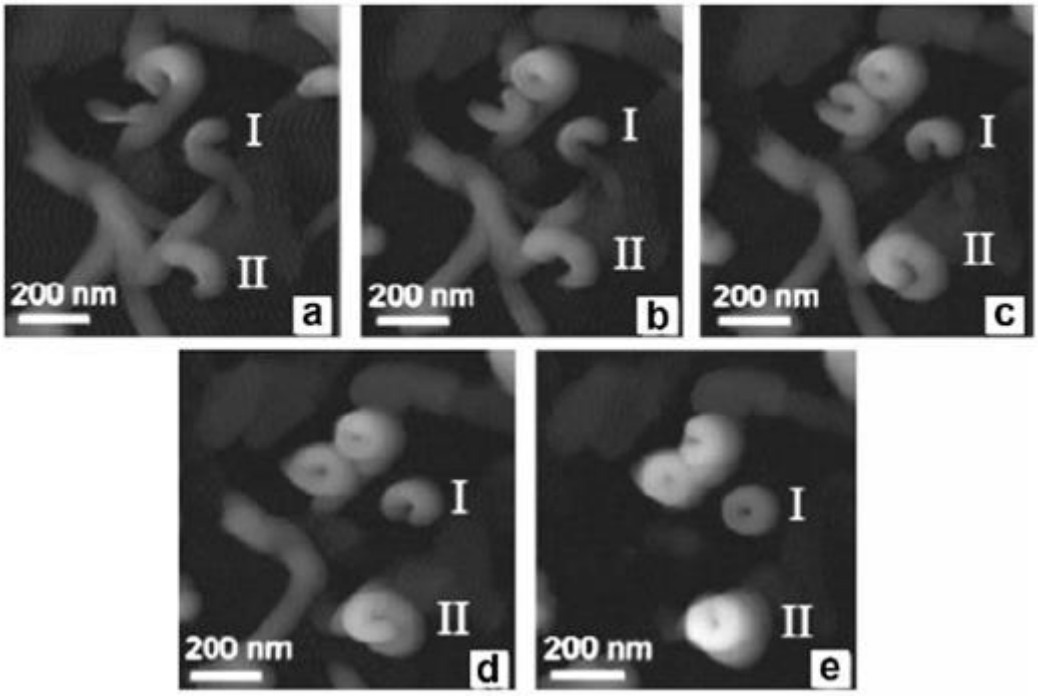

Figure 1.12 – AFM images of the self-assembly of nonacosan – 10 – ol tubules. (a) 65min curved rodlets start forming, (b – e) growth of the rodlets into tubules (Koch et al., 2009b).

1.5 Models of the leaf surface.

1.5.1 Extracted waxes

There have been a number of models used to study the impact of the chemistry and structure of the IW and EW of leaf surfaces on transport of agrochemicals. These have led to understanding of certain properties of the wax surface. Each model provides different possible studies and techniques that could be used.

Extracted waxes have been used to study the different aspects of the IW and EW. EW are used when the cuticle cannot be isolated without damage. Extracted waxes are often used in studies that investigate the self-assembly of EW. These studies have looked into the impact of individual compounds that produced the three dimensional structure of the fully formed EW, such as tubules and plates using SEM (Jeffree et al., 1975). This was achieved by dissolving the plant's waxes in organic solvent and allowing the solution to move through a porous material. As the solvent evaporates the wax undergoes self-assembly into either plates or tubules, as shown in figure 1.13.

The advantage of the extracted wax model is the study of individual components of the waxes or the classification of chemical composition of leaf waxes is possible. The major disadvantage of the extracted wax model is the loss of structure to the overall waxes, that being lost of cutin/cutan, topology and morphology and hence the impact of such macro-organisation on agrochemical wetting and transport is lost.

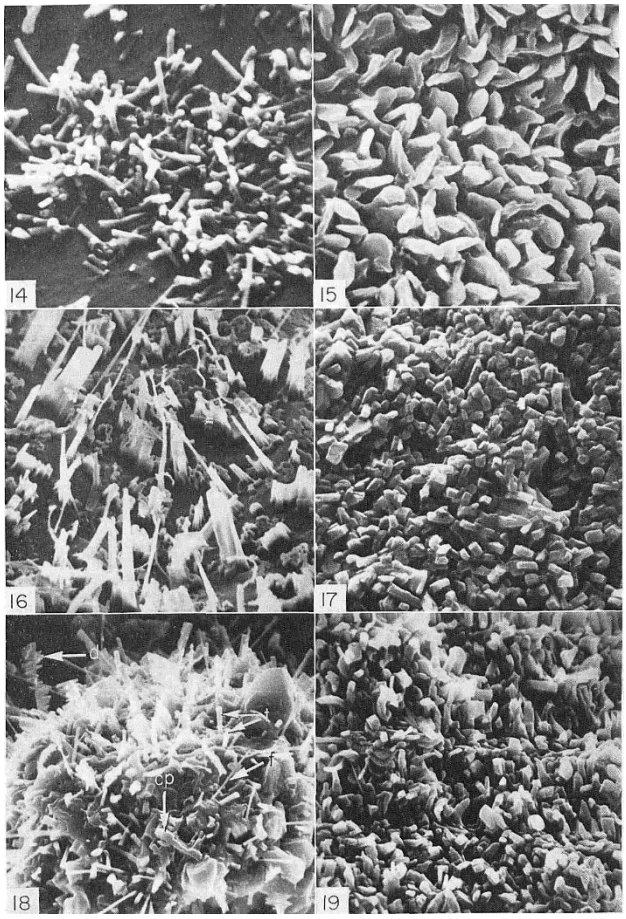

Figure 1.13 - SEM of leaf surfaces and recrystallized extracted waxes from *Agathis australis* (14 leaf surface & 15 Recrystallized wax) and *Brassica oleracea* (16,18 leaf surface & 17, 19 recrystallized wax) (Jeffree et al., 1975)

1.5.2 Isolated cuticles

The use of isolated intact cuticle is the most commonly used approach for studying the impact of compounds movement through the cuticle. Typical experiments used for this model requires the isolated cuticle to be fixed between two compartments, one compartment contains the solute being investigate and the other is the receiver compartment (Baur et al., 1997a). Though the major disadvantage of isolated cuticles model is if the surface of the leaf is too thin or the surface has stomata or trichromes then the isolated cuticle will be difficult to obtain intact and will have holes in it which will allow uninhibited transport.

Isolated cuticles have been used to investigate the impact of adjuvants on the structure of the cuticle, with many different techniques. These include x-ray photoelectron spectroscopy, time-of-flight secondary ion mass spectrometry, AFM, SEM and SThM (Perkins et al., 2005a, Perkins et al., 2005b, Perkins et al., 2008). The utility and ease of this model has made it useful to study agrochemicals, though it should be noted that isolated cuticles have removed the overall topology although they do maintain the morphology of the wax crystals.

1.5.3 Intact leaves

Intact leaves are an ideal model to study interaction and properties that arise from the chemistry, topology and morphology, this is because the overall structure of the cuticle and shape of the cuticle are unaffected (Schreiber and Schonherr, 1993). Since the overall chemistry is not altered in a significant way, thermal characteristics could be described (Perkins et al., 2005a) and the study of the impact of surfactants could be performed.

The main technique used to study intact leaves is SEM. SEM has been used to image intact leaf surfaces to characterise the surface topology and morphology of leaf surfaces to gain an understanding between different species of the same genus (Bussotti and Grossoni, 1997), shown in figure 1.14, and improving the nomenclature of EW structures (Koch and Ensikat, 2008).

An uptake study has also been conducted on intact leaves using different surfactants, these require the use of radioactive ^{14}C-glyphosate and ^{14}C-2, 4-dichlorophenoxyacetic acid (Liu). After a predetermined time, the remaining radioactive material was washed off and assumed the missing material had moved into the cuticle. It was found that high ethylene

oxide content improved the glyphosate uptake; low ethylene oxide content improved the 2, 4-dicholorophenoxyacetic acid uptake.

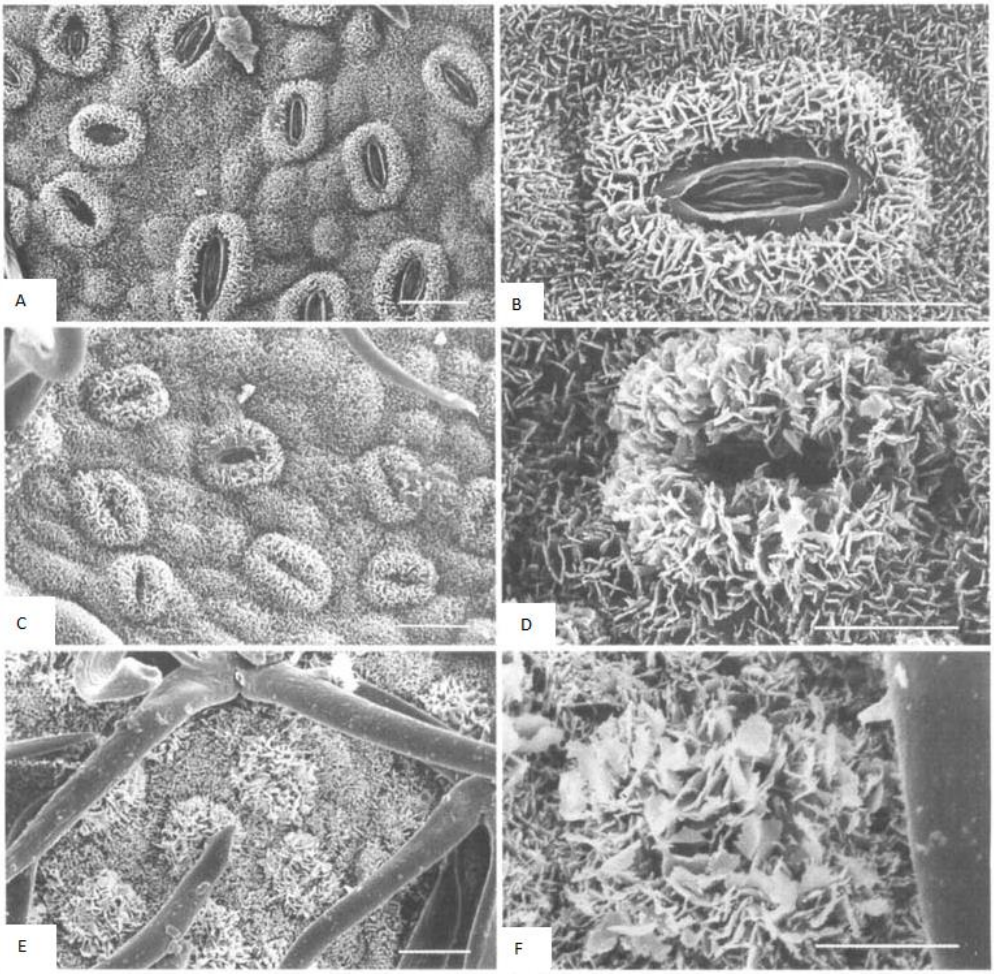

Figure 1.14 - SEM showing the main wax structure of different species of oak leaves A & B *Quercus petraea*, C & D *Quercuz pubescents*, E & F *Quercus faginea*. A, C & E scale bars 20µm. B, D & F scale bar = 10µm. (Bussotti and Grossoni, 1997)

1.5.4 Live leaf studies

Other models have been used to study the time dependent aspects of the leaf surface. For example, EW of *Prunus laurocerasus* were extracted at different leaf ages, marked in

days, and the chemical composition monitored (Jetter and Schaffer, 2001). The study does show the changes in chemical composition over the time of the experiment. Showing certain waxes are important in the early development of the leaf, like alcohol, while later alkanes have an increased presence. An observation is the changing of the overall wax coverage over time. This shows the important potential live leaf studies have on understanding the leaf surface.

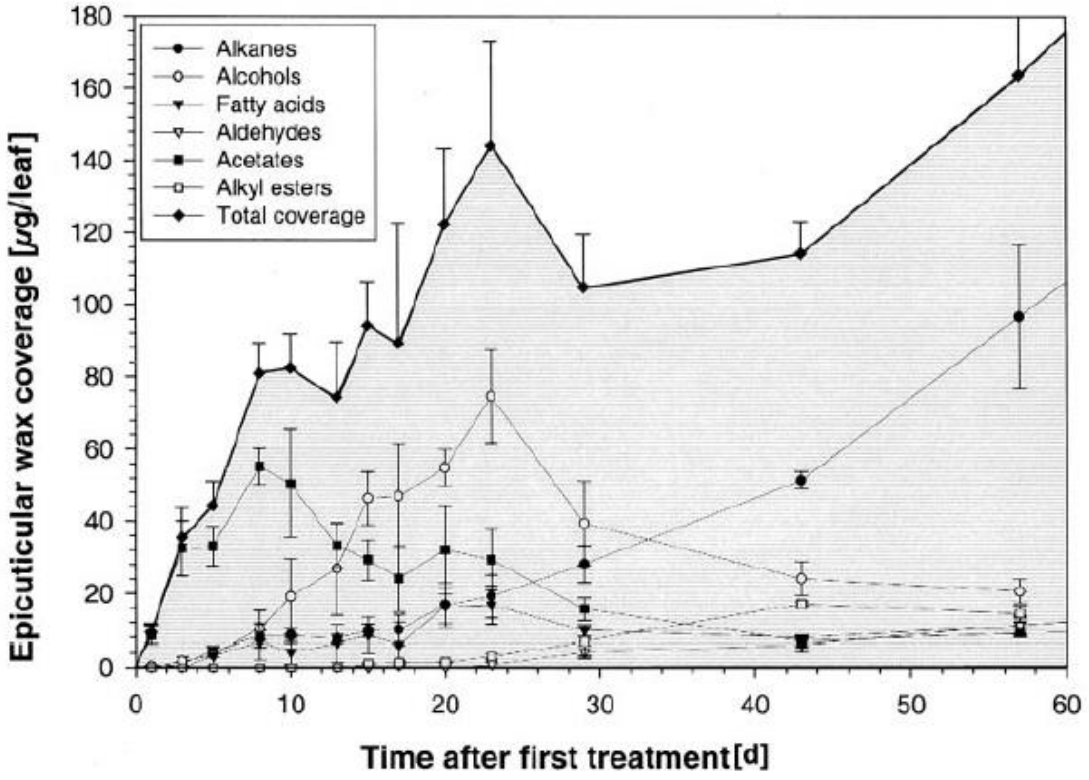

Figure 1.15 - Development of the epicuticular waxes on the adaxial surface *of Prunus laurocerasus* leaf, over 60 days. Removed and analysed with gas chromatography. (Jetter and Schaffer, 2001)

Live leaf is my own term to describe the leaf that is attached to the rest of the plant, it is an intact leaf but alive which allows important dynamic processes to continue. Live leaf

studies are the least used model, this is because most techniques like scanning electron microscopy and time of flight secondary ion mass spectrometry require the sample to be under vacuum. This would preclude live plant tissue for studies. Ambient techniques such as optical microscopy and scanning probe microscopy do allow imaging and characterization of live leaves. Live leaf studying would allow the processes that are associated with living leaves to be characterized (Koch et al., 2009a).

An example of live leaf studies and the potential information gained from the model is shown in AFM studies (Koch et al., 2004, Koch et al., 2009a). The studies imaged live leaves of various plants to assay wax regeneration abilities of the EW and study the movements of EW through the cuticle. The studies used both intact leaves, which were kept hydrated, and live leaves. The intact leaves could only be maintained up to 2 hours before the cells stopped producing the waxes for the EW. The live leave could be imaged indefinitely. Figure 1.16 shows Koch's study using AFM to image the wax generation on the dewaxed surface of *Euphorbia lathyris.* The study shows the regeneration of the leaf wax over the time of 20 hours, starting with a single layer of wax being regenerated and ending with a multilayer forming at the end of imaging.

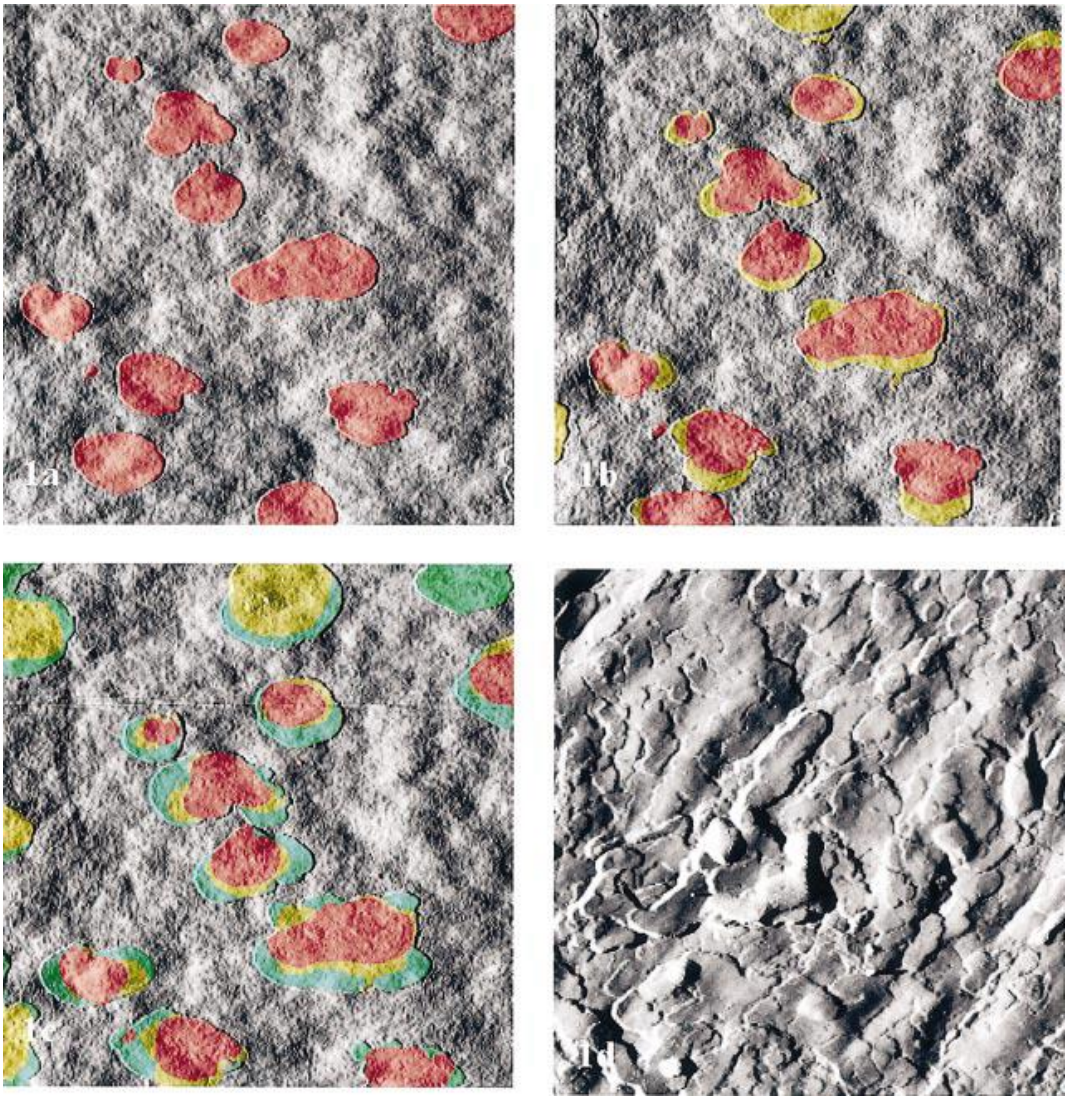

Figure 1.16 - AFM showing the wax regeneration of dewaxed surface of *Euphorbia lathyris* 3x3 µm. (1a) T=1h 38min, showing the start of was regeneration. (1b) T= 2h 11min, further accumulated wax, coloured yellow. (1c) T=3h 3min, more accumulated wax, coloured green. (1d) T=20h showing multi-layered wax regenerated. (Koch et al., 2004)

These studies have shown the potential that live leaf imaging and characterisation might have on the studying of agrochemical interactions. The natural processes involved, like transpiration, translocation and repair mechanisms could have an impact of chemicals and the properties of the leaf surface.

1.6 Aims of the Thesis

Plant cuticles are a dynamic and complex structure of the leaf surface, with different plant species having different cuticular structures. These structures control the properties of the surface of the leaf, from wetting to self-cleaning. To investigate how the properties of the cuticle are related to the structures of the EW and the rest of the cuticle new analytical approaches are required, preferably using live leaf imaging. The research and aim of this project focuses on the use of scanning probe microscopy (SPM) to image and characterise the impact of agrochemicals on leaf surfaces and physical properties of the leaf surface, of intact leaves and live leaf surfaces.

The first part of the project was to utilise scanning ion conductance microscopy (SICM) for imaging the surface of leaves. SICM is a liquid based imaging technique that uses conductance through a pipette to map the topology of surfaces. This relatively new technique has mainly been used to image living cells because it is non-contact, reducing potential damage. This technique has not been used before to image leaf surfaces. Since SICM hasn't been used to image leaf surfaces, a range of leaves were selected, including English ivy, strawberry and pea. This was to investigate if SICM can image a range of leaf surfaces with different EW crystalline structures, like pallets and filaments. This was to compare to other imaging techniques that have been used to image the surface of leaves, comparing SICM with atomic force microscopy (AFM) and scanning electron microscopy (SEM).

SICM, being a native liquid imaging technique, could be used to describe the impact of liquid formulations and interactions of liquids with the leaf surface. SICM was used to investigate the wetting of a droplet on a hydrophobic leaf surface. Imaging over time the interaction of the droplet with the leaf surface, investigating the changes in wetting as the

droplet dries. Another area of investigation is the effects of drying formulations on a leaf surface, looking to see if the formulation impacts the leaf surface during the drying stage.

The second part of the project was to use scanning thermal microscopy (SThM) to characterise the differences between thermal profiles of an intact leaf surfaces and live leaf surfaces. The experiment was to establish the thermal profile of recently dissected (with water present) or live leaves and a dried intact leaf of the same plant. This is to understand how water content affects the leaf surface and the thermal profile. Also to examine the differences between leaver with EW and IW surfaces. Then SThM and AFM was used to probe the effects of plasticizers and surfactants on the live leaf of the field bean.

There are a number of different leaf surfaces that are used throughout this work. This thesis will look at the surfaces of *Festuca* grass, *Pisum sativum, Hedera helix, Brassica napus, Fragaria ananassa* and *Vicia faba*.

Chapter 2

Main Experimental Methods

2.1 Scanning Electron Microscopy

2.1.1 Theory

Scanning electron microscopy (SEM) was created from the development of the electron beam scanner by Knoll 1935. The first SEM with a sub-micron probe was developed by Von Ardenne 1938 (McMullan, 1995). These SEMs were then followed by many other designs due to advances in technology or need for imaging different surfaces. Conventional SEM requires high vacuum to be used whilst imaging takes place so as to allow sufficient beam path length of the electrons. The advent of environmental (ESEM) and variable pressure SEM (VP-SEM) now make it possible to image under low vacuum and high humidity conditions (Stabentheiner et al., 2010, Talbot and White, 2013).

The electrons from the SEM are produced from a number of sources which include; tungsten hairpin, thermionic emission and field emission source. The electrons are then brought into focus using electromagnetic lenses. The SEM electron beam can interact with the surface to produce various physical responses. These include secondary electrons (SE), backscattered electrons (BSE) and Auger electrons, as well as x-rays, cathode-luminescence and electromotive force (McMullan, 1995, Birks and Brooks, 1957). These are utilised to produce images and/or the characterization of the sample.

The primary electrons (PE) from the electron source make random elastic and inelastic collisions. These collisions produce SE and BSE. SE are produced by the excitation of valence electrons of the atoms of the samples, which then propagate through the sample to the detector. Back scattered electrons are primary electrons that have been deflected by atoms in the sample, where the electron path takes it through the sample and back out surface (Stokes, 2008). BSE and SE are then used to produce the SEM image. SEM produce images

by using the electron beam scanning the surface of a sample in a raster pattern. The coating of samples with a thin conductive layer is standard with conventional SEM, since without a coating the PE beam would damage and charging of the sample at high energies. The coating also provides a number of other advantages. These include; stable imaging with increase beam energies, reduction in penetration of PE, increase SE emission, increased surface detail, increased lateral resolution, increased mechanical and thermal stability (Stokes, 2008).

The development of ESEM and VP-SEM allows samples to be imaged in or close to their native hydrated state without the need for a conductive coating. Sample preparation, however, remains important.

The removal of water is important because the sample will undergo high vacuum condition, which would put stress on hydrates samples. The sample would need to be fixed, by air drying, freeze drying, critical point drying or chemical fixation (Pathan et al., 2008).

2.1.2 SEM instrumentation.

The SEM images used in this thesis were captured using JEOL-JSM-6060Lv SEM (JEOL Ltd). Samples were coated in a thin layer of gold using a sputter coater EM SCD005 (leica Microsystems). Samples were sputtered for 300 seconds at 30mA. Samples were mounted on an aluminium stud and fixed using carbon discs

2.1.3 Applications of SEM to imaging leaf surfaces

SEM has been the most used high resolution technique to image and analyse plant surfaces. It has been used to study the surfaces of fruits (Bargel and Neinhuis, 2005), roots

(Walker et al., 2004), leaves (Kim et al., 2009), petals (Feng et al., 2008) and other surfaces (Koch et al., 2008). It has been used to study many processors that occur on these surfaces, such as self-assembly (Koch et al., 2004) , wetting (Nairn et al., 2011) and chemical up take (Uzu et al., 2010).

The application of SEM to leaf imaging has included the study of micromorphologies of waxes on the plant surface, and the classification of epicuticular waxes (EW). This work has improved the terminology and classifications of leaf surfaces. Classified structures include thin films, massive crusts, granules, plates, platelets, filaments, rods and tubules (Koch and Ensikat, 2008).

In terms of investigating agrochemical formations SEM has been used to image the impact of adjuvants of the surface of leaves (Orbovic et al., 2001). More recently SEM has been used as a complimentary higher resolution imaging technique to support other more novel analytical approaches such as atomic force microscopy, micro thermal analysis and time of flight secondary ion mass spectrometry (Perkins et al., 2005b).

2.2 Atomic Force Microscopy

2.2.1 Theory

An alternative imaging technique to SEM is the use of the various instruments with the scanning probe microscopy (SPM) family. SPMs interrogate surface by using a sharp proximal probe that scans the surface of the specimen while recording a defined interaction, either physical of chemical, between them. An SPM that could be used for imaging leaf surfaces is the atomic force microscope (AFM).

AFM is a nanoscale imaging technique first developed in 1986 by Binnig and Quate (Binnig et al., 1986). AFM was designed as a tool to investigate the surfaces of insulators on the atomic scale. In AFM the surface of the sample is imaged using a sharp probe in contact with or close to a surface. The probe is mounted on a flexible cantilever. To monitor the motion of this cantilever a laser is reflected from the back of it on a position sensitive detector. The tip of the probe is moved across a surface in a raster fashion while changes in the vertical cantilever deflection are monitored. The scanning is achieved by using piezo ceramic crystals, which allow the movement of the probe or the sample in the X, Y or Z axes; with sub-nanometre precision as indicated in figure 2.1. This type of imaging means no conductive coating is required and sample may be imaged in air or liquids in their native state.

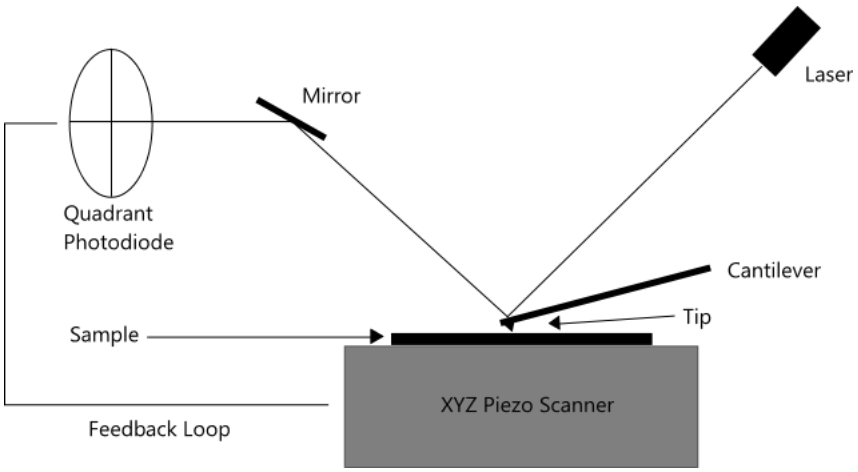

Figure 2.1- Schematic of the principle of AFM

AFM can be operated using different modes depending on the sample and the information required. There are two main modes that are used, these are contact mode and tapping mode. In contact mode atomic force microscopy (CM-AFM) the probe is kept at a constant force and in continuous contact with the surface. So as the probe increases or decreases in height with topographic features. The signal from the reflected laser is used in a feedback system to control the piezo ceramic crystal scanner so as to increase or decrease the Z position of the probe/sample to maintain a constant force. Since CM-AFM is always in contact with the surface it offers the greatest height sensitivity, however the lateral forces of the probe on the surface during scanning can often cause damage soft biological samples such as leaf surfaces (Novak et al., 2009).

To counter the lateral forces of contact mode, tapping mode atomic force microscopy (TM-AFM) was developed (Shao et al., 1995). TM-AFM uses a probe that oscillates at its resonant frequency above the surface of the sample while the tip periodically touches the surface on each oscillation cycle (Kasas et al., 1997). As the tip interacts with a sample this affects the amplitude of tip oscillation, a signal which can then be employed in a feedback loop to map surface topography. The main advantage of TM-AFM is the reduction in lateral forces applied to the sample, although TM-AFM still uses contact forces to image the sample

surface and damage on some samples is still reported (Fritz et al., 1993). TM-AFM can also use the sine wave movement of the cantilever, with respect to the drive frequency, to acquire spatially resolved phase data as well as topographical information. Phase imaging can identify changes in tip sample interaction, which can be used to map physical and chemical properties at the nanoscale (Chen et al., 1998).

2.2.2 AFM instrumentation

The AFM images in this report were acquired using a DI 3000 AFM (BrukerNano, Coventry, UK). This instrument has a maximum scan size of 90 x 90 µm with a maximum Z (vertical) limit of 6 µm. Samples up to 200mm in diameter can be accommodated, including live leaf samples.

TM-AFM was used to acquire the AFM images in this report, phase images were obtained simultaneously with topology images, with a 512 x 512 pixel resolution. In air the tips used were 0.01 – 0.025 Ohm.cm^{-1} Antimony doped Si (BrukerNano), with a resonant frequency between 347 – 393 kHz.

2.2.3 Application of AFM to characterisation and imaging the leaf surfaces.

The flexibility of AFM, without the need for coating and imaging in ambient has allowed an increased usage for leaf imaging. One of the first uses of AFM to image a leaf cuticle surface was a study using CM-AFM to image isolated English Ivy leaf cuticles (Canet et al., 1996). In this study the AFM images were shown to be comparable to SEM images of the isolated cuticle, with higher resolution and quantified 3D information. Since this time the AFM has been used to image a number of different plant leaf surfaces.

TM-AFM has also been used to image complex leaf structures including the recrystallized waxes of the wheat (Koch et al., 2006). The platelet structures on grapevine leaves (Bensalem-Fnayou et al., 2009) and the surface of dissected Lotus and Colocaisa (Bhushan and Jung, 2006) have been analysed. It should be noted that all these studies are of relatively small scan sizes and relatively flat surfaces, this can be explained by the small Z ranges of most AFMs. Hence, it is difficult to employ AFM on leaf surface in general as most display to much roughness for analyses. However, on suitable samples TM-AFM has been shown to provide additional information to topography data by acquiring phase images. This was utilised to map variation in surface properties of English Laurel by using a hydrophobic tip (Perkins et al., 2005b), using amplitude-phase-distance to monitor the attractive and repulsive regions of the leaf cuticle.

AFM opens up the possibility, as yet largely unexplored of imaging live leaf surfaces. An example of live leaf imaging with TM-AFM was the study on imaging the self-assembly of waxes that make the EW. The study investigated this by removing the EW then imaging the wax regeneration on the leaf as it moved through the cuticle (Koch et al., 2004). The regeneration of EW were studied on different surfaces. This allowed a mechanism of wax

formation to be proposed (Koch et al., 2009a). Live leaf imaging of the cuticle in the future could provide more information on how herbicides and other agrochemical formulations interact with the plant surface.

2.3 Scanning Ion Conductance Microscopy

2.3.1 Theory

Another possible SPM method able to image the surface of leaves is scanning ion conductance microscopy (SICM). SICM was developed in 1989 by Hansma (Hansma et al., 1989). This instrument was able to image the surface of an insulating acetate film, though, the sample and the imaging micro-pipette would often be damaged during the imaging process. It wasn't until 1997 when specific scanning parameters where developed to prevent sample damage (Korchev et al., 1997), that significantly improved imaging was achieved, allowing for example the imaging of living tissue.

SICM is a probe microscopy like AFM. Unlike AFM, SICM uses the conductance of ions in a solution instead of contact force to image the surface of a sample. SICM uses a micro/nanopipette filled with an electrolyte solution and an electrode. When in contact with a reservoir of electrolyte solution with the corresponding electrode and a potential voltage difference then the conductance of ions through the pipette pore will occur. The position of the pipette relative to the surface of an object influences the ion current (Korchev et al., 1997). As the pipette moves closer to an object the ion current is restricted and this can be used to monitor and control the position of the probe relative to a surface, as shown by the approach curve in figure 2.2.

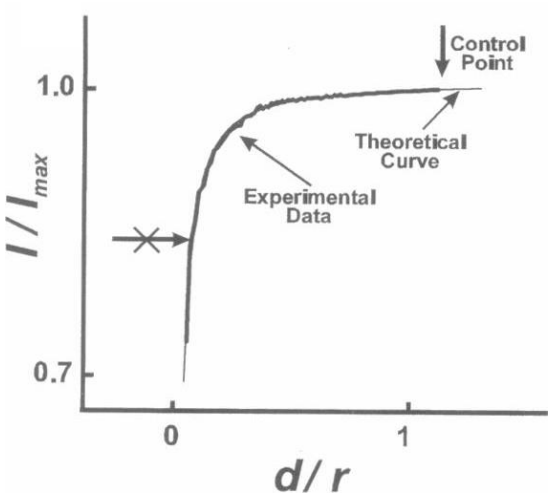

Figure 2.2 –Comparison of expected and observed tip current (I) as a function of distance (d). (r) is radius of tip (Korchev et al., 1997).

There are three standard modes which can be utilised with the SICM, these are DC or scanning mode, AC mode and hopping mode. Scanning mode SICM images the surface of a sample in a raster scanning pattern, while using the ion conductance to maintain a constant distance from the sample. This is shown in figure 2.3, showing the differences between the two modes. This mode of imaging proved to be useful for imaging of live cells and was able to resolve nuclear pores, which where 50 nm in diameter (Ying et al., 2005). This mode of imaging is suited for relatively flat surfaces, but if topology of the sample changes dramatically there is a chance that sample or probe could be damaged, which would affect image quality (Novak et al., 2009). In AC mode the tip vibrates, while still maintaining a close distance to the sample, the vibration height can be around 100 nm (Pastre et al., 2001). While this mode improves sensitivity and allows the pipette tip to be closer to the sample there is still a significant issue related to damage to the pipette and sample for relatively rough samples.

Since these scanning modes can cause damage, to both, sample and probe when imaging rough samples a new mode was introduced. Hopping mode, unlike the scanning modes, does not use a continues feedback, but instead at each imaging point the probe is

approached from above the sample, until the pipette reaches a percentage set point reduction of the ion current value. Once this value is achieved the Z position is recorded as the height at that specific point (Korchev et al., 1997, Novak et al., 2009). .

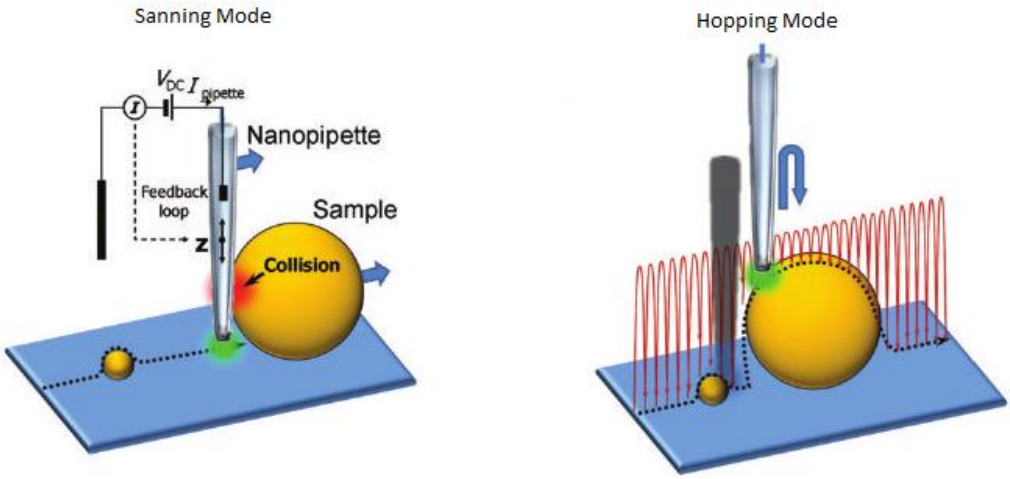

Figure 2.3 - Images representing the two main modes of SICM. (Left) Scanning mode and problems associated. (Right) Hopping mode (Novak et al., 2009)

The resolution of SICM has been studied using experimental and computational methods. Hansma and colleagues used a well-defined periodic sample to assess the resolution of the micropipettes used (Hansma et al., 1989), though the sample does not allow the lateral resolution to be derived. It wasn't until Rheinlander and Schaffer in 2009 that a computational model to describe image formation and resolution was produced (Rheinlaender and Schaffer, 2009). They found that the lateral resolution is three times the inner opening radius (r_i), r_i being shown in figure 2.4.

Experimental studies have claimed the SICM has a range of lateral resolutions. A study comparing SICM to AFM and SEM suggested a lateral resolution of 50 nm (Ushiki et al., 2012), while another study, looking into imaging of proteins, claims a resolution between 3 – 6 nm (Shevchuik et al., 2006). Computational studies has shown the resolution to be

either 2ri or 3ri, which doesn't seem to agree with experimental data. The difference between

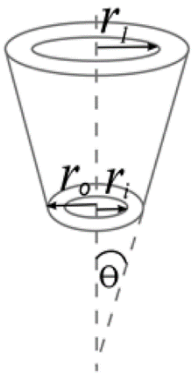

Figure 2.4 - The lateral resolution of the SICM is controlled by the tip. The important parameters are r_i, inner radius, r_o, outer radius. (Del Linz et al., 2014)

the two experimental studies are the r_i of the pipette tip, 100nm and 6.25nm respectively. Showing This shows that r_i or tip size is important to resolution, though the experimental work show the lateral resolution is below that of r_i, showing it could be more complex (Edwards et al., 2009).

2.3.2 SICM instrumentation

The SICM used throughout this work was a ScanIC SICM (Ionscope, Melbourn, U.K). This instrument has a maximum scan range 90 x 90 µm with a maximum z limit of 25 µm. Hopping mode was used to image the surface, with 512 x 512 pixel resolution. Phosphate buffer saline (PBS) (Fisher Scientific) was used as the electrolyte solution made up in ultrapure Milli-Q water.

Pipettes were either obtained from Ionscope or pulled in house using a p-97 flaming/brown micropipette puller (Sutter Instruments). Standard wall borosilicate tubes, with an outer diameter of 1 mm and an inner diameter of 0.5 mm (Sutter Instruments) were used as the starting material. Images were processed using SICM image viewer (Ionscope).

2.3.3 Applications of SICM for biological imaging.

There are no published studies of SICM being used to image leaves, although, SICM has been widely used to image biological systems under physiological conditions. These range from studies of living neuroblastoma cells (Liu et al., 2011) to imaging proteins on *Bacillus sphaericus* cells (Shevchuik et al., 2006). SICM is well-suited to cell imaging because of the non-contact imaging process in physiological environments (Del Linz et al., 2014), and its ability not to disrupt the cells natural processers by physical contact.

There are significant differences between SICM and AFM as a result of the non-contact nature of SICM and the very different contrast mechanism employed. SICM and AFM were used to image myoblast cells and the data compared (Rheinlaender et al., 2011). AFM was found to cause the width, height and, by association, volume to be distorted due to tip convolution effects and sample compression, while in SICM the measurements were accurate (Rheinlaender et al., 2011). AFM was shown to have superior spatial resolution but caused damage to these cell, while the SICM left the cells undamaged. Sharp vertical steps are also resolved efficiently (Ushiki et al., 2012), a problematic feature for AFM. This shows that SICM could be useful in imaging the delicate waxy features of the leaf surface, with for example their often dramatic vertical crystalline structures.

Since there are no studies with plants the potential to utilise SICM with its other abilities to study leaves can be ascertained. In addition to imaging SICM is also able to deliver chemicals to a localized area of a sample from the pipette. This was demonstrated in 2002 with the delivery of DNA though the pipette and onto a sample surface (Ying et al., 2002, Bruckbauer et al., 2002). This was possible because the negatively charged phosphate groups of the DNA allowed the SICM to manipulate the DNA to force it out of the pipette via an electrophoretic effect. The injection capability was then utilised to map individual ion

channels and receptors in living cells (Babakinejad et al., 2013). This is achieved using The ability to deliver compounds locally to a leaf surface to image the effects could provide a wealth of knowledge in terms of leaf response and localised effect of herbicidal compounds.

SICM also as the ability to be combined with other techniques by adapting the probe, with addition controls or with separate techniques. These include scanning electrochemical cell microscopy (Snowden et al., 2012), patch clamp (Yang et al., 2011) and confocal microscopy (Shevchuk et al., 2013). All these studies have shown the capabilities and potential of SICM to imaging of biological samples, and by association plant surfaces.

2.4 Scanning Thermal Microscopy

2.4.1 Theory

SThM is also a part of the SPM family and was first proposed in the 1986 by Williams and Wickramasinghe. SThM is a combination of SPM and thermometric sensor which replaces the tip of the AFM or scanning tunnelling microscopy (STM), as a result there are two possible constructs to the SThM, as shown in figure 2.5 (Gmelin et al., 1998).

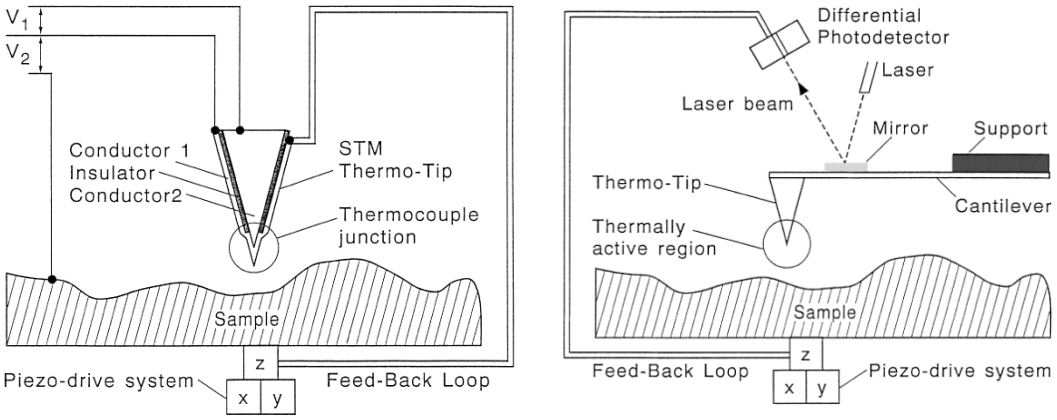

Figure 2.5 - Schematic of the principle of (left) STM SThM and (right) AFM SThM (Gmelin et al., 1998)

The differences between the STM-SThM and AFM-SThM are the methods in which the tip interacts with the sample to create the feedback loop. The STM-SThM requires the tunnelling of electrons between the tis to the sample to maintain distance, which requires the surface to be conductive. The AFM-SThM controls tip sample distance by the use of the laser and the photodetector in a similar manner to the AFM (Gmelin et al., 1998). Since the AFM-SThM doesn't require a conductive sample it can be used on more samples.

The tip of the AFM-SThM consist of a silver wire with a fine platinum core bent into a V shape, this is called a Wollaston wire (Price et al., 1999). The tip can image the sample surface like CM-AFM and can hold a constant temperature, which allows the mapping of the

surface thermal conductivity (Hammiche et al., 1996a). This is achieved when a current is passed through the wire, while the scan is moving in a raster pattern over the surface.

The SThM can also utilise the tip to perform local thermal analysis (LTA) of a sample. For LTA, the tip remains stationary and the temperature of the tip is ramped to a predetermined point. As the temperature is increased the AFM feedback system measures Z axis deflection on the feedback loop (Hammiche et al., 1996b). When a thermal transitions occurs such as a melting or glass transition point the z axis deflection is affected.

2.4.2 SThM Instrumentation

The SThM used was a Topometrix Explorer SPM equipped for SThM (BrukerNano). This instrument had a maximum scan size of 100 x 100µm with a maximum height of 10µm. The tip was a Pt/Rh thermal resistor, with a temperature coefficient of 0.00165k, and a nominal resistance 2.1 Ohms (BrukerNano). This was achieved by measuring the melting point of three crystalline polymers and room temperature. These included polyethylene glycol (PEG), polypropylene (PP) and nylon-6. The Tm of these polymers are 62 °C for PEG, 158 °C for PP and 217 °C for nylon-6.

2.4.3 Applications of SThM to analysis of surfaces.

SThM has been used to both image and perform LTA on many different surfaces. It has imaged resins and tablet (Price et al., 2000), polymer blends and their phase separation (Zhang et al., 2003). It was also utilised to image and perform LTA on polymorphic forms of a drug (Sanders et al., 2000). This has led to the improvement of the technique to the point where nanothermal analysis can be achieved, which has shown to provide thermal

information on delicate samples (Zhang et al., 2011) and pharmaceutical solid dispersions (Zhang et al., 2009) at nanoscale resolution. This is achieved using a silicon based nanothermal probe of a similar geometry to a standard AFM probe.

SThM has been used to characterise the effects of two non-ionic alcohol ethoxylated surfactants, being Synperonic A7 and A20, were used on the surface of English Laurel leaves (Perkins et al., 2005a). In this study the *in situ* SThM and LTA where compared to the bulk technique of differential scanning calorimetry (DSC). This was achieved by performing DSC on isolated cuticular wax that had been mixed with the surfactants. SThM and LTA were performed on intact leaves, where the surfactant had dried. The study showed the surfactants were able to reduce the melting point of the cuticle, with A7 showing disruption to the crystalline structure. The SThM with LTA also showed the A7 surfactant effected regions of the deposit differently, with depressions in the melting point being higher at the rim. This is the only study to date that has used SThM for leaf characterisation.

2.5 Plants species

2.5.1 Plant choices

In this thesis there are a range of plants that was used, this was to allow for a range of surface features and topologies to be imaged, to test the different microscopic techniques and allow comparison. Also the different leaves were chosen because of the different surface properties, this is shown with the hydrophobic study.

Hedera helix was used because it grows on the Nottingham University campus, allowing easy access to samples, while growing all year round. The surface of the leaf shows not surface features and is relatively flat, making it ideal to image with SPM.

Festuca grass, grows on the Nottingham University campus and it easily acquired. The surface of the leaf had hydrophobic properties and allowed the testing of SICM ability with hydrophobic surfaces. The surface of the leaf has a large density of platelet features

Fragaria ananassa (strawberry) was used because the surface of the leaf had not been imaged by SPM. It was chosen to test the abilities of SICM to image leaves that couldn't be imaged by AFM. The surface features, filaments and rodlets, were

Pisum sativum (Pea) and *Brassica napus* (Oil Seed Rape) are important agricultural crops. The surface of the leaves being hydrophobic, resulting in a different wetting regimes, compared with *Festuca* Grass. This plant was investigated because of this property allowing the wetting study. Also they have different morphological structures, with pea having platelets and oil seed rape having tubules.

Vicia faba (Field Bean) is, also, an important agricultural crop, which lacks surface features. Allowing easy imaging with SPM. This plant was used for the SThM study because

there is no EW crystals on the surface, which would interfere with the thermal profiling of the surface.

2.5.2 Plant growth

For studies of *Hedera helix* (English Ivy) and *Festuca* grass, leaves were harvested from plants continuously grown on the University of Nottingham's grounds. *Fragaria ananassa* (Strawberry) plants were sourced locally (Homebase Ltd). The leaves were not washed, to prevent damage to the EW Structures. Grown and maintained by myself in my house, near a window. This was to prevent damage and debris from the surface of the cuticle

Pisum sativum, *Brassica napus* and *Vicia faba* plants were grown from seed (Syngenta, Jealott's Hill, Berkshire, UK). Using compost and watering daily, the plants where grown next to windows, allowing the surface to be maintained and clean, while allowing light for growth. The plant was monitored to gage the age of the leaves, with the first day beginning from bud breakage. This was to allow the age to be followed and to reduce the variable of old from studies.

2.6 Materials and Method

2.6.1 Chapter 3 Materials and Method

2.6.1.1 Plant Information

Hedera helix (English Ivy) leaves where chosen at random, then they were washed with deionised water, with resistivity of 18MΩ cm, obtained from Milli-Q water purification system (Millipore Cooperation), before imaging to remove any debris from the leaf surfaces. Young *Fragaria ananassa* (Strawberry) were used without cleaning the leaf surface, this was to prevent damage of the surface features.

2.6.1.2 Samples for SEM, AFM and SICM Imaging

SEM samples were prepared by dissecting the leaf and leaving the segment to dry over a day. Once the segment was dried it was then secured onto an aluminium stud and coated in a layer of gold. AFM samples leaves were dissected and fixed to a steel stud with double sided sellotape, and imaged immediately. SICM samples the leaves were dissected and fixed to a petri dish with double sided sellotape. The petri dish was then filled, and the sample was allowed to equilibrate with the PBS solution for 10 minutes.

2.6.2 Chapter 4 Materials and Method

2.6.2.1 Plant Information

Festuca grass was carefully sampled from around the Nottingham University campus, by cutting the leaf into segments. The *Pisum sativum* (Pea) leafs were kept whole, but removed from the stem of the plant by the base of the leaf, with the leaves being less than two weeks' old. The leaf was not washed to prevent damage to the platelet structures. *Brassica napus* (Oil seed rape) leafs were kept whole, but removed from the stem of the plant by the base of the leaf, with the leaves being less than two weeks' old. The leaf was not washed to prevent damage to the platelet structures.

Hedera helix sample leaves for the SEM Resolva study were marked, to indicate which leaves had a droplet of the 90:10 Resolva: PBS solution. Then left for either one or five days before being desiccated and left to dry for a day. The SICM study the leaves were washed with deionised water with resistivity of 18MΩ cm, obtained from Milli-Q water purification system (Millipore Cooperation).

2.6.2.2 Samples and solutions for SEM and SICM

Festuca grass was fixed to a petri dish with double sided sellotape, then a droplet of PBS was applied to the surface and the electrodes placed in the centre top of the droplet to reduce distortion on of the droplet and then the leaf surface was imaged. For full wetting of surface sample imaging of hydrophobic surfaces, Tween 20 (Sigma Aldrich, Missouri, US) was added to make a 5% w/w droplet, then left for 5 min to allow the surfactant to equilibrate before imaging took place.

Pisum sativum and *Brassica napus* wax fixed to a petri dish with double sided sellotape, then a droplet of PBS was applied to the surface and the electrodes placed in the

centre top of the droplet to reduce distortion on of the droplet and then the leaf surface was imaged, to image the liquid/vapour interface. Tween 20 (Sigma Aldrich, Missouri, US) solutions were made to a 1% and a 0.5% w/w solution in PBS. The solutions were added to the 4ml droplets of PBS on the leaf surfaces, to make a finial concentration of 0.0012% and 0.0006% w/w Tween PBS solution

2.6.3 Chapter 5 Materials and Method

2.6.3.1 Plant Information

Hedera helix (English Ivy) leaves where chosen at random, then they were washed with deionised water, with resistivity of 18MΩ cm, obtained from Milli-Q water purification system (Millipore Cooperation), before imaging to remove any debris from the leaf surfaces. *Vicia faba* (Field Bean) leaves were under 2 weeks old, the leaves were left on the stem while performing AFM imaging and SThM characterisation. SICM imaging of Field Bean leaves are desiccated samples.

2.6.3.2 Surfactant solutions

The surfactants/adjuvants used was Brij 98 and TEHP (Syngenta, Jealott's Hill, Berkshire, UK). Brij 98 is a non-ionic alcohol ethoxylated surfactant, TEHP is a phosphoric acid ester known for its effect as a plasticizer. Solution were prepared to concentrations of 0.2% w/w with deionised water, resistivity of 18MΩ·cm, obtained from a Milli-Q water purification system (Millipore Corporation). The solutions were heated to ~50 °C and stirred overnight, this was to allow the adjuvant to make a homogenous solution. Structures of the adjuvants are shown in figure 6.1.

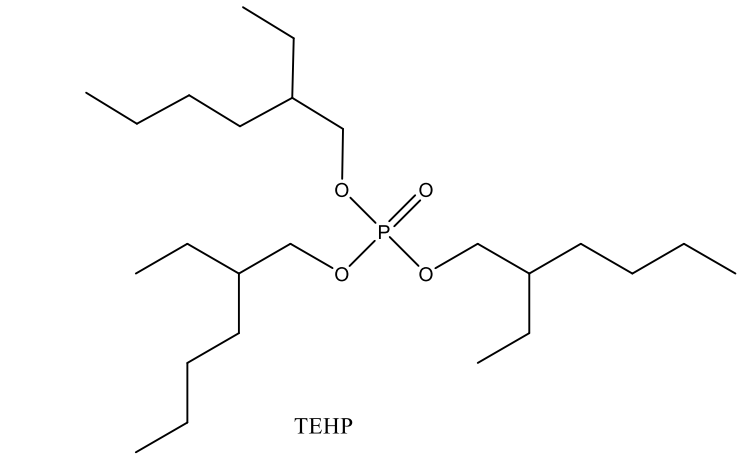

TEHP

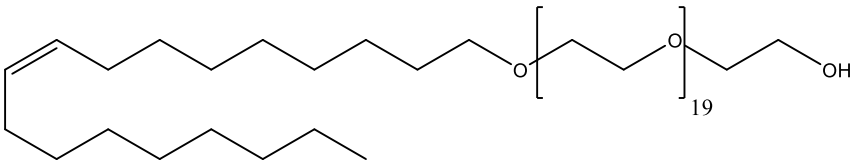

Brij 98

Figure 2.6 - Chemical structures of the adjuvant TEHP and surfactant Brij 98

Chapter 3

The investigation of SICM as a technique for characterizing leaf surfaces

3.1 Introduction

3.1.1 Imaging the Leaf Surface

Imaging of leaf surfaces has mostly been performed using conventional techniques; such has scanning electron microscopy (SEM) (Koch and Ensikat, 2008). SEM is used to image the topological and morphology of the leaf surfaces, showing a range of different surface variations and crystalline constructs relating the double structure of leaf surfaces.

SEM typically requires samples to be dry, coated in a thin conductive film and imaged in vacuum. This can induce artefacts and precludes studies on live leaves (Jeffree, 2006). Low-pressure or Environmental SEM (ESEM) can address this issue to some extent but this tends to compromise resolution and still fails to provide access to imaging live samples. Though advances in ESEM have allowed imaging at high spatial resolution of non-coated samples the primary electron beam still can cause damage to the waxes on leaf surfaces at high magnifications (Stabentheiner et al., 2010).

An alternative is to use scanning probe microscopes (SPM) such as the atomic force microscopy (AFM). AFM has been used to image isolated cuticles (Canet et al., 1996), which showed AFM is comparable to SEM but with higher spatial resolution. Furthermore tapping mode AFM (TM-AFM) was used to image the surface of *Prunus laurocerasus* (Perkins et al., 2005b) and the lotus leaf (Bhushan and Jung, 2006). For live leaf imaging there are only a few studies, most likely due to difficulties imaging surfaces that is mechanically connected to a large body. Notably, imaging of wax regeneration of the epicuticular waxes (EW) at the nanometre scale was achieved (Koch et al., 2004). Critically AFM of leaves has been carried out in ambient and liquid environments opening up the potential to view dynamic processes

on live samples. AFM though is unable to image most leaf surfaces due to their micro scale roughness and hence is limited to species with particularly flat cuticle surfaces.

A similar technique, called scanning thermal microscopy (SThM), utilises a tip that can be heated to record topographical and map surface thermal conductivity data, as well as acquire local thermal analysis. This technique has been used to measure the plasticizing effects of non-ionic surfactants on native leaf surfaces (Perkins et al., 2005a), to gain information on how chemicals affect certain areas of the cuticle, but this is the only study that uses SThM on leaf surfaces.

3.1.3 Potential of Scanning Ion Conductance Microscopy

Another SPM is the scanning ion conductance microscopy (SICM), a techniques which images surfaces in the presence of an electrolyte using a hollow nano-pipette (Korchev et al., 1997). SICM has to date been primarily used for imaging live cells at up to molecular resolution (Shevchuik et al., 2006, Liu et al., 2011). Unlike AFM, it is a true non-contact imaging technique (Del Linz et al., 2014), and hence has been shown to cause less damage to soft samples (Rheinlaender et al., 2011).

Hopping mode SICM has been shown to allow imaging of relatively large variations in the z-axis of sample surfaces (Novak et al., 2009), as well as sharp inclines of the surface (Shevchuk et al., 2011). Figure 3.1, by Shevchuk, shows the impact of continuous and hopping scanning modes on auditory hair cells, with the continuous mode distorting the sample with the pipette colliding into the structures. This is because of the feedback loop maintains a constant distance from the surface, result in sudden changes in topology not affecting the conductance through the pipette pore. The hopping mode, shows the image of

the auditory cells when the pipette approaches from above, preventing interaction with the sample, and improving the image and the Z range of SICM. This improved mode of imaging can be an advantage to leaf imaging.

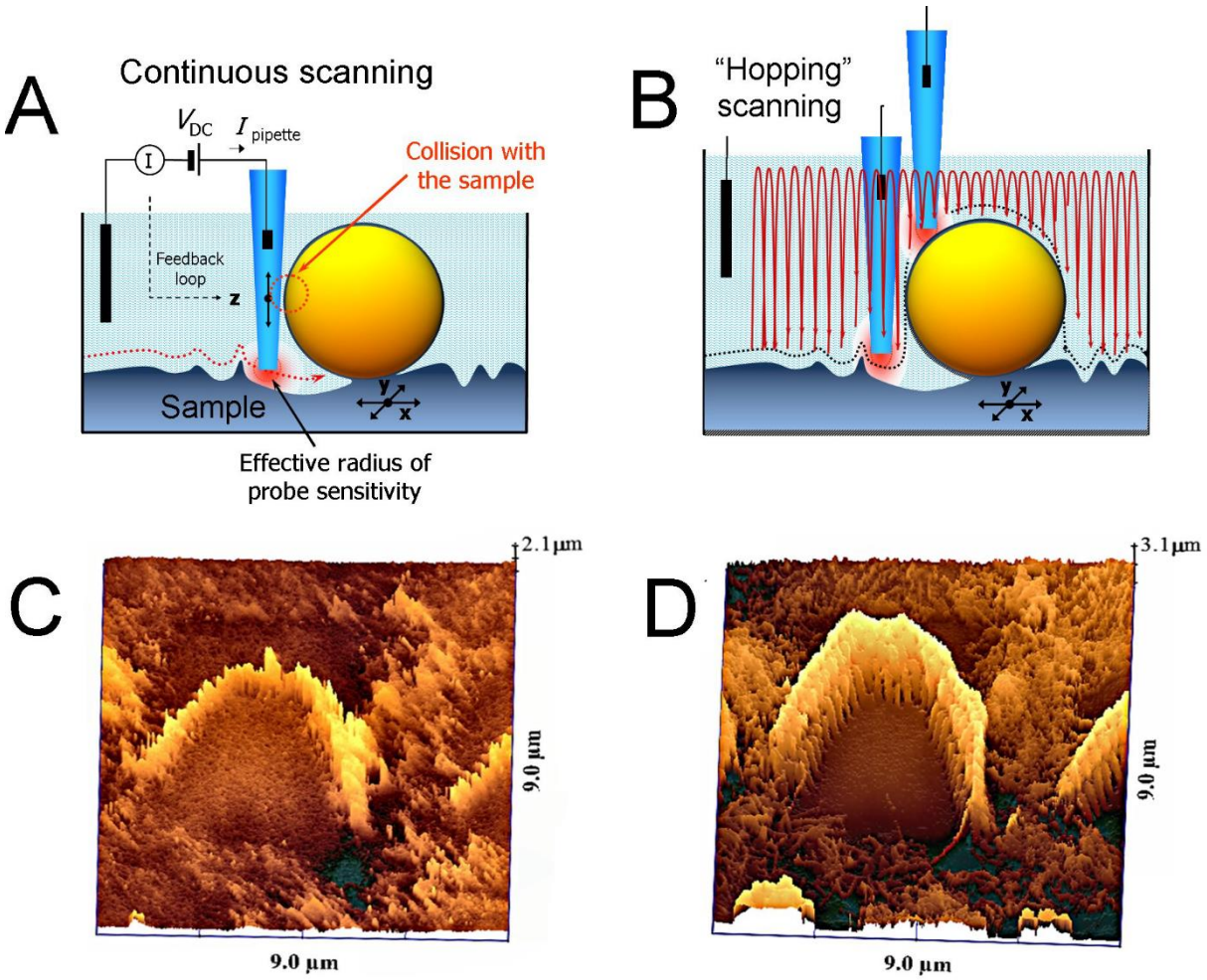

Figure 3.1 - Image showing the comparison of continuous and hopping scanning modes for SICM, with images of mechanosensitive stereocilia of auditory hair cells. (A &B) images showing the different modes and the how they acquire images. (C) shows the impact of continuous mode and the distortion of the surface structures. (D) shows the results of hopping mode and the unaffected surface and structures (Shevchuk et al., 2011).

SICM, as a technique, could be useful to imaging leaves surfaces under liquid and the ability to imaging large variations in height could provide a wealth of knowledge on biophysical processes and agrochemical effects. The noncontact ability combined with the

hopping mode will allow large and delicate structures to be images at the nanoscale, while maintaining relatively large areas of imaging.

3.1.2 Chapter description

This chapter looks into the use of SICM to image a verity of different leaf surfaces, to image the different EW wax structures and, by comparison, relatively large structure of the stomata. This is to allow a direct comparison between SICM with other imaging techniques like SEM and with more in-depth comparison with AFM. SICM was also used to image the strawberry leaf surface, this is because the AFM is unable to image the surface due to long hairs (trichromes) that protrude from the leaf, which prevent the cantilever, and there for the tip, from engaging the surface. Also, strawberry was used to ascertain if SICM can image more complex surfaces, imaging both the adaxial and the abaxial surfaces, both having different EW features.

3.3 Results

3.3.1 Imaging of abaxial and adaxial sides of *Hedera helix* (English Ivy) leaves surfaces with SEM, AFM and SICM.

English Ivy is an evergreen plant that grows commonly in Europe, America and Asia. It is a climbing plant using aerial rootlets which cling to objects that can stabilize the plant, and is considered an invasive plant in some countries. The English Ivy is an ideal surface to begin to compare the capabilities of the SICM, in imaging of leaf surfaces, with that of the SEM and AFM. This is because of its relatively smooth surface, which allowed the SICM and AFM to image. The surface of a *Hedera helix*, on the adaxial side (the surface of the leaf facing towards the axis of the plant) of the epicuticular wax shows no features, like rods or platelets, but the cuticle does show regular "undulating hillock" pattern which are located on the surface of the leaf, as seen in figure 3.2.

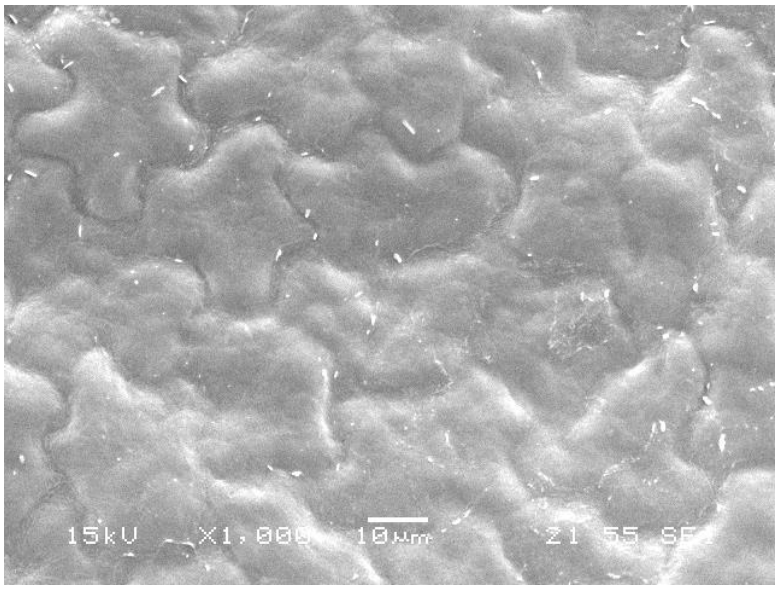

Figure 3.2 - SEM of the adaxial surface of the English Ivy

These patterns are the result of the epidermis cells and the cuticle showing the anticlinal walls of the cells. AFM was used to image the adaxial of the cuticle to image the topology and an area of individual "undulating hillocks", as shown in figure 3.3. The height AFM image shows the surface of the cuticle to be relatively smooth with the main globular structure. The length of the structure is ~ 21µm, from end to end, with a width of ~ 8µm. This is only one globular structure and as the SEM suggest the patterns vary in shape and size according to the epidermis cells.

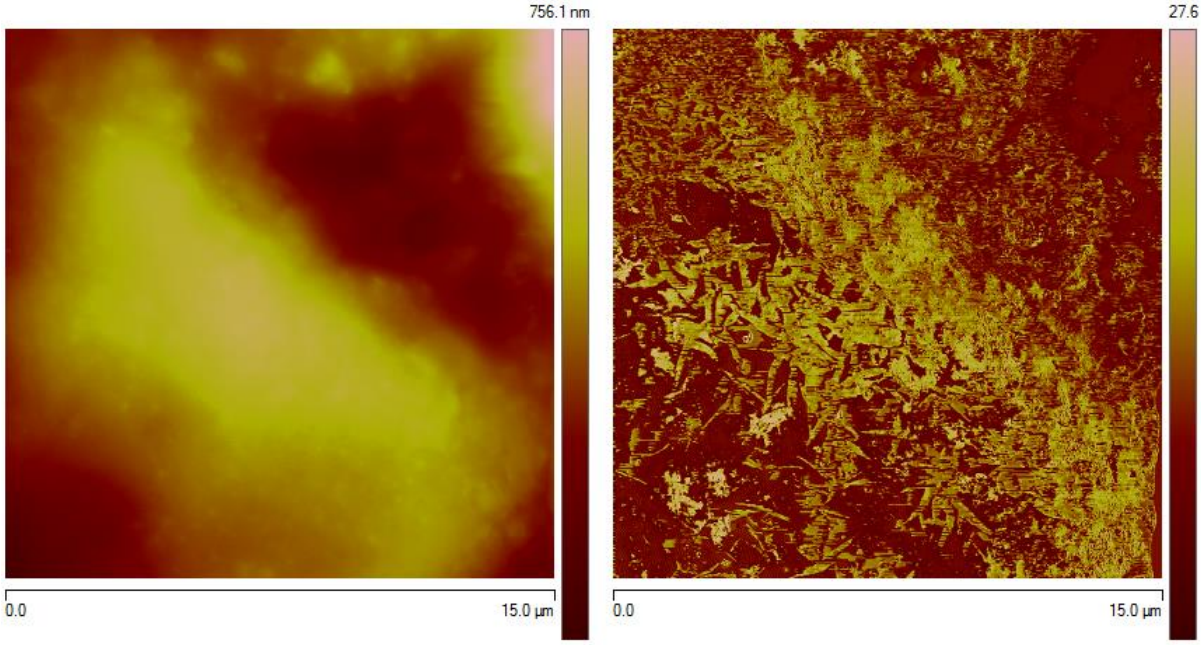

Figure 3.3 - AFM images of the surface of *Hedera helix* leaf. (Left) Height image. (Right) Phase image.

The phase image of the AFM image of figure 3.3 shows how the different region of wax are proposed to be related to crystalline and amorphous areas of the cuticle. The apex of the "hillock" appears to consist of different proportions of either needle-like crystalline or amorphous regions compared to that of the valley, the anticlinal walls. The AFM could not image larger scan sizes because it became difficult due to the excessive roughness and the limited z range of the AFM, denying the ability of larger areas to be imaged.

SICM was also used to image adaxial surface, the SICM was able to image a larger area than the AFM in a scan, to the maximum of 90x90 µm, shown in figure 3.4. SICM, as

with AFM and SEM, shows the surface of the leaf to be smooth with the “hillock” patterns clearly visible. The larger scan size is the result of the use of hopping mode, which allows large variations in topology to be imaged. Since the SICM was able to image a larger area the variety shape and sizes are shown, as the SEM suggests. Also the images can be used to generate a 3D image of the area, which allows the study of topology more in-depth, these are shown in figure 3.4.

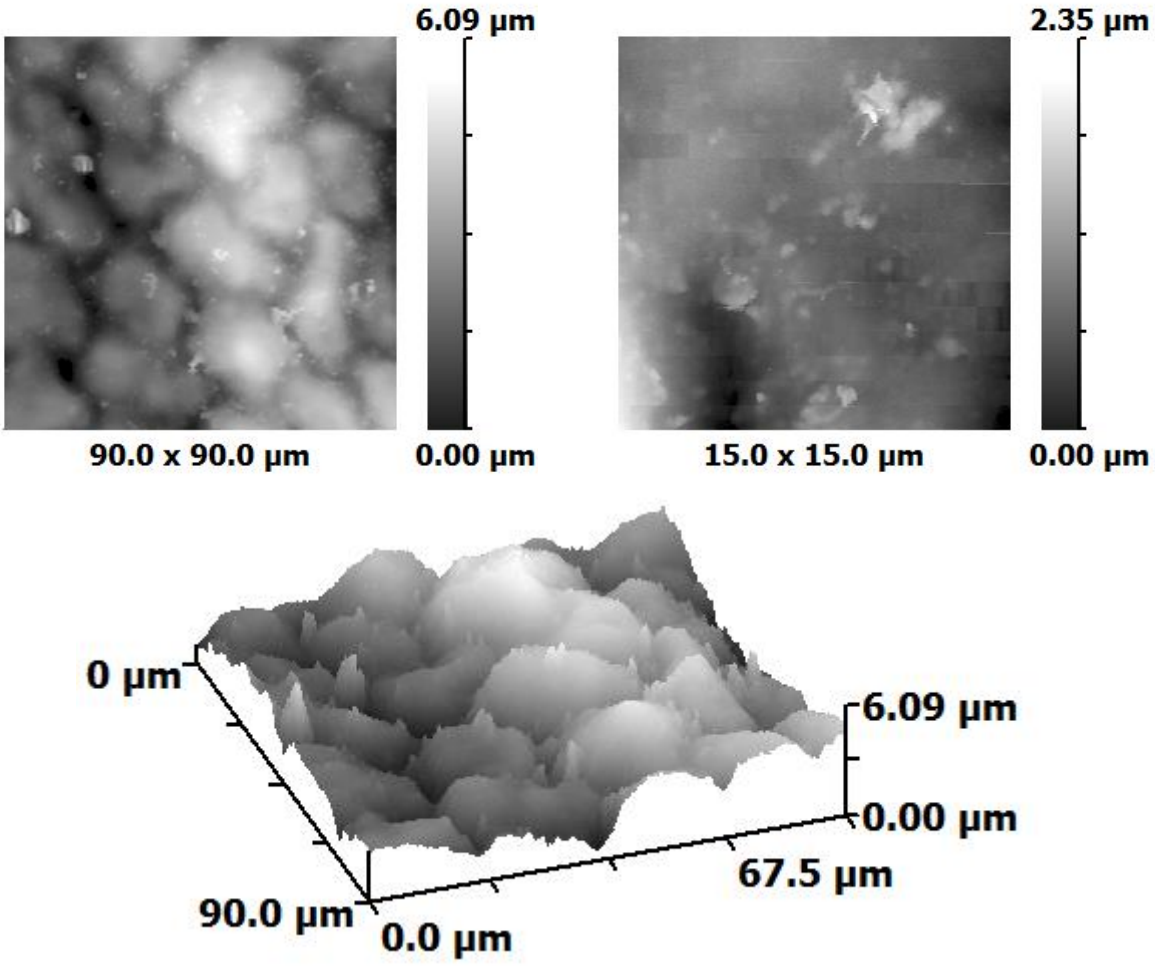

Figure 3.4 - SICM images of the surface of *Hedera helix*. (Top left) 90 x 90 µm 2D with height scale bar. (Top right) 15 x 15 µm with height scale bar. (Bottom) 3D representation of top left.

The SICM images show the "undulating hillocks" vary in height; also the trenches of the anticlinal walls vary in depth, which is most likely dependent on the underlying epidermis cells. The SICM is able to image at high resolutions with a scan size comparable to that of AFM. Both SICM images show contamination of the surface from debris from the environment. These help show the SICM is able to resolve smaller features and that these are not disturbed in data acquisition and the ability to resolve particulates on the leaf surface.

The abaxial side of the leaf shows the main density of stomata are located here, and are of some interest to plant biologists. The stomata are relatively large structures consisting of the two guard cells and surrounding wax cuticle, and they are required for gaseous

exchange between the plant and the environment (Kinoshita et al., 2001). Both the AFM and SICM were used to image this important plant structure to perform a more in-depth comparison between hopping mode of SICM and tapping mode of AFM.

AFM data show the guard cells, which are open, and the pore that the cells create. The guard cells appear to be similar in size and to have a relatively smooth surface. There is a wax chimney structure that surrounds the guard cells is shown to be an elliptical structure. Also the AFM imaged the valleys before and after the wax chimney (Barthlott et al., 1998), but couldn't image further from the stoma. This was due to the increase of vertical (z) height of the surrounding cuticle, and the limited z range of the AFM. The SICM was able to image the individual stoma, like the AFM, with the same features like the guard cells and the wax chimney being distinguished. SICM was able to image the surrounding area of the guard cells with more detail. Figure 3.5.

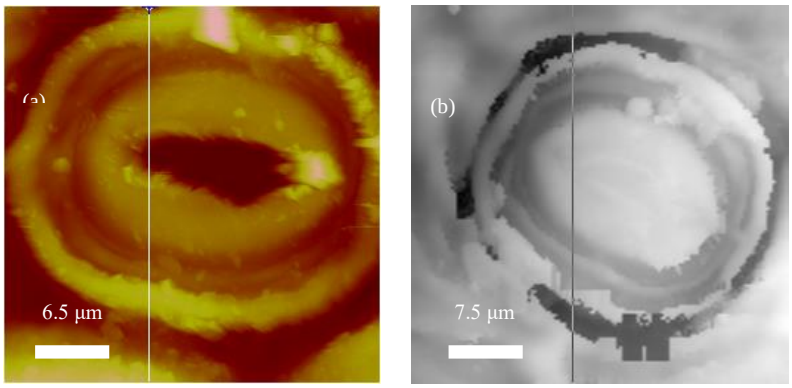

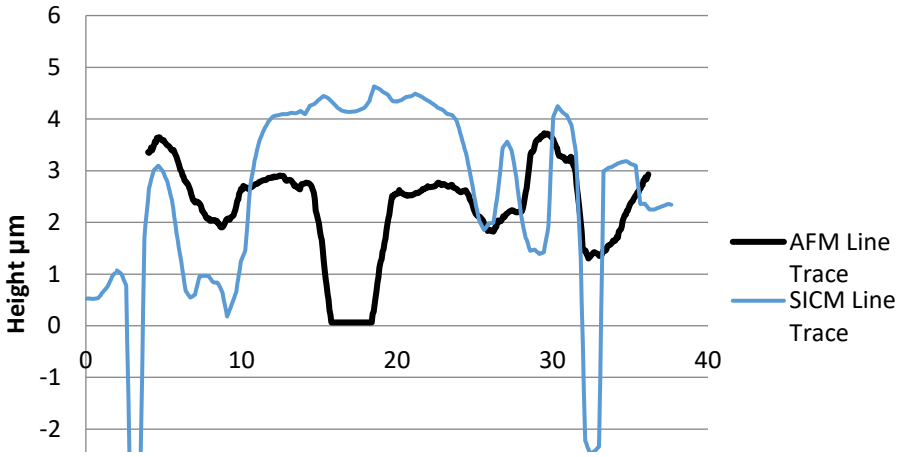

Figure 3.5 - Images of stomata from the adaxial surface of *Hedera helix*. (Top left) AFM image, line shows the path of the line trace. (Top Right) SICM image, line shows the path of the line trace. (Bottom) AFM and SICM line traces of the stomata, showing changes in topography.

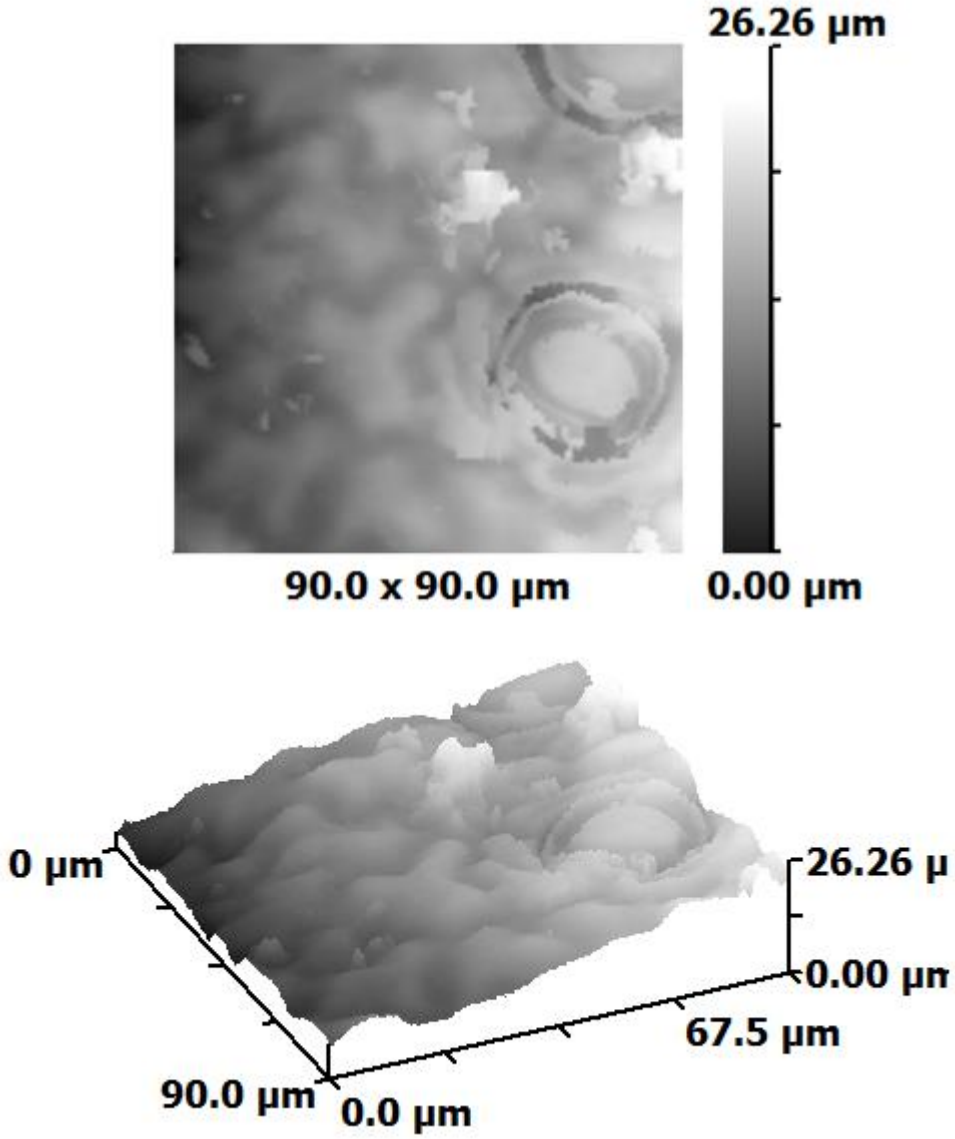

Figure 3.6 - 2D and 3D SICM images of the abaxial surface of the *Hedera helix* and the stomata located there.

The wax chimney is shown to be one continuous structure, as the AFM suggests, but the valley between the guard cells show a smaller inner chimney. The AFM was not able to image the inner chimney because the AFM tip was not able to penetrate into the valleys (Rheinlaender et al., 2011). A line trace of both the SICM and the AFM images show the differences between the AFM and SICM ability to penetrate into deep valleys on the cuticle surface. The deepest point of the AFM, from the line trace, is the pore of the stoma, from the

apex of the left guard cell to the bottom most point imaged, which is 2.5 μm. The deepest points from the SICM are the trenches beyond the wax chimney, with the deepest being 6.6 μm. This is because the SICM pipette tip approaches the surface from above but without interference from the pipette itself. The SICM images show the stomata to be closed, this might not be the case. This is because if the stoma is open then it is possible that a trapped pocket of air remains, with the SICM only imaging in liquid would measure the liquid gas interface as the surface, which would show as a closed stoma. This false positive is a disadvantage of the SICM being an only in liquid imaging technique. Though if the SICM is able to image the liquid gas interface then SICM can be used to image wetting of the leaf surface.

The SICM was also able to image the surrounding area of the stoma, shown in figure 3.6. This shows the similar “undulating hillock” pattern of the adaxial surface. The image shows the same stoma as the previous SICM image, showing some (but not all) of the detail that is shown at a lower scan size. The 3D representation of the topographical data shows the varying terrain the AFM could not image, the SICM shows clearly the incline of the surface. The surface still shows particles from the environment on the surface.

3.3.2 Imaging complex leaf structures, *Fragaria ananassa* (strawberry)

Another leaf species, and surface, imaged with SICM is the adaxial surface of Strawberry. Figure 3.7, shows a SEM image of the surface, which is populated with low density of "web" like structures, which are EW features related to the main group of filament structures (Mackerron, 1976). These features are AFM was not able to image the surface because of trichromes, hairs, located on the surface; the trichromes blocked the cantilever and prevented the tip from tapping the surface of the leaf. SICM is able to avoid these, and able to image the surface without hindrance.

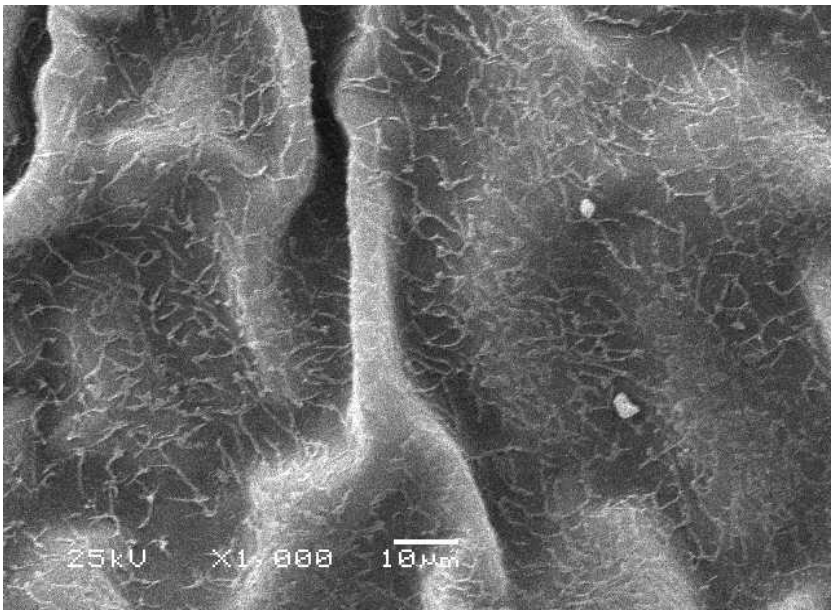

Figure 3.7 - SEM image of the adaxial surface of the *Fragaria ananassa*.

The SICM was also able to image these filament features but without a metal coating and in the electrolyte (figure 3.8). The images also provide additional information on height, with these features ranging from a height of 0.1 µm to 1 µm with a width of approximately 0.5 µm. The SICM also revealed that the surface comprises of even finer features between the main filament structures. These finer features are much thinner, with larger filaments being approximately 2 µm in length and have a higher density on the surface of the cuticle. Where

the finer features meet there appear to be “nodes” (figure 3.7) which vary in size, potentially composed of wax, and are connected to many thinner filament features. This illustrates the spatial resolution of SICM and its ability to image delicate structures without damage. These fine features were not seen by SEM, either due to a lack of resolution of the instrument used or more likely loss of structural details due to the sample preparation employed.

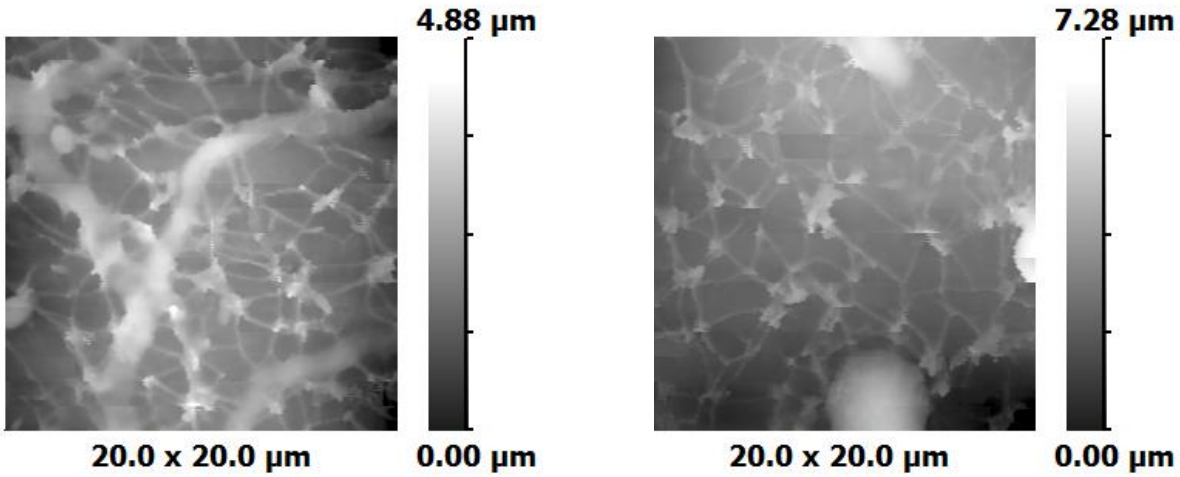

Figure 3.8 - High resolution images of the adaxial surface of the *Fragaria ananassa* leaves.

The abaxial surface of the strawberry plant was also imaged using SEM (figure 3.9). The surface appears to be more complex than the adaxial surface, the SEM used was unable to resolve these features to helpfully classify them into an EW group. Though a published paper shows the surface features to be rodlets (Kim et al., 2009). These rodlets are of high density in some areas of the surface, while some areas are clear from them.

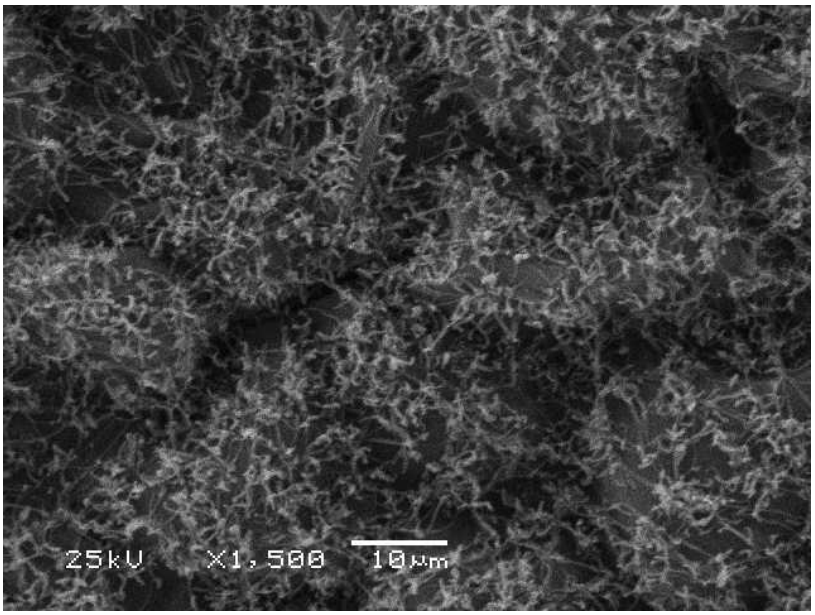

Figure 3.9 - SEM image of the abaxial surface of *Fragaria ananassa*

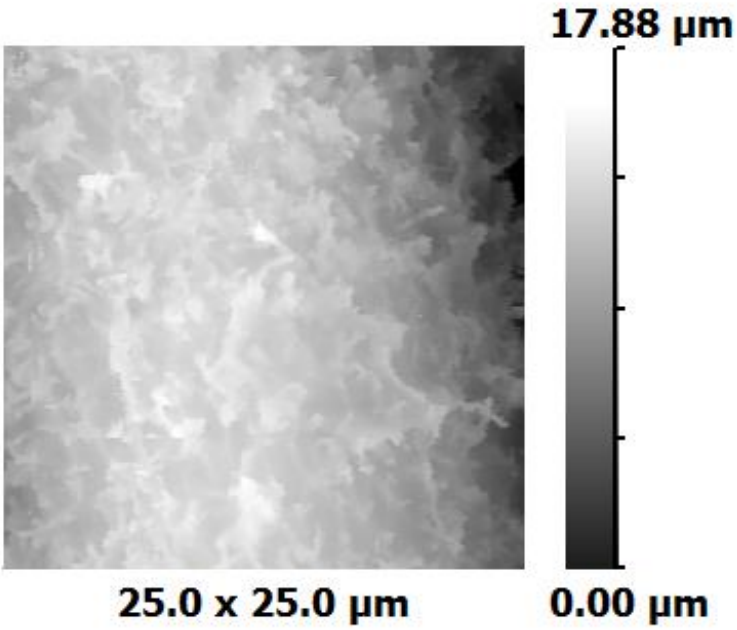

Figure 3.10 - SICM of the abaxial surface of *Fragaria ananassa*.

The SICM was able to image this surface and the rodlets features (figure 3.10). The features appear to have a higher density compared to that of the SEM, from my own images

and that of published work (Kim et al., 2009). The features vary in size, which is shown by SEM, and range from 0.5 μm to 2 μm. The SICM has imaged the features from above and also imaged some from the side (depending on their orientation), showing they have a rough top and the thickness to be approximately 0.4 μm.

3.4 Conclusions

In this chapter we have used three imaging techniques for surface characterisation of features of selected leaves. SEM, which has been widely used in studies more than the others, was used to gain knowledge of the surfaces of all the leaves studied. AFM was used to compare with SICM and to understand the differences between the two scanning probe microscopies (SPM). SICM was used to assess the abilities and possible research paths the technique could achieve. All three techniques were able to image the leaf surface and provide surface detail, while all showed their limitations.

The SEM showed the different features of the leaf surface from imaging of the filaments, platelets, rodlets and tubules. Its largest advantage compared to the other two techniques is its large field of view, making it easier to locate areas of interest before imaging at higher magnifications. Another advantage is the speed at which images are produced and the small amount of preparation required. Making capturing a large number of images rapid and the study of large number of sample surface possible. There are many studies that utilise the SEM to image the surface of leaves to high resolution, it is still limited to what can be imaged. For example, it is unable to image in droplets of water and study possible interactions. Also even with uncoated samples there is still damage being produced with ESEM and VP-SEM (Stabentheiner et al., 2010, Zheng et al., 2009, Talbot and White, 2013) making studying live leaves continuously difficult. The resolution of ESEM and VP-SEM has increased in recent years to the point where nanoscale features can be imaged (Kim et al., 2009, Koch et al., 2008, Bargel et al., 2006).

SEM can be used to image the effects chemicals have on live leaf surfaces, the investigation would have allowed the chemical to affect the leaf surface while the droplet

dries. This would allow change over time to be observed with the results being imaged. This would give us the end result but not the process of how it is achieved.

AFM, which is not often used to image plant EW and cuticles, can be used to image relatively flat surfaces (Canet et al., 1996, Bhushan and Jung, 2006). The imaging of EW features is achievable, with studies imaging different EW structures showing it is possible (Bargel et al., 2006, Burton and Bhushan, 2006) allowing higher resolution images of the features and the cuticle to be generated. Though AFM is mainly a contact method and would still damage soft and delicate surfaces, as seen on the strawberry leaf.

The advantages of AFM are the operating in ambient and liquid conditions and the lateral resolution is the best compared to the other two techniques. Since AFM is a contact technique the tip can be used to gain information of physical properties of the surface. The disadvantage comes to large variation or surface inclines, the cantilever/tip can interact with the surface and can over exaggerate the surface and disrupt results (Rheinlaender et al., 2011). This is seen when imaging the stomata chimney waxes of the English Ivy, though for flat surfaces the AFM could provide a wealth of knowledge of agrochemical interactions that could be complementary to SEM and SICM.

SICM imaging of the surface of leaf cuticles and EW has provided details that have not been seen with AFM or SEM. SICM has the advantage of being a non-contact technique, which aided with the imaging of the delicate strawberry leaves rodlets and filaments. Hopping mode of the SICM was also shown not to damage and or disrupt the wax structures, the vertical approach of the pipette avoids the steep variations of the surface structures.

In this study the SICM was able to image the surfaces of the leaves and resolve the features present. These included the large cellular constructs of the stomata and the waxes on the surface with filaments, rodlets, platelets, tubules and chimneys. Imaging of hydrophobic

surfaces was also possible, though if the electrolyte traps pockets of air between the surface and itself then the full surface cannot be imaged without the addition of surfactant to collapse such bubbles. This allows the SICM to image wetting, and the study of the interaction of droplets with hydrophobic surfaces.

The resolution of the SICM is not shown in this work to its full potential as relatively large diameter pipettes were used. The resolution of SCIM, both lateral and height, are dependent, mostly, with the inner radius of the pipette tip. The best lateral resolution reported to date is between 3 – 6 nm from a tip with r_i, inner radius of the tip, of 6.25 nm (Shevchuik et al., 2006). Computational/experimental (Del Linz et al., 2014, Rheinlaender and Schaffer, 2009) suggests that SICM resolution should be 2 to 3 r_i, but experimental work does show it to be smaller.

Chapter 4

Imaging leaf surfaces under liquid – Imaging wetting and drying formulations

4.1 Introduction

4.1.1 Wetting of plant surfaces

Leaf cuticle surfaces can have different wetting properties, from super hydrophobic to super hydrophilic. This behaviour is the result of the chemistry and structure of the cuticle surface (Koch and Barthlott, 2009, Barthlott et al., 2010). For example, hydrophobic properties of the leaf surface are governed by the roughness of the cuticle surface, with the roughness increased by the EW wax structures and the topology of the cuticle (Bargel et al., 2006). These properties are, further, enhanced by other surface structures like trichromes (Koch and Barthlott, 2009).

Studies of wetting of leaves have found certain properties that result in the different wetting regimes. These include the lotus effect (Marmur, 2004), salvinia effect (Barthlott et al., 2010) and the petal effect (Feng et al., 2008). The properties are the result of one or more forms of differing region of surface properties, for example, the petal effect is the result of areas of super hydrophobic and hydrophilic structures (Feng et al., 2008). These properties are of interest to replicate for biomimetic materials (Bargel et al., 2006).

The main technique used to study the interaction of droplets of water with the surface of plants is contact angle measurements (Neinhuis and Barthlott, 1997), along with variations of SEM and AFM to image the surface (Bargel et al., 2006, Nairn et al., 2011), so as to relate the roughness to the contact angle observed. This is because the contact angle is used to define the properties of the surface, shown in figure 4.1 (Koch et al., 2008). Wetting, and by association, hydrophobicity can be determined by the contact angle between the surface and a droplet of water (Koch et al., 2008). Several factors influence the contact angle, like free

energy, roughness, cleanliness and droplet size (Whitesides and Laibinis, 1990, Bhushan, 2005, Jung and Bhushan, 2007).

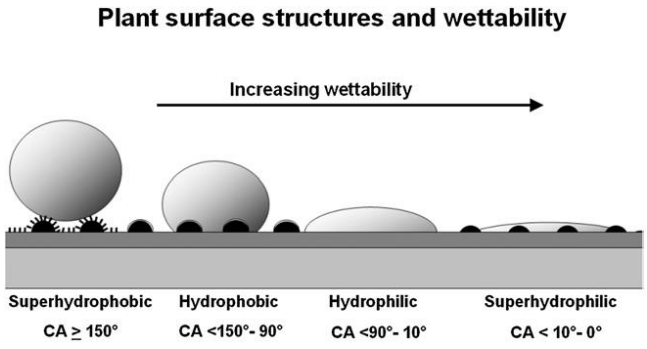

Figure 4.1 - Schematic showing the four classes of surface wettability, characterised by their static contact angle (Koch et al., 2008).

SEM and AFM have been used to image droplets of liquid on surfaces to image contact angles of droplet, of plant and synthetic surfaces (Delcheva et al., 2015, Koch et al., 2008). SICM could be used to image inside the droplet, allowing an investigation on how surfactants affect droplets on the surface at the nanoscale.

As well as imaging wetting, SICM can also be used to image the effects of formulations as they dry. This has mostly been studied with SEM, time of flight secondary ion mass spectrometry and AFM (Perkins et al., 2005a, Perkins et al., 2008). However, these approaches only image after the droplet has dried, not during. Since SICM has been shown to image in the droplet of PBS, it is possible that it can image inside a formulation, that is able to conduct between the two electrodes.

4.1.2 Young, Wenzel and Cassie-Baxter wetting

There are three regimes of wetting for a static droplet on smooth and rough surfaces, these are the Young, Wenzel and Cassie-Baxter droplets (Whyman et al., 2008). Young's wetting regime describes the contact angle of a droplet on the on a smoot surface (Degennes, 1985), with is . Wenzal's wetting regime describes a homogenous droplet on a rough surface but fully wetted, where water fills the gaps between structures (Marmur, 2003). Cassie-Baxter's wetting regime describes a heterogeneous droplet that rest on top of features not full wetting (Marmur, 2003). These wetting regimes are showed in figure 4.2.

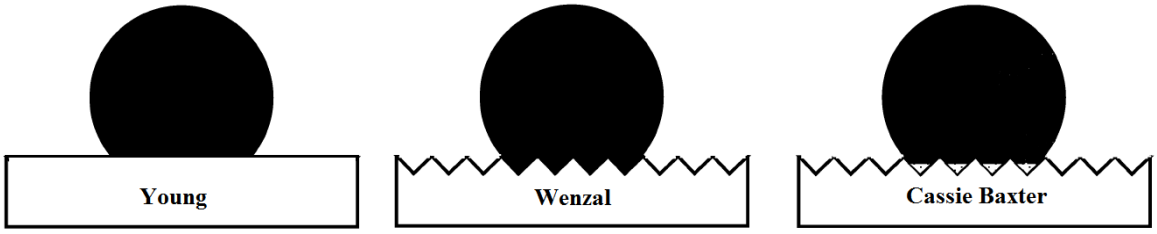

Figure 4.2 - Image showing the droplet and surfaces of the different wetting regimes of Young, Wenzel and Cassie-Baxter (Marmur, 2003).

The different regimes are governed by three equations (1,2 and 3). The equations associate the contact angle ($\theta_{\gamma,}$ $\theta_{w\ and}$ θ_{CB}) with surface tension, where γ_{lv}, γ_{sv} and γ_{sl} are the surface tension at the liquid/vapour, solid/vapour and solid/liquid interfaces (Whyman et al., 2008). The roughness of the Wenzal and Cassie-Baxter equations needs to be added, with r being roughness ratio, r_f being the roughness ratio of the wet area and f being the fraction of the projected area of the solid (Marmur, 2003).

$$\gamma_{lv} \cos\theta_{\gamma} = \gamma_{sv} - \gamma_{sl} \text{ (1)}$$

$$\cos\theta_{w} = r \cos\theta_{\gamma} \text{ (2)}$$

$$\cos\theta_{CB} = r_f f \cos\theta_{\gamma} + f - 1 \text{ (3)}$$

The transition from a Cassie-Baxter to a Wenzel regime of wetting has been imaged with reflection interference contrast microscopy, and it was found that the transition occurs from the centre of the droplet moving out wards (Moulinet and Bartolo, 2007). The technique does have disadvantages, including the need for transparent material to allow light to pass through, also the limited resolution.

4.1.3 Chapter description

SICM is an in liquid non-contact imaging technique, as shown in the previous chapter. In this chapter this SICM is used to image different hydrophobic surfaces, since SICM require a conductive liquid hydrophobic surfaces might be a more challenging surface to image. SICM could also be used to image the solid/liquid and liquid/vapour interfaces of a droplet on the leaf surface. SICM is used to investigate the ability to image these interfaces and look at the effects of surfactant on the droplet.

Since SICM can image inside a droplet then it is possible to image inside a conductive agrochemical formulation and image, over time, the impact of the formulation on the surface of the lead. This in conjunction with SEM, to image what occurs when a formulation dries.

4.3 Results

4.3.1 The use of SICM to image hydrophobic surfaces.

Leaf surfaces can be hydrophilic, hydrophobic, superhydrophilic and superhydrophobic (Bhushan and Jung, 2006, Koch and Barthlott, 2009), depending on the surface chemistry and structure. Successful SICM imaging of a surface depends upon complete wetting of that surface by the electrolyte, with previous images showing full wetting of the surface and no complications in imaging. Hence hydrophobic and super hydrophobic surfaces present a potential challenge, particularly if they are rough as this can promote micro-bubble formation (Feng et al., 2008). Whist a challenge to SICM imaging this also presents an opportunity to study wetting processes at surface *in situ* using the SICM to image liquid-air and liquid-solid interfaces as a solution wets a surface.

A grass leaf from the genus of *Festuca* possesses a hydrophobic surface, which is a surface that exhibits a droplet contact angle above 90° but below 150° (Koch et al., 2008). This property of hydrophobicity is the result of the chemistry and structure of the leaf surface. A SEM image of the adaxial surface of *Festuca* grass leaf shows the surface consists of a highly convoluted surface, showing the double structure of the cuticle (Figure 4.3). With rows of cells, providing the majority of topographical variations, and the added morphological structures of the epicuticular wax platelet structures (Holloway, 1969).

The SICM was able to image the surface of the leaf (Figure 4.4) which shows the platelet structures. These structures have similar shape but vary in size and orientation. Since the electrolyte solution penetrated between the platelet structures it can be conferred that water was able to wet the surface between the platelet features. This regime of wetting does

not prevent the SICM from imaging the surface, since the electrolyte solution can be in contact with the entire surface and still allow conductance between the two electrodes.

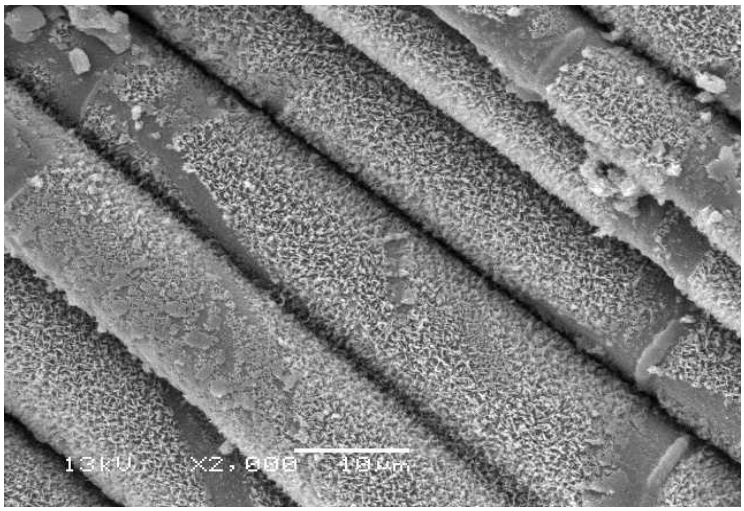

Figure 4.3 - SEM image of the abaxial surface of the *Festuca* grass leaf.

There are differences between large and small scan sizes, the large scan sizes show the topology that the cells create and the wide variation in height (figure 4.4). Also the wax platelet structures are not fully resolved but noticeable. At smaller scan sizes the platelet structures can be imaged with higher detail. The difference is because of the resolution of the imaging, increasing resolution would increase the time taken to acquire, and there is a restriction of high resolution or large scan size.

The higher resolution image (figure 4.4) shows the same differing orientations of the platelet features, like the SEM. Though the SEM doesn't provide quantitative topographical information beyond dimensions. Like the platelet structures these are shown to be of varying height but average around 1 μm, with an average length of 0.5 μm and a width of 50nm. Also in the 3D images, of both large and small scan size, the curvature of the underlying cells are imaged, giving a better understanding of the impact of the cells on topology and how it relates to the leaf's properties.

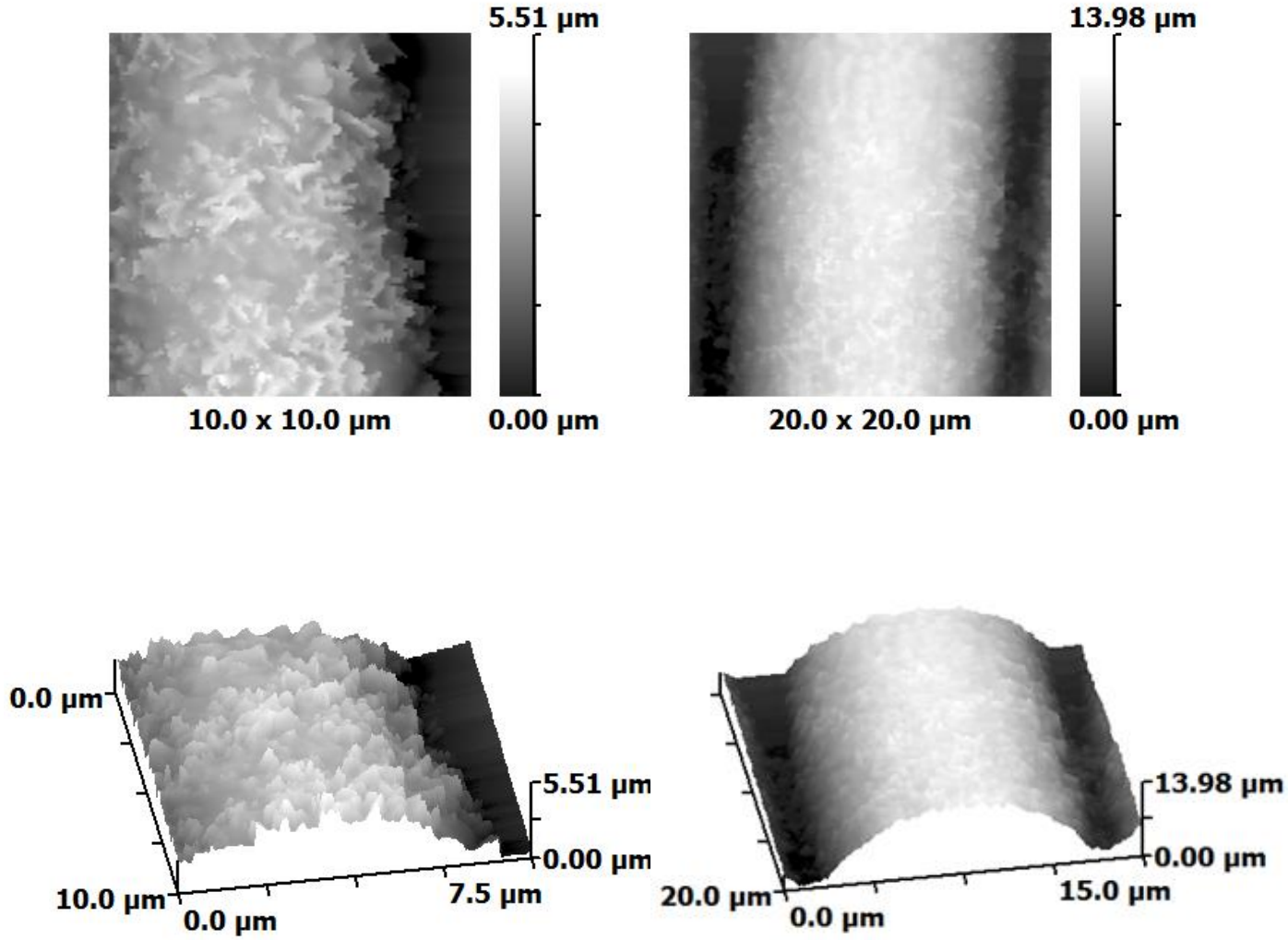

Figure 4.4 - SICM images of *Festuca* grass leaf. (Top) 2D images showing the difference between scan sizes. (Bottom) 3D representation of the 2D images, showing the detail of morphology and the effect of the underlying cell on topology.

The leaves of *Brassica napus* and *Pisum sativum* also possess hydrophobic surfaces (Gniwotta et al., 2005). These leaf surfaces only have a small fraction of the droplet in contact with the surface due to trapped air pockets (Marmur, 2004). *Brassica napus* and *Pisum sativum* have differing structures (Figure 4.5 Top left and right). *Brassica napus*

surface is highly convoluted with the EW composed of tubules crystal features with amorphous wax between the features, *Pisum sativum* consists of a high density of crystal platelet feature, like *Festuca*, although the surface is not as convoluted.

The droplet, of electrolyte solution, is hence not in contact with the entire surface of the leaves. This is evidenced by considering the SICM data in (Figure 4.5 Middle left and right). The images show that the SICM probe is not imaging the leaf surface and we propose is detecting the liquid/gas interface of micro air pockets trapped at the surface. For *Brassica napus* (Figure 4.5 Middle left) this interface was smooth showing no protruding leaf structures. For the *Pisum sativum* (Figure 4.5 Bottom left), the SICM image shows some disruption of the interface, indicating that the apex of the platelet crystals are submerged in the electrolyte. This is consistent with a Cassie-Baxter wetting regime (Figure 4.2) (Marmur, 2003).

To lower the surface tension of the electrolyte and promote complete wetting of the leaves a surfactant (Tween 20) was used (Lee et al., 2008). Tween 20 was used because it is a mild surfactant and would not disrupt the leaf surface. After adding the surfactant, the electrolyte solution was in contact with the entire surface, which allowed the surfaces to be imaged. SICM images of *Brassica napus* (Figure 3.12 d) depict tubules of the EW to be of varying size and shape, also the SICM has imaged into some of the tubule holes. Compared to the SEM image (Figure 3.12 a) the SICM is able to image the tubule structures clearly showing the variations between size and shape of the crystals. For *Pisum sativum* the SICM (Figure 3.12 e) clearly shows a large number of crystal platelet structures in a valley of the cuticle. Some of the platelets are imaged from above and some are imaged from their side. The SICM shows the platelet structures clearly, which is comparable to SEM, the additional height information provided for the platelet structures show that the average height is approximately 1 µm.

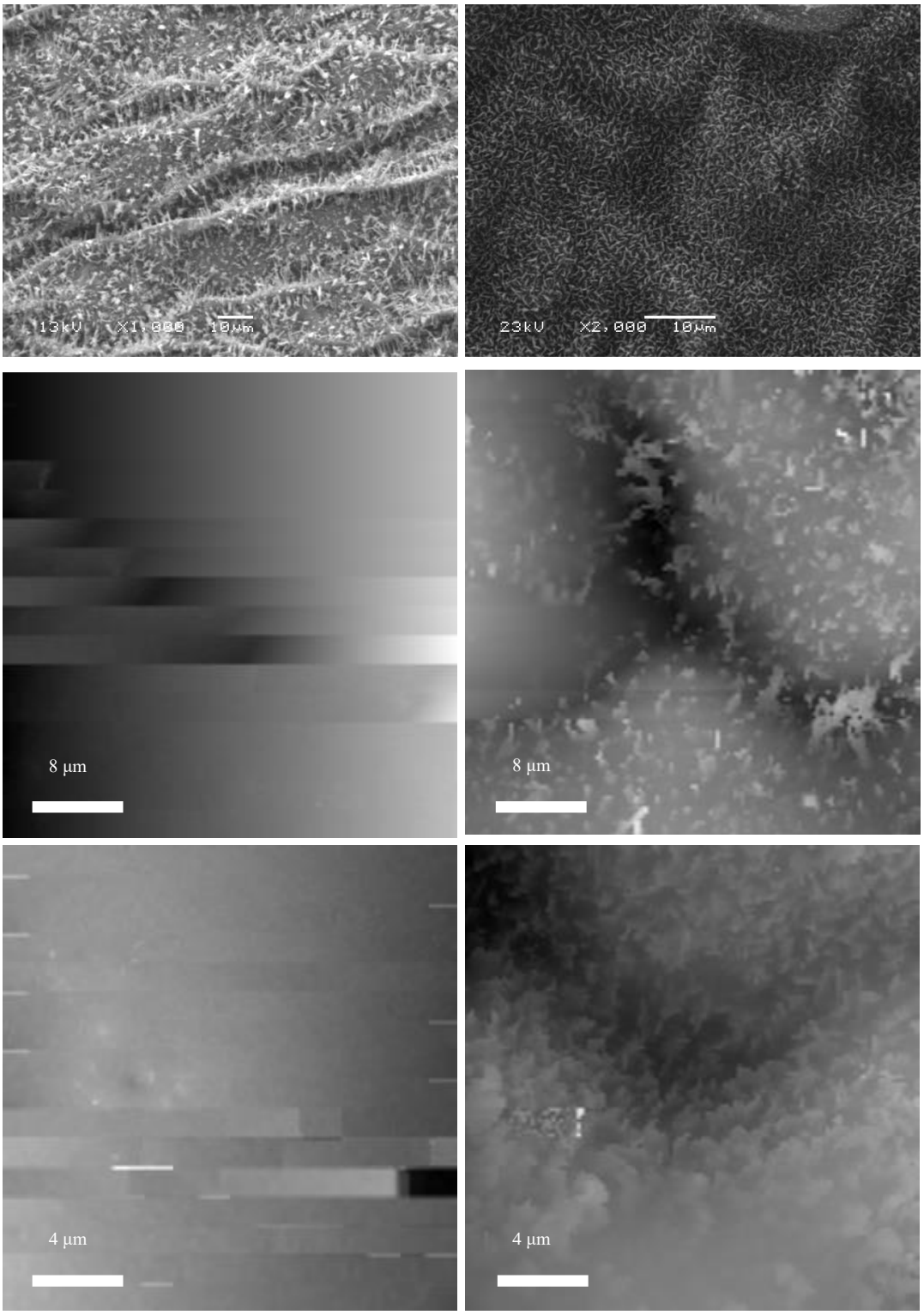

Figure 4.5 - Images of the abaxial surfaces of *Brassica napus* and *Pisum sativum* (Top left) SEM of the surface of *Brassica napus* (Top right) SEM of the *Pisum sativum* (Middle left) SICM image of the liquid/gas interface of the droplet on *Brassica napus* (Middle Right) SICM image of *Brassica napus* after surfactant was added to the droplet (Bottom left) SICM image of liquid/gas interface of the droplet on *Pisum sativum* (Bottom Right) SICM image *Pisum sativum* after surfactant was added to the droplet.

4.3.2 Imaging wetting from inside the droplet

It is possible to image the leaf surface at the liquid/vapour and solid/liquid interface of a droplet, which was resting on a hydrophobic leaf surface. The use of relatively high concentrations of Tween allowed the SICM to image the hydrophobic surfaces of Pea and Oil Seed Rape. This study was to look into the possibility of imaging wetting with the SICM and describe the transition from a non-wet state (Cassie-Baxter) to a full wet state (Wenzal). The pea leaf was chosen because the SICM can resolve the features, the platelets structure, and also the ease with which the leaf can be handled.

Imaging of the interface of the liquid on the hydrophobic surfaces with the SICM allowed the study of the effect of small concentrations of Tween on the wetting regime. Figure 4.6 shows the surface and the interface of the droplet on the surface of Pea leaf, before adding 1 % w/w tween 20. The liquid/vapour interface can be seen in the majority of the image, with the surface features just beginning to penetrate in the top left hand corner. This shows that wetting is not uniform. The penetration of the platelet structures is not fully complete; this can be seen by comparison with figure 4.6 and 4.7.

Figure 4.8 shows the surface after adding the Tween 20 solution to the droplet, the image was recorded 2 minutes after tween was added. This suggests that the concentration used for these images is too high to be able to image the effect of the surfactant on the liquid/vapour and solid/liquid interface. The SICM image shows a large density of platelets, previously shown in with the images of *Festuca* grass.

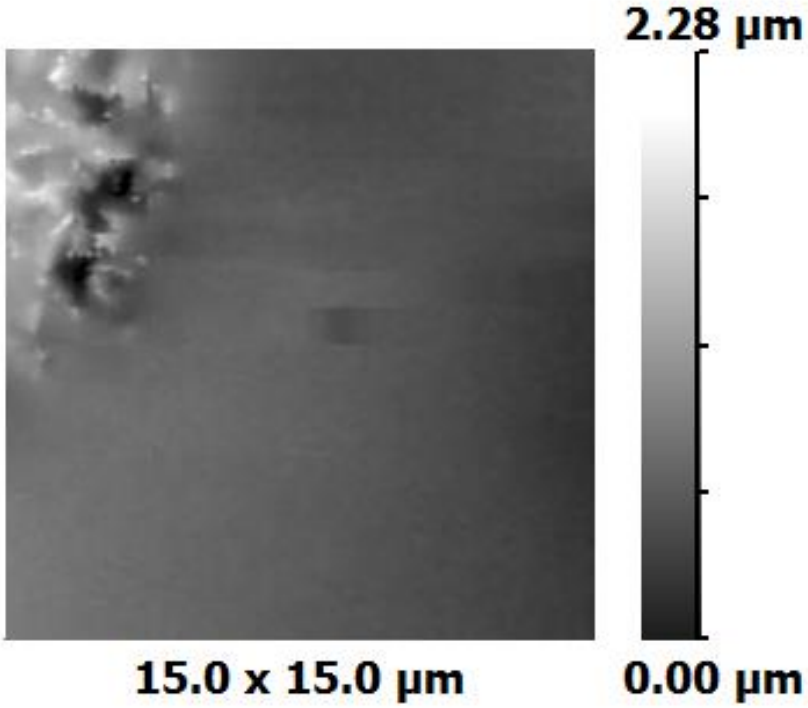

Figure 4.6 - SICM image showing the gas/liquid interface of a droplet on a Pea leaf. With partial penetration of platelet features

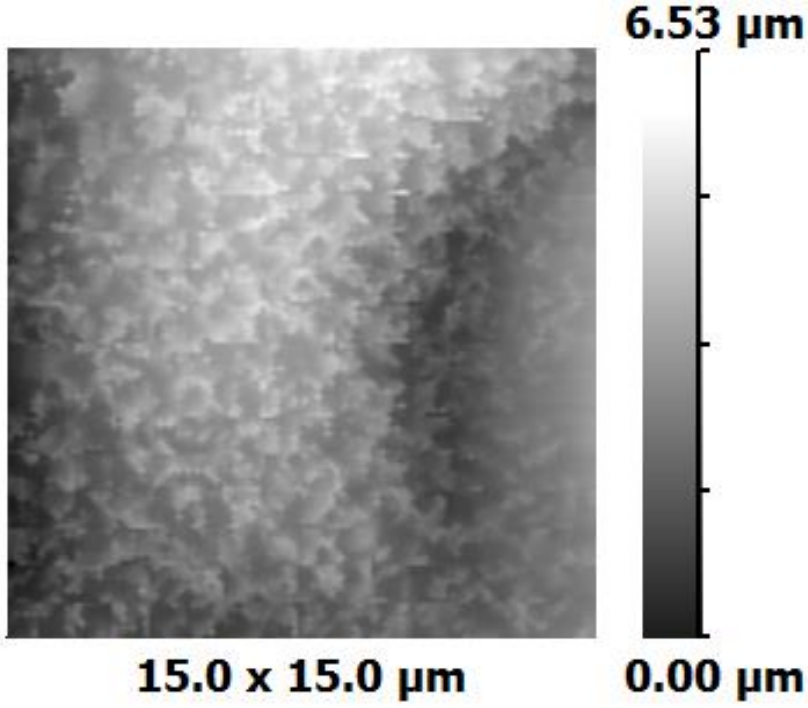

Figure 4.7 - SICM image of the Pea leaf surface, showing the platelets features after tween was added.

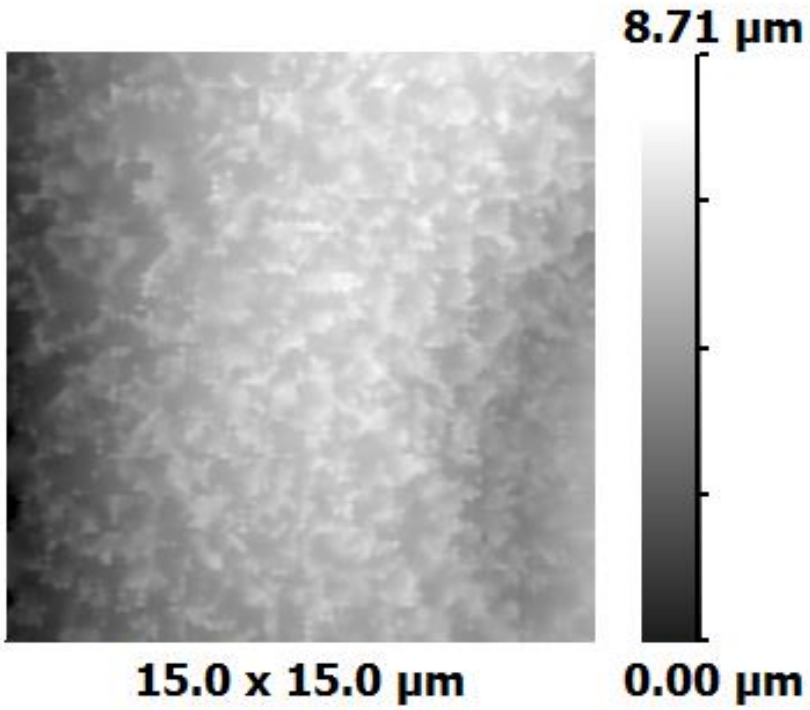

Figure 4.8 - SICM image showing the pea leaf surface after additional tween was added.

After the imaging process was complete some more Tween was added to compare the two SICM images to see if the surface was completely wetted by the droplet, this is shown in figure 4.8. The surface of the cuticle can be seen, with a large density of platelet as in figure 4.7. This shows that the concentration of Tween used is too high to study the effects of the surfactant.

The concentration of the Tween solution was reduced to 0.5 % w/w and the experiment repeated. Imaging of the interface of the liquid on the hydrophobic surfaces with the SICM allowed the study of how small concentrations of Tween affect the wetting regime.

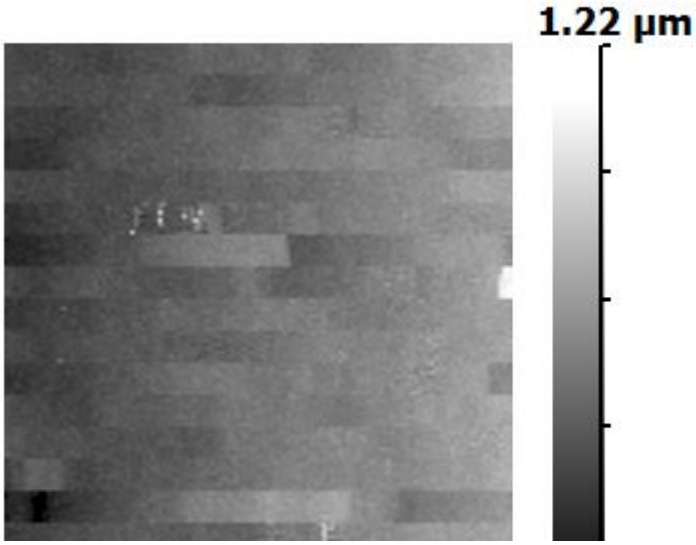

Figure 4.9 - SICM images of Pea leaf and the liquid/gas interface before adding a small concentration of Tween 20.

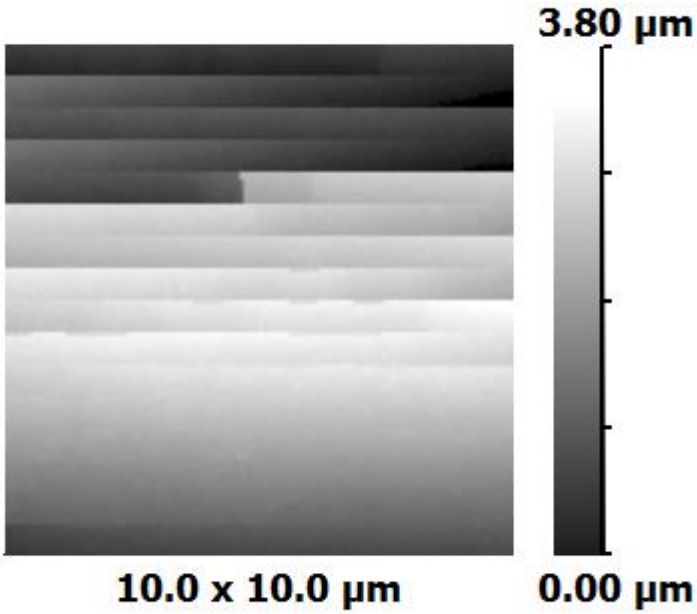

Figure 4.10 – SICM mage after 5 minutes of adding the surfactant, the image shows the interface remains intact, though there is a collapse.

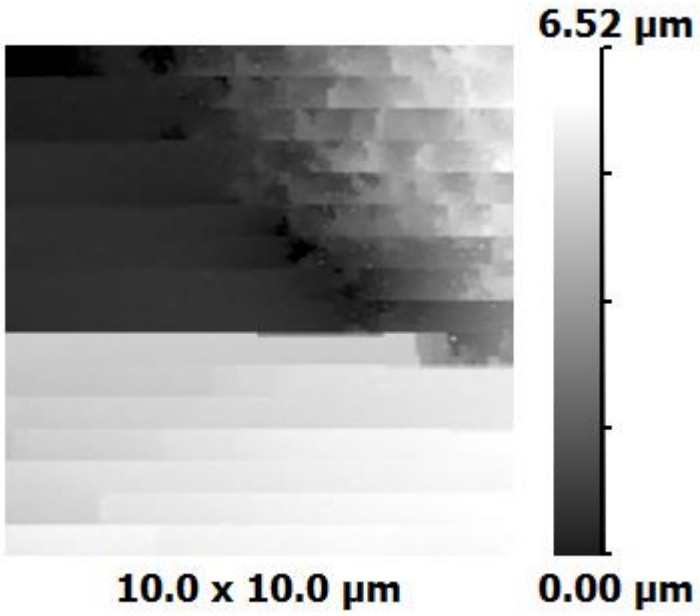

Figure 4.9 - Image after 30 minutes of adding the surfactant, the image shows another collapse, this resulted in the leaf surface being exposed to be recorded.

Figure 4.9 shows the liquid/vapour interface of the Pea leaf surface. After adding the Tween solution, the interface still remained after 5 minutes (Figure 4.5), though there is a collapse in the interface while imaging. The collapse of the interface is shown as a change in height of in the interface, resulting in the sloped being imaged, this is seen in figures 4.10 and 4.11. With the interface getting closer the to the plant surface after each line of imaging. This collapse is seen again after 30 minutes of adding the surfactant, but this collapse resulted in the surface of the leaf being imaged.

Clearly the introduced surfactant to the electrolyte solution has caused a reduction in surface tension and a collapse of the trapped microbubbles (Ying et al., 2005). This set of images, figure 4.9 – 4.11, show the droplet, at this location, is not in contact with the surface below. This shows the droplet is static and stable at the beginning of the experiment, without all parts of the droplet base in contact with the platelets. Even when the surfactant is added

the interface is not in contact with the surface. This suggests air pockets are not just trapped between the surface features but also between the overall curvature of the cuticle.

4.3.3 *In situ* imaging of a formulation drying

The study of imaging the drying of formulations onto a leaf surface could provide insight into how the formulation affect the plant surface. The SICM was used to study the effects of a commercially available weed killer, Resolva. SICM is potentially able to perform *in-situ* imaging while the droplet evaporates, to investigate the effect of the solution of the weed killer on the surface. First SEM was used to image the effect of the weed killer on the surface of dissected leaves of English Ivy. English Ivy was used because of its relatively flat featureless surface and ease of imaging with SICM.

The SEM images in figure 4.7 show the effect of the Resolva on the surface of the leaf. After one day of exposure the cuticle of the leaf shows large fractures in the wax, this is likely caused by the surfactants in the Resolva solution. Surfactants are used to increase uptake of herbicides and/or pesticides and are added to most formulations (Riederer and Friedmann, 2006a). Also the regular globular structure of the cuticle seems to be altered, but this is only on the outer rim of the exposed area. This is the result of the drying process, as the droplet of Resolva dries the chemicals in the solution goes toward the outer edges of the drop, increasing the concentration of the chemicals on the surface.

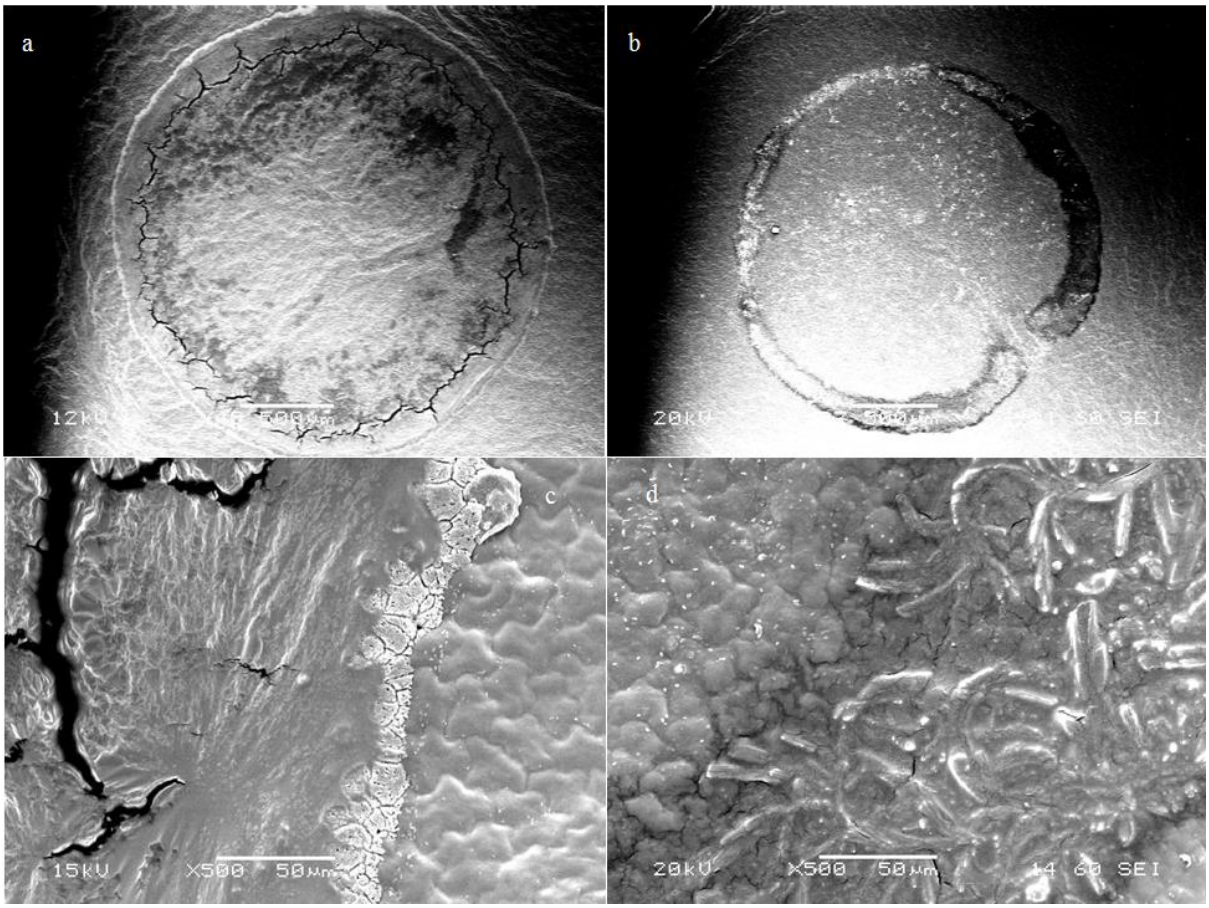

Figure 4.10 - SEM images of the area exposure to Resolva weed killers. (a) Area of exposure after one day. (b) Area of exposure after 5 days. (c) Close up image of one of the cracks from image a. (d) Close up image of disrupted area from image b.

After five days the Resolva solution causes an increasing amount of damage/disruption of the cuticle. Also present on the surface is, what seems to be, a crystalline structure, in image d from figure 4.12. The disruption of the “undulating hillock” pattern at the edge of the deposit would be the result of the formulation.

Figure 4.13 shows an area of the cuticle that was treated with Resolva where the “undulating hillock” structures of the surface still remain. This area still shows the cuticle fractures are present even from the outer edges of the deposition area. Also the image shows either small spots of disrupted waxes or residual film from the weed killer.

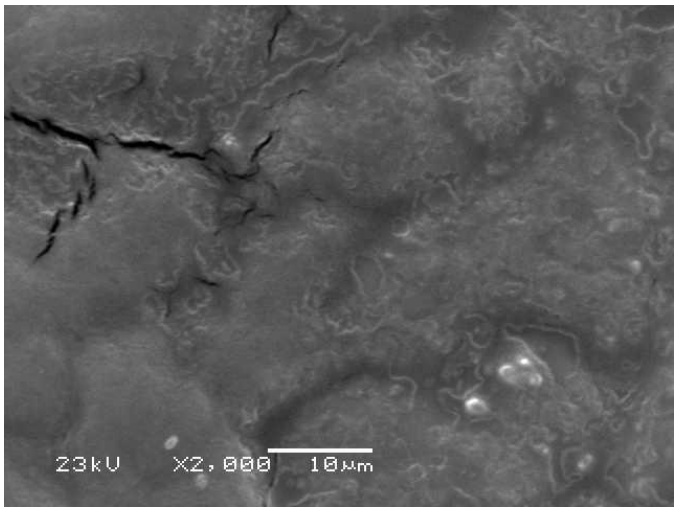

Figure 4.11 - Close up SEM image of an exposed area after 1 day, image is in the centre of the exposed area.

The SICM was used to image the same area as a droplet of Resolva was drying to image *in-situ* the effect of the weed killer on the structure of the cuticle. Figure 4.14 shows the result of repeated SICM images of the same area after being treated with Resolva and during drying, the droplet dried after 272 minutes. The images show that as the droplet dries the "undulating hillock" structure of the surface do not appear to change; this shows that the solution has no measurable effect when drying. This means the disruption in the cuticle occurs when the deposit has fully dried. This might be because a critical concentration of surfactant needs to be present before any measurable effect can be imaged, as surfactant would need to penetrate into the leaf's cuticle to have an effect and this is a diffusion dependent process (Santier and Chamel, 1996).

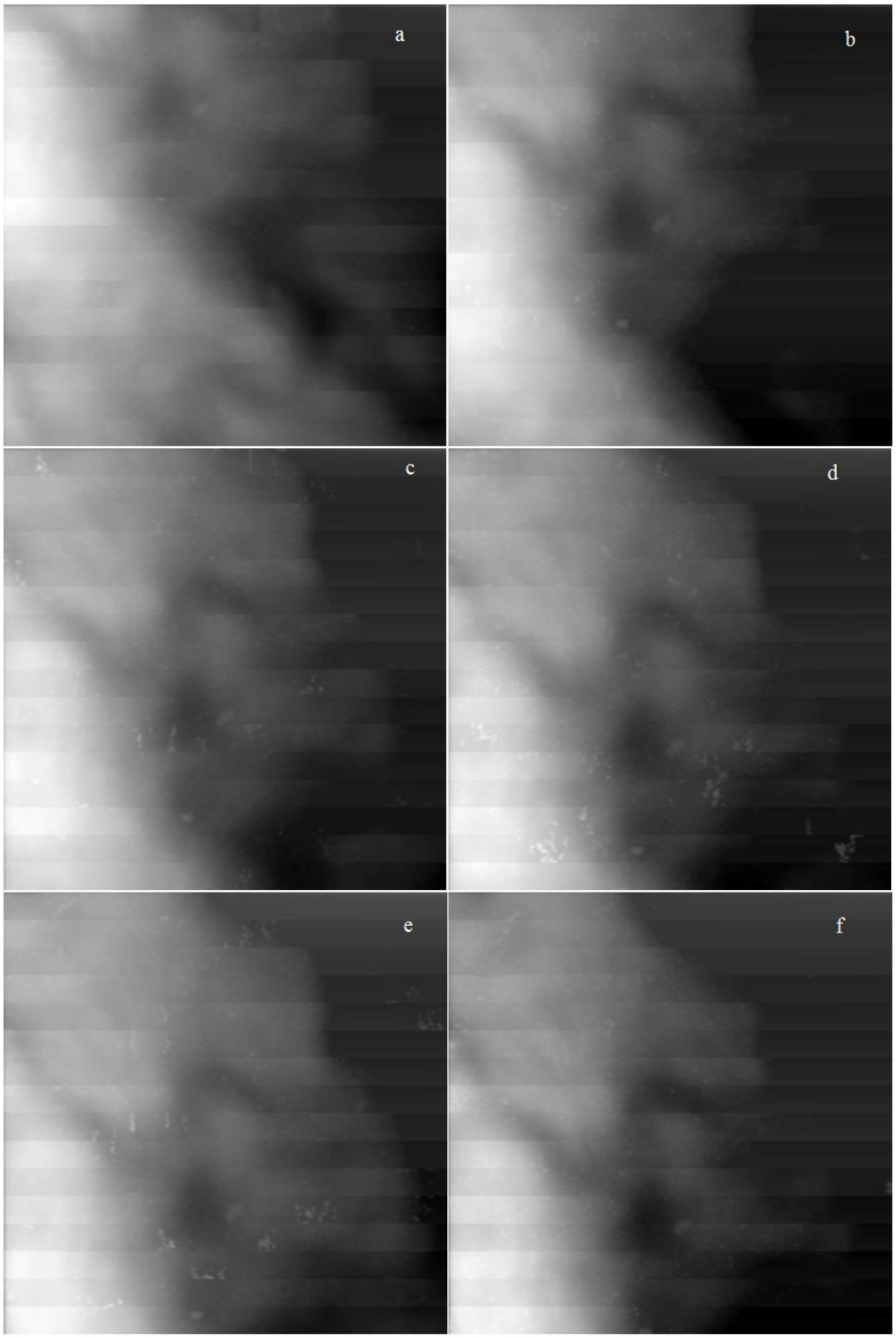

Figure 4.12 - Repeated SICM images of an area that was treated with Resolva, all images are 40 x 40 μm (a) 65 min after exposure. (b) 120 min after exposure. (c) 152 min after exposure. (d) 182 min after exposure. (e) 209 min after exposure. (f) 240 min after exposure.

After 24 hours the same area was imaged again, using PBS as the electrolyte solution, the SICM image is shown in figure 4.15. This was performed because SICM requires a minimum amount of liquid to image, as the droplet of dried it became increasingly challenging to image the leaf surface. This is shown in figure 4.14, has the imaging progresses there is an increase in observable artifacts on the images. The area shows the same fine residual structure that SEM was able to image in figure 4.13, these weren't imaged in figure 4.14 because the chemicals that cause this disruption hadn't reached a critical concentration, this occurs at the very end of the drying process.

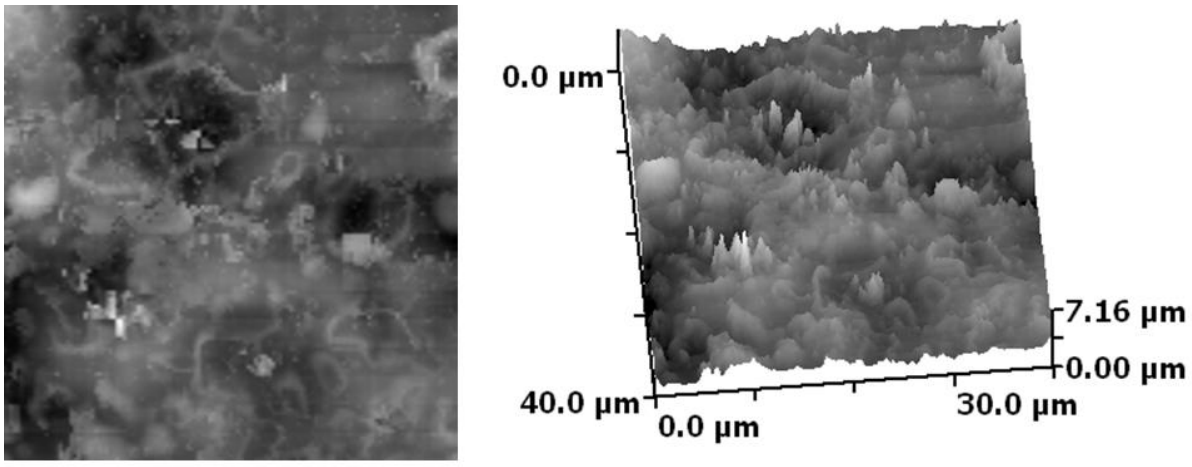

Figure 4.13 - SICM image of the same area of continues scans. (Left) 2D SICM image. (Right) 3D SICM image

4.4 Conclusion

In this chapter we have applied the use of SICM to image hydrophobic leaf surfaces and two potential processes of interest, that being wetting and to image a formulation as it dries. The SICM is a non-contact in liquid imaging technique (Del Linz et al., 2014) that has been shown to image inside of bulk solution (Korchev et al., 1997, Novak et al., 2009) and a droplet, as shown in this chapter. The SICM is mainly used to image the surface of cells and events that occur at the surface (Shevchuk et al., 2013) which has allowed the study of certain surface processors. For plant imaging, SICM has been shown it is able to image the surface features of leaves and the gas/liquid interface of the droplet of PBS. This is the result of improved imaging modes, like hopping mode, that has increased the speed of acquisition of images (Novak et al., 2009, Liu et al., 2011). In this chapter we have shown that it can be used to image the process of wetting. Using SICM to image hydrophobic surfaces inside of a droplet was successful, with the wetting of the droplet being the main factor in allowing imaging of the full surface. If the droplet wets fully then imaging is unobstructed, if the static droplet forms a Cassie-Baxter wetting regime then SICM is unable to image the full surface, though this allowed imaging of wetting to be investigated.

The use of surfactants to wet a surface has allowed imaging of the transition between different wetting states and has imaged the collapse of a micro bubble The disadvantage of SICM is the speed at which it images, in the images of the transition it takes ~30 min to perform a full image, increasing the speed would compromise the resolution or scan size.

The wetting experiments have shown the trapped pockets of air is not just confined to between the features of the Pea leaf surface, which is generally reported in the literature (Koch and Barthlott, 2009), which suggests the droplet would be in continuous contact with the features of the leaf. A situation when there is not continuous contact is seen with super

hydrophobic surfaces involved with the lotus effect (Koch et al., 2008). For hydrophobic surfaces, the literature reports the trapped pockets of air are between the surface features and the droplet (Moulinet and Bartolo, 2007). This could be the result of the simple surfaces used during their experiment and the lack of other variations in surface topology than surface features. Also, SICM images the penetration of platelet features of the leaf surface through the air-liquid interface of the microbubble at the beginning of wetting before any surfactants are added. This shows SICM could be a useful technique for developing materials that possess certain wetting abilities, like the petal effect or the lotus effect which require minimum contact to aid in frictionless contact for example (Koch and Barthlott, 2009).

The surfactants impact on wetting is a well-studied topic. Surfactants reduce surface tension, this is achieved by the adsorption of the surfactant compounds to the solid/liquid and water/vapour interface (Lee et al., 2008). The analysis of the impact of surfactants on wetting is generally done with contact angle measurements (Zhang and Basaran, 1997, Farris et al., 2011). The SICM has shown that surfactants do not gradually remove trapped pockets of air slowly over time but in relatively sudden changes that results in full surface wetting. This is shown in the SICM image has sudden changes in height of the liquid/vapour interface.

Resolva was used to test the abilities of the SICM in imaging a drying deposit of a formulation. The SEM analysis has shown the effect that Resolva has on the surface of English Ivy leaves. The formulation disrupts the cuticle with edge of the deposit being the area with most change. This is related to the so-called “coffee ring” effect, which is caused when evaporation drives a radially outwards flow within the droplet, so the formulation components concentration builds up on the deposits edge when drying (Erbil, 2012). Though, it should be noted that some material is also deposited near the center of the deposit area.

The imaging of drying with SICM showed that the SICM could image over the same area for a prolonged period of time with minor drift seen. Due to the different compounds in the electrolyte solution the SICM can cause artifacts to appear on to the images, as can be seen in figure 4.9 c, d and e. These artifacts are caused by sudden changes in the voltage measured between the two electrodes and might be the result of ion current rectifications due to a nonlinear current voltage response (Edwards et al., 2009).

The deposit, as it dried, did not show any signs of disruption to the surface of the cuticle, this suggests the effect Resolva has on the surface is caused towards the last moments of evaporation of the droplet or the first moments after the droplet as dried. Though the SICM was not able to image the disruption via in-situ imaging. The technique is able to image in complex solutions and hence indicates the potential role in formulation development studies, allowing the study of a range of compounds and imaging the effect, if any, that these have with the plant cuticle.

Chapter 5

Thermal profiling of intact and live leaf surfaces

5.1 Introduction

5.1.1 Thermal profiling of leaf cuticles

To study the interactions of agrochemicals with live leaves at the micro and nanoscale the surface has to be characterised. Most techniques used to characterise the cuticle require non ambient conditions like high vacuum, for example, SEM (Pathan et al., 2008) and time of flight mass spectrometry (Perkins et al., 2008) or requires the isolation of the cuticle (Perkins et al., 2005a).

SPM can be used to characterise plant surfaces in ambient conditions, which would allow the characterisation of live leaves. AFM, for example, has been used to characterise the cuticle by measuring the elastic modulus. Another SPM used to characterise intact leaf surfaces is scanning thermal microscopy (SThM). It was demonstrated that SThM could perform local thermal analysis (LTA) of a leaf surface. The thermal analysis of the intact leaf model of *Prunus laurocerasus* leaf was comparable to differential scanning calorimetry (DSC) of the isolated cuticle (Perkins et al., 2005a). Showing a solid-solid transition thought to be the change of orthorhombic to a hexagonal crystal lattice structure and then a melting transition.

The cuticles of plants are generally a complex structure of a range of different chemicals and chain lengths, which are involved in the structures of polymers, crystals and amorphous areas (Riederer, 1995, Merk et al., 1998, Jetter et al., 2006). The microscopic structure of the cuticle is unknown, though it is thought to be composed of isolated crystals in a sea of continuous amorphous wax (Baur et al., 1996). This structure of the cuticle is the main barrier to penetrating agrochemicals.

As well as the wax and polymer/monomer components there is also another significant component of the cuticle that effects the structure, this is water. The cuticle can contain between 1 – 8 % of its weight in water (Chamel et al., 1991, Luque et al., 1995), with the polysaccharides being the responsible for cuticular sorption of water (Chamel et al., 1991). Water can increase softening, which can decrease the elastic modulus between 35 – 50 % (Round et al., 2000, Dominguez et al., 2009), though this would require high humidity of between 60 -80 %. Water content importance is significant for hydration to be incorporated into extracted wax models of the cuticle (Fagerstrom et al., 2013).

The use of SThM and LTA on the surface of dried and live leaf could provide information on the impact of water in the cuticle. To date there is no thermal analysis of the live leaf surfaces, SThM and LTA has proven to provide essential data of an intact cuticle. The same technique could be used to study live leaf surfaces.

5.2.1 The effects of adjuvants on cuticular uptake

The movement of compounds through the cuticle is discussed in chapter 1, which describes the mobility and solubility in the cuticle as key factors (Riederer et al., 1995, Schreiber and Riederer, 1996). Another parameter that needs to be considered is tortuosity, which is the path length of penetrating compounds (Buchholz et al., 1998, Baur et al., 1999a). The cuticle is built up of amorphous and crystalline segments, with the diffusion of agrochemicals occurring in the amorphous regions (Riederer et al., 1995). The crystalline areas are impermeable for actives, which cannot diffuse through and so increases tortuosity, which increases the diffusion path (Baur et al., 1999a).

Surfactants, and other enhancers, have been incorporated into formulations to increase the uptake and efficacy of actives, and are considered an important part of a formulation (Riederer et al., 1995, Burghardt et al., 1998, Riederer and Friedmann, 2006a). Studies have shown surfactants increase uptake by increasing the solubility (Schreiber et al., 1997) and mobility (Schreiber, 2006) in the cuticle wax.

The impact on the tortuosity is less studied but surfactants have been shown to effect the crystalline regions. Differential scanning calorimetry and scanning thermal microscopy (SThM) with local thermal analysis (LTA) have shown that different surfactants have different impacts on the crystal structures of the surface of *Prunus Laurocerasus*, English Laurel (Perkins et al., 2005a).

5.2.1 Chapter description

In this chapter, SThM is used to investigate the impact water as on intact and live leaf surfaces. Using SThM to gain the thermal profiles of live/fresh leaf surface and dried leaf surfaces. This gives a clear indication on how water interacts with the cuticle and understanding the effect of water of the thermal profile, by comparison, of the dried and live leaf waxes. An investigation on how a surfactant and a plasticizer effects live leas cuticles, utilising tapping mode atomic force microscopy (TM-AFM) to image the effects of two different adjuvants, one being a surfactant Brij 98v and the other being a plasticizer Tris (2-ethylhexyl) phosphate (TEHP). Combined with SThM and LTA, to characterise the impact of the adjuvants on live leaf surfaces with comparisons of the native state of the leaves.

5.3 Results

5.3.1 LTA of intact and live leaf surfaces

5.3.1.1 LTA of *Hedera helix*

Two states of intact leaves were used, these are dried and fresh leaf surfaces, this is to compare the thermal profiles to gauge the impact of water on LTA trace. The LTA thermographs are displayed as first order derivatives of the sensor, with respect to temperature, which shows the changes in surface topology against temperature increases. A transition in the cuticle is recorded as an abrupt change in the sensor signal.

LTA of dried *Hedera helix* surfaces show two different phase transitions that could be recorded, and are shown in figures 5.1, 5.2, 5.3 and 5.4. The main phase transition that occurs is a melting transition (T_m), with a double peak shown is thermogram 18. LTA traces also show some thermographs to have no phase transitions. Shown in figure 5.1, 5.3 and 5.4, traces 4, 20, 24 and 29. This is an instrument error, with the SThM tip disengaging for the surface during characterisation.

Table 5.1 shows the T_m of all the thermograms relating to the dried *Hedera helix* surface, with two distinct groups of values being recorded. The first group (group 1) shows a high T_m with a mean T_m of 91.54 ^oC and a range from 87.98 ^oC to 99.62 ^oC, with a standard deviation of 2.67 ^oC. Showing a low variance between the T_m of group 1, meaning that these transitions could be considered different to group2.

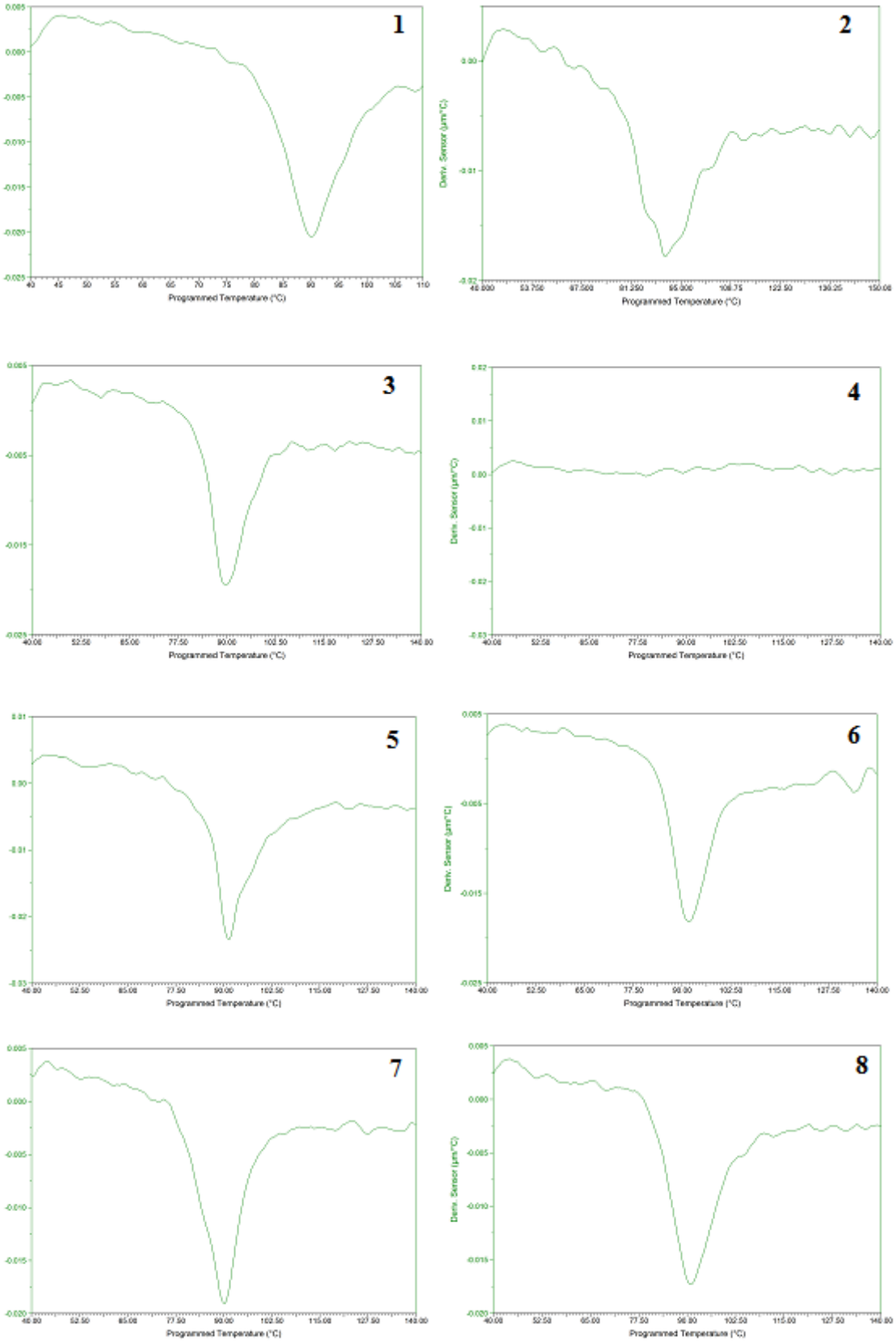

Figure 5.1 - LTA traces of dried *Hedera helix* (1-8), showing the melting point of the cuticle and no phase transition (4), at different locations on the intact leaf surface.

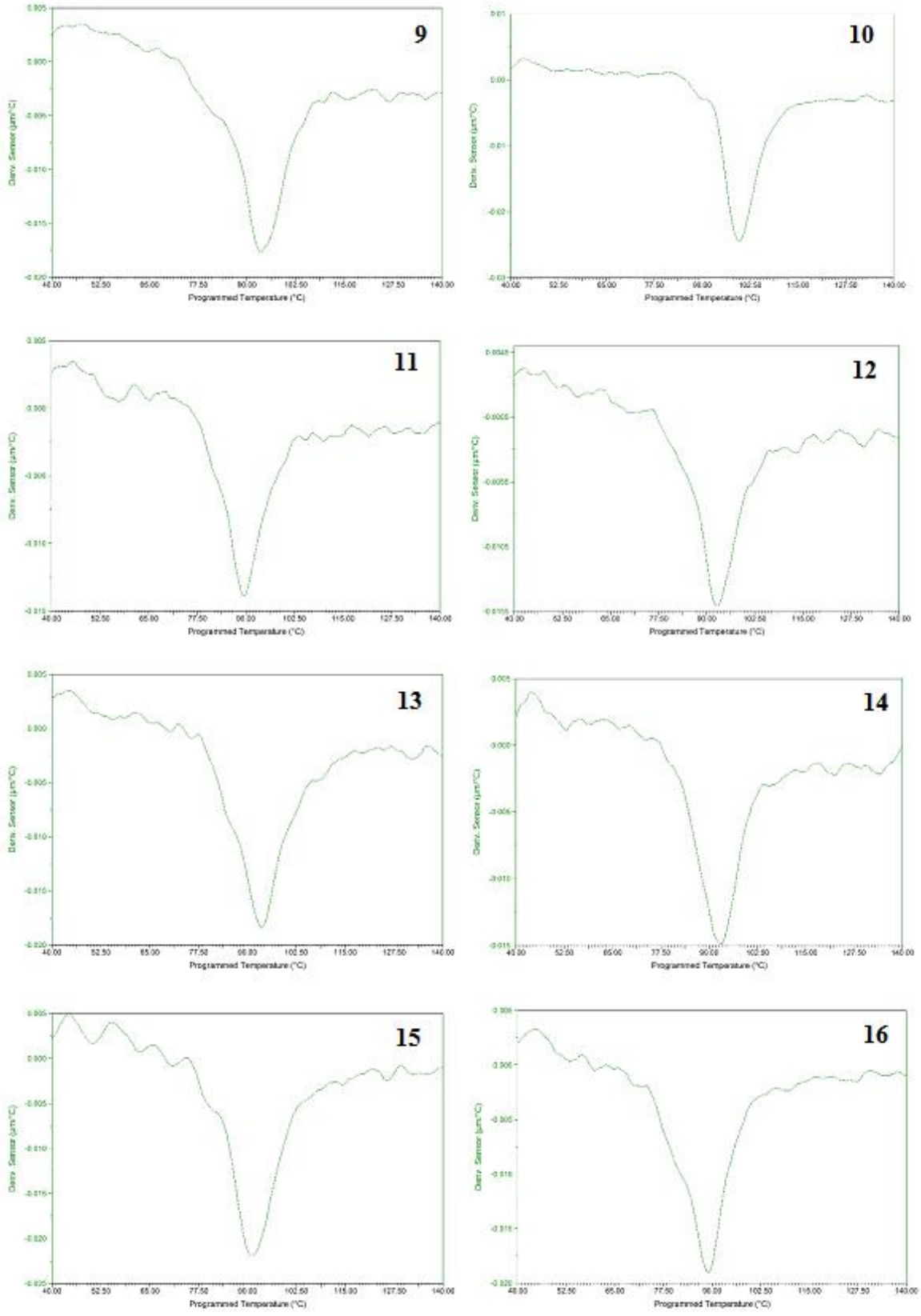

Figure 5.2 – (Continuation) LTA traces of dried *Hedera helix* (9-10), showing the melting point of the cuticle at different location on the intact leaf surface.

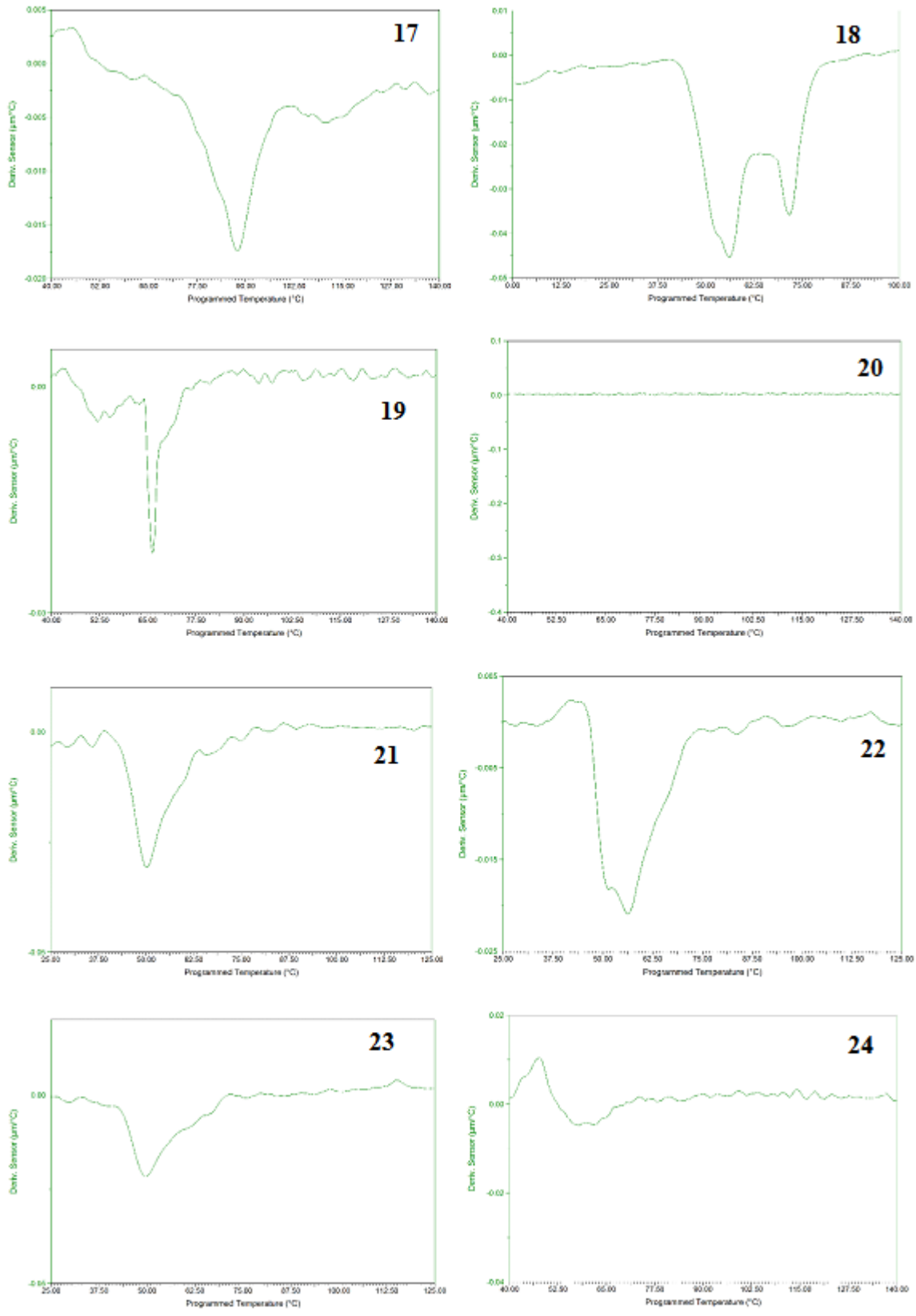

Figure 5.3 -– (Continuation) LTA traces of dried Hedera helix (11-24), showing the melting point of the cuticle at different location on the intact leaf surface. Also the double peak of a solid-solid transition (18) and no phase transition (20).

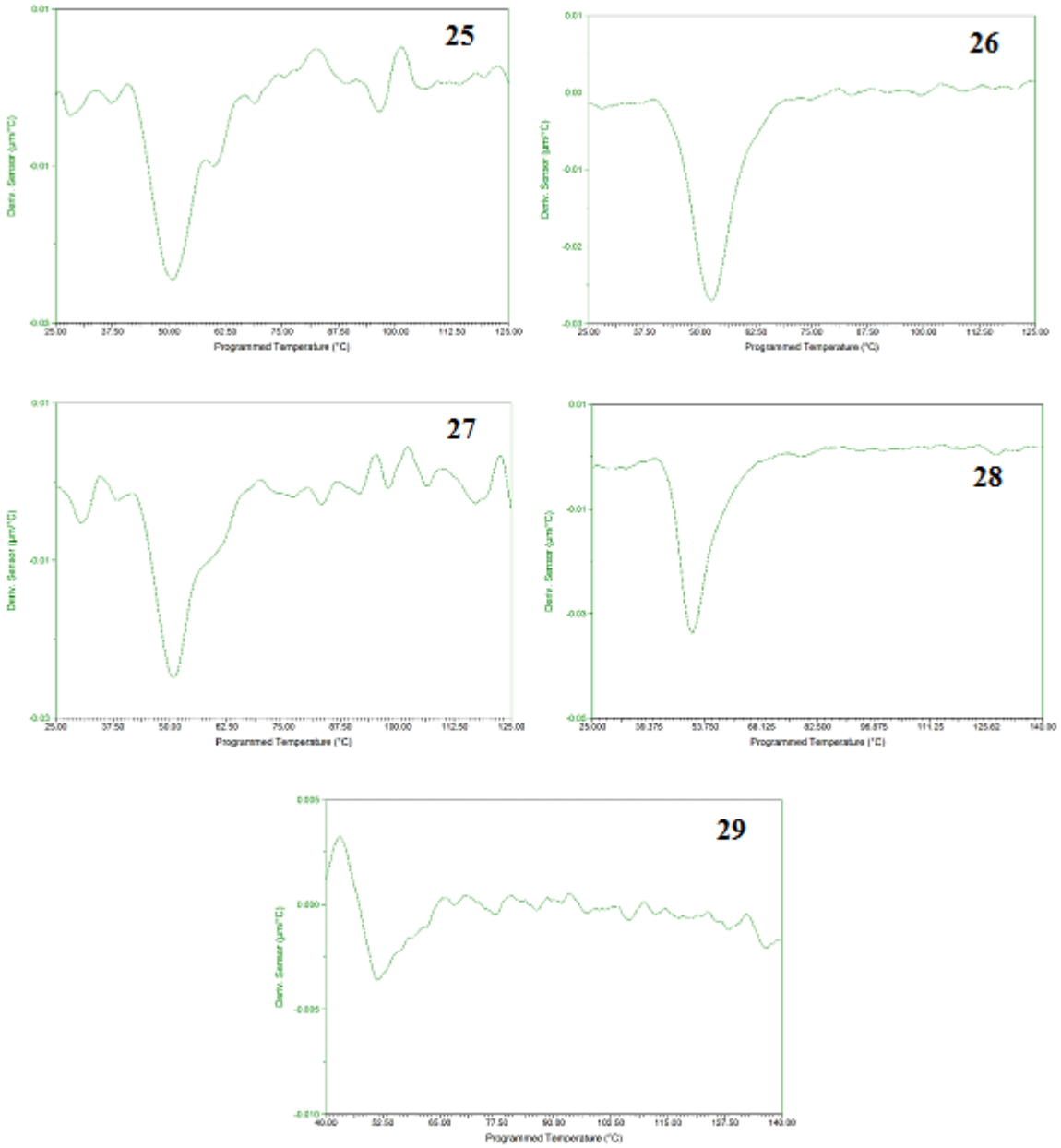

Figure 5.4 - – (Continuation) LTA traces of dried Hedera helix (25-29), showing the melting point of the cuticle at different location on the intact leaf surface and not phase transition (29).

Table 5.1 - Table showing the Tm of the LTA of dried *Hedera helix*

Trace number	T_m (°C)		Trace number	T_m (°C)
1	89.91		16	89.14
2	90.79		17	87.98
3	89.78		18	71.58
4	N/A		19	66.38
5	91.26		20	N/A
6	91.79		21	50.22
7	90.21		22	56.36
8	90.83		23	49.58
9	93.37		24	N/A
10	99.62		25	50.85
11	89.56		26	52.54
12	92.63		27	50.74
13	93.69		28	50.47
14	92.85		29	N/A

15	91.26			
The mean, maximum and minimum of the two groups of melting transitions.				
Group 1 (°C)			Group 2 (°C)	
Mean	91.54		Mean	51.54
Max	99.62		Max	56.36
Min	87.98		Min	50.22
σ	2.67		σ	2.31

The second group (group 2) of melting transitions are lower than group 1, with a mean Tm of 51.54 and a range from 49.58 to 56.36, with a standard deviation of 2.31 °C. This shows there is a low variance in the Tm measured, defining the two groups as different. This suggests that the surface has two different areas and is heterogeneous in structure, this could be the result of different fatty acid chain length structures occurring at the different sites, which would account for the differences in T_m.

The other trace that is observed is shown in figure 5.3, thermograph 18. It shows a two-point peak which shows a solid-solid transition and then T_m of the cuticle and is seen in the literature with other leaf surfaces (Perkins et al., 2005a). The solid-solid transition peak of figure 5.3, thermograph 18 is at 55.95 °C and the Tm is 71.58 °C. This thermograph is only observed once in this data set, but has been observed in other repeats of this study. This suggest that there might be a third area of the cuticle, which would be crystalline. The phase

transition is thought to be a change of orthorhombic to a hexagonal crystal lattice structure, observed from long chain fatty acids (Koch et al., 2009b, Perkins et al., 2005a).

For fresh *Hedera helix* a number of peaks are seen in the traces, figures 5.4, 5.5, 5.6 and 5.8, with thermograms 21 to 26 showing marked peaks. Comparison, with fresh and dried *Hedera helix* traces, there is a distinct difference between the thermographs. The melting transition that was present in the dried traces is no longer present in the fresh sample. This suggest that water has an impact of the cuticle structure resulting in different thermograms.

The fresh traces show that there are many phase transitions occurring in the area of the SThM tip, there is no clear way to distinguish between the peaks. They could be either Tm peaks or solid-solid transitions but this can't be discerned from the traces, because of resolution of SThM, it is most like a combination of both. There is a pattern which is shown in traces 21 to 26, with peaks label a, b, c, d and e.

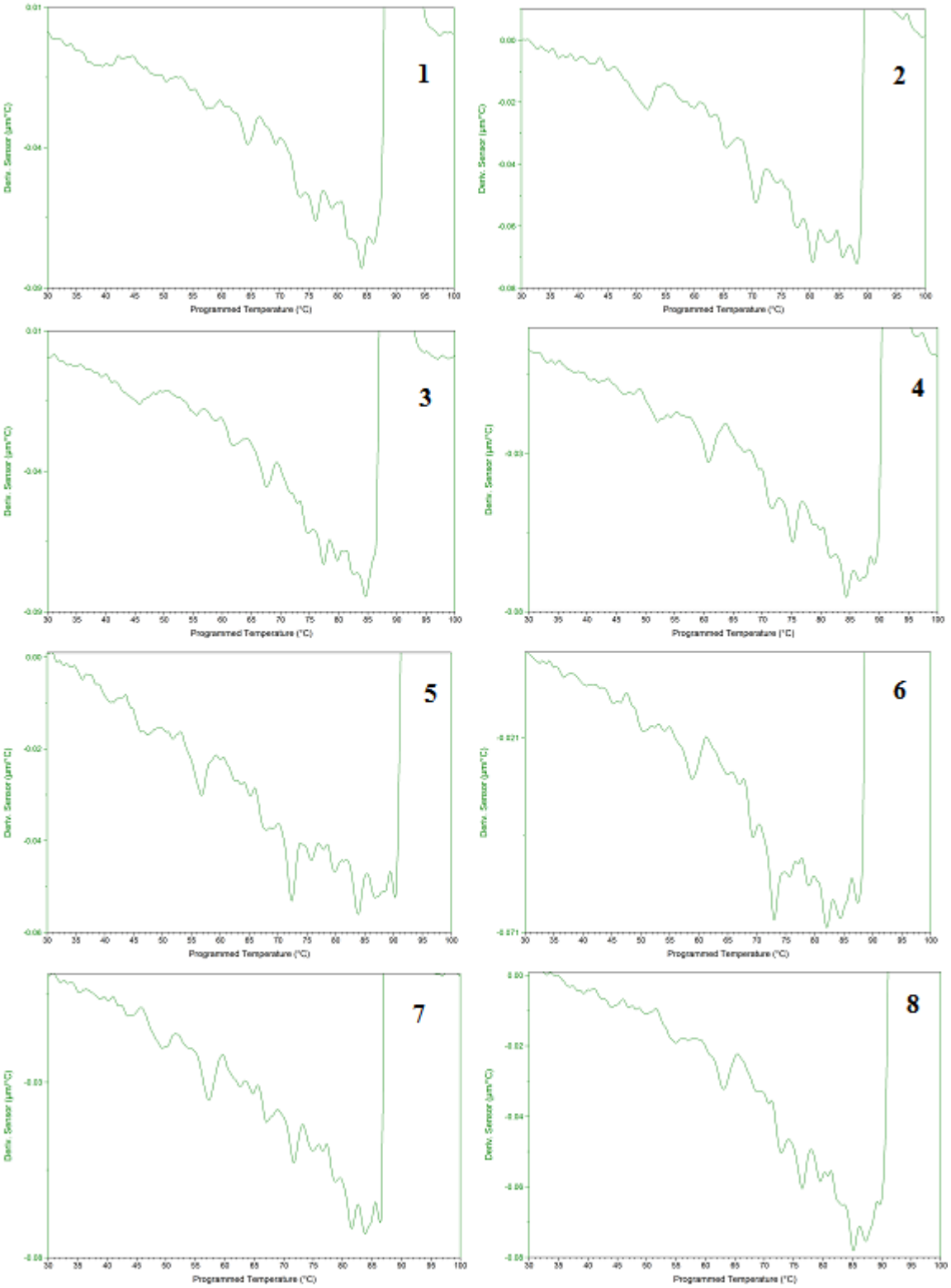

Figure 5.5 - LTA thermograms of fresh *Hedera helix*, showing multiple transitions.

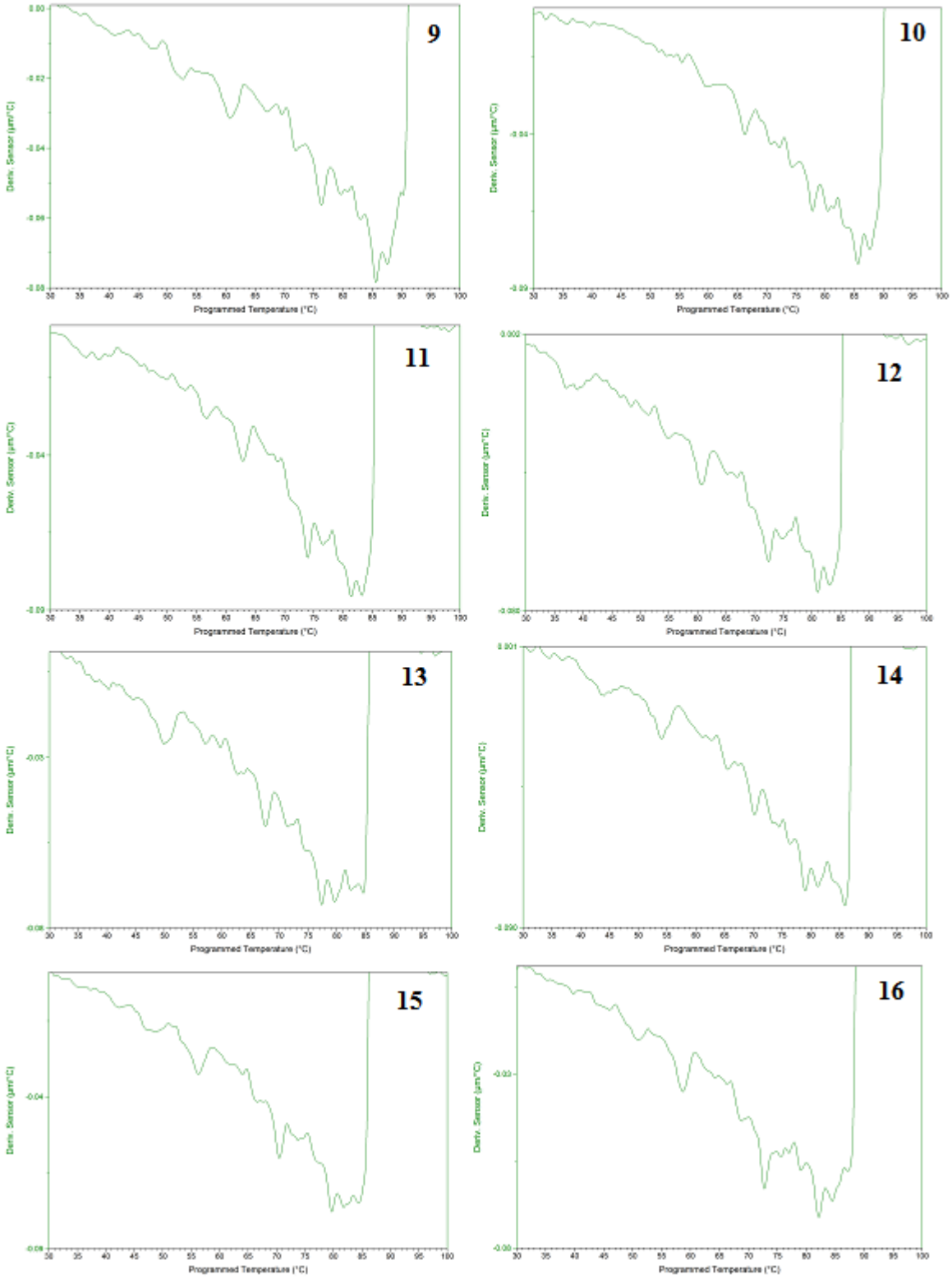

Figure 5.6 - (Continues) LTA thermograms of fresh *Hedera helix*, showing multiple transitions.

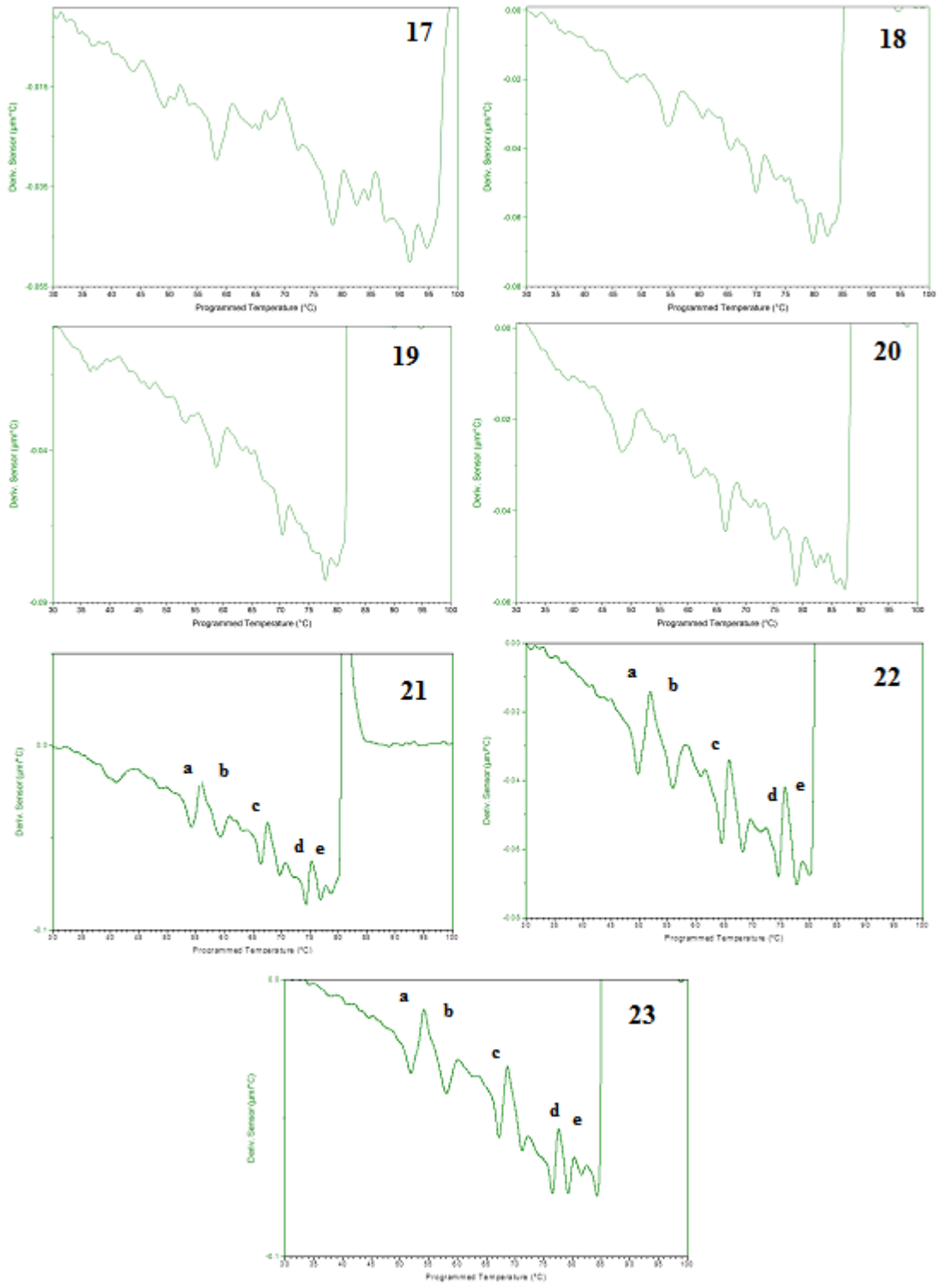

Figure 5.7 – (Continues) LTA thermograms of fresh *Hedera helix*, showing multiple transitions. Peaks a, b, c, d, and e shows the pattern of the thermograph.

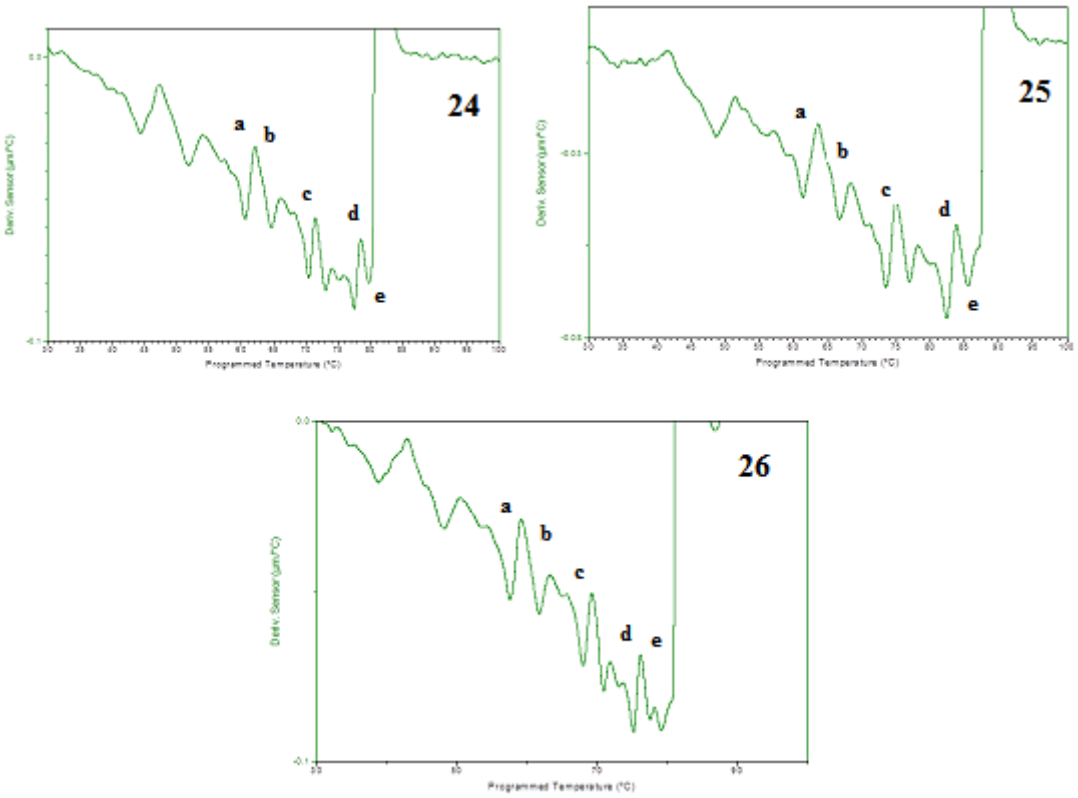

Figure 5.8 - (Continues) LTA thermograms of fresh *Hedera helix*, showing multiple transitions. Peaks a, b, c, d, and e shows the pattern of the thermograph.

The six traces with marked peaks show that multiple trace show the same pattern. Though the phase transitions values of the five peaks vary, shown in table 5.2, they can still be clearly identified by their position within the thermogram. Table 5.2 shows there is variation in peak values, while the image shows the pattern to remain the same. For example, the largest range is associated with peak (a), from 49.73 to 61.36, being 11.63 °C but the peak can be identified by the location of peak b and c.

The pattern of the thermographs shows that there are areas of similar composition. The standard deviation of each peak, with the transition temperatures, shows there is a large variation in peak transitions, by 3 to 4.7 °C. This shows that areas that of similar composition

contain something that result is these large variations, this could be water being a known and abundant plasticizer (Round et al., 2000, Dominguez et al., 2009).

Table 5.2 - Tables showing the phase transition at a, b, c, d and e of live *Hedera helix* surface.

	Phase Transitions °C				
Trace Number	a	b	c	d	e
21	54.17	59.21	66.47	74.33	76.92
22	49.73	55.95	64.47	74.48	77.74
23	51.80	58.03	67.21	76.48	79.22
24	60.54	64.62	70.40	77.37	79.74
25	61.36	66.70	73.51	82.33	85.52
26	57.58	61.73	68.03	75.22	77.51
Mean	55.86	61.04	68.35	76.70	79.44
Min	61.36	66.70	73.51	82.33	85.52
Max	49.73	55.95	64.47	74.33	76.92

σ	4.73	4.09	3.19	3.00	3.16

5.3.1.2 Living vs intact, profiling of *Vicia faba*

Field Bean (*Vicia faba*) leaf surface is relatively smooth like English Ivy, this is shown in the SICM images in figure 5.9. The image show that the surface has no features and have large variations in the z-axis. The use of this leave are to compare the different thermal transitions between live leaf and intact leaf (dried) model and to ascertain if it could be used to study surfactant on live leaves.

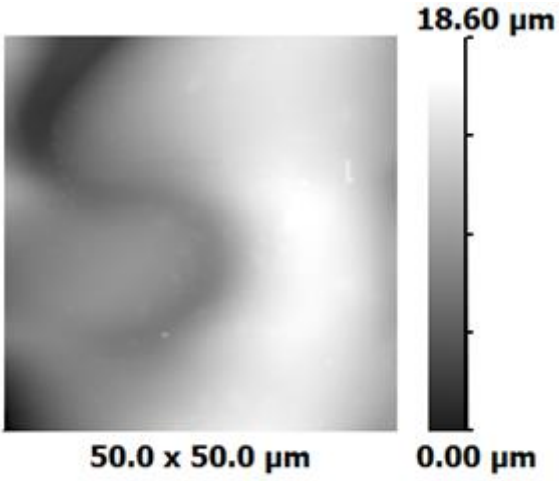

Figure 5.9 - SICM images of (Left) Field Bean and (Right) Sugar beet with z scale bars

Dried LTA trace of Field Bean is seen in figure 5.10, 5.11 and 5.12, which shows a multitude of different thermographs, that show different transition of the cuticle. Examples of the typical thermograms can be seen in traces 1, 4, 5 ,12 and 15, these show multiple transition through the temperature range, these could be considered melting transition as they show only one peak over a broad range.

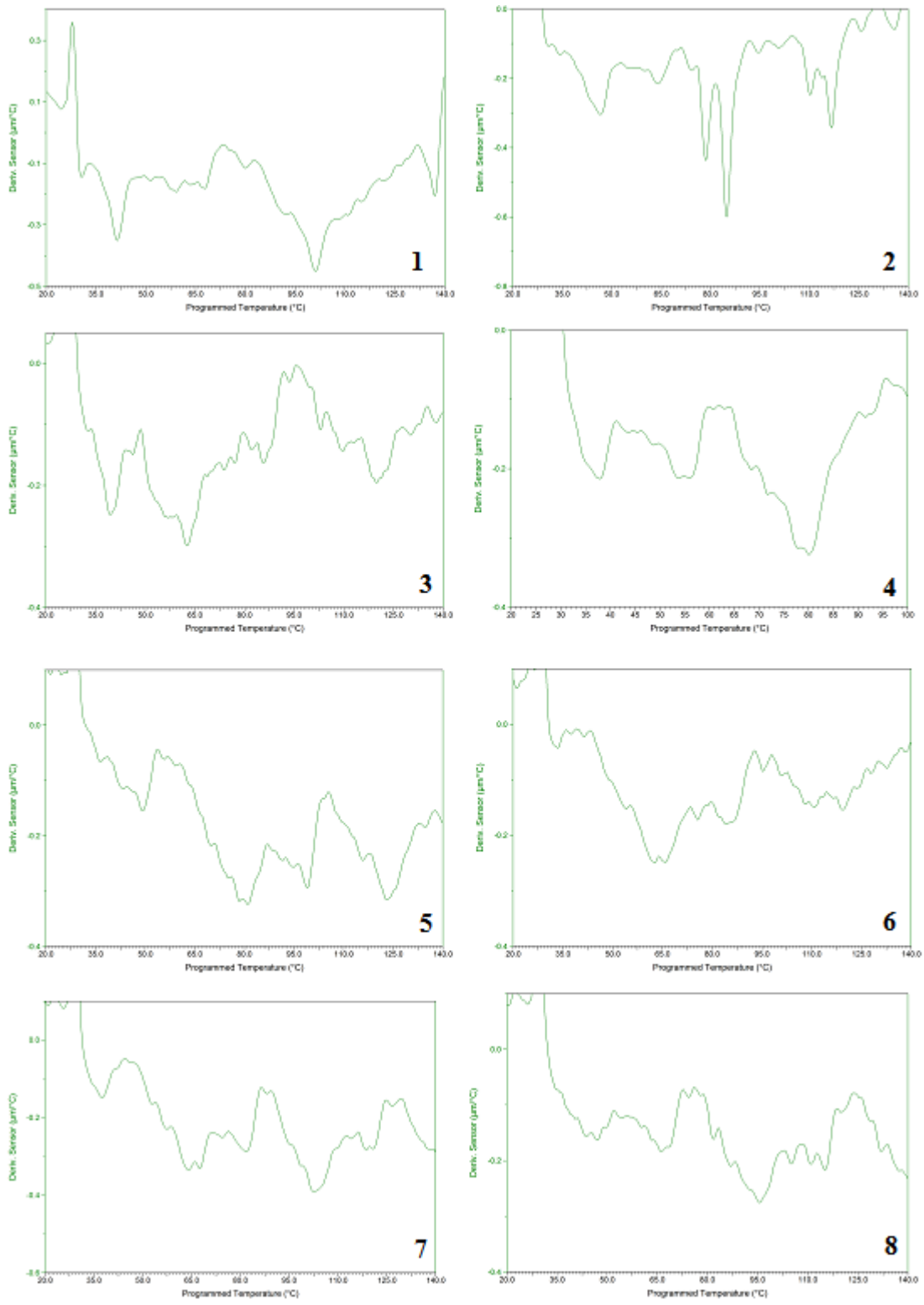

Figure 5.10 - LTA trace of dried *Vicia faba*, showing multiple transitions.

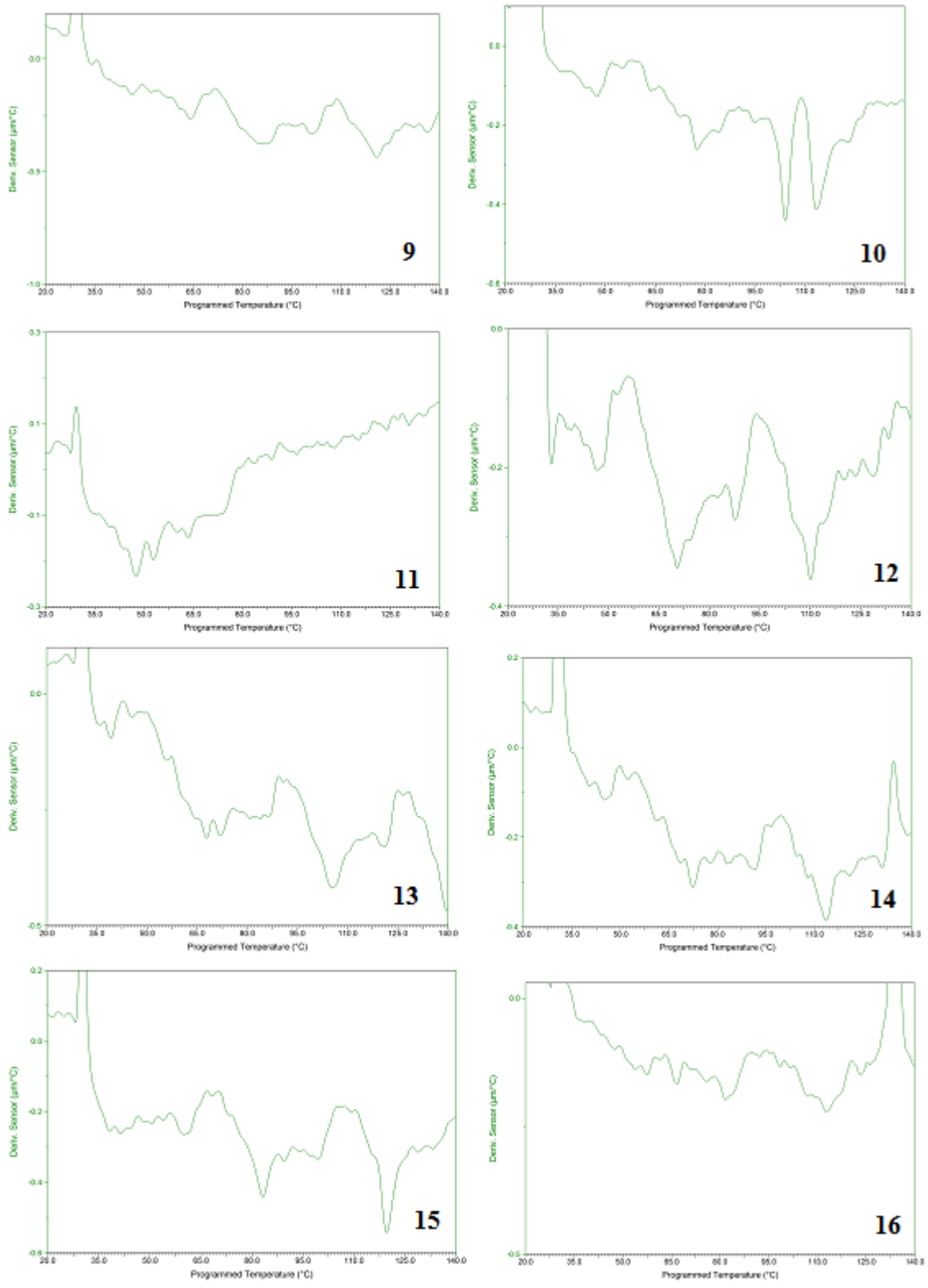

Figure 5.11 - LTA trace of dried *Vicia faba*, showing multiple transitions.

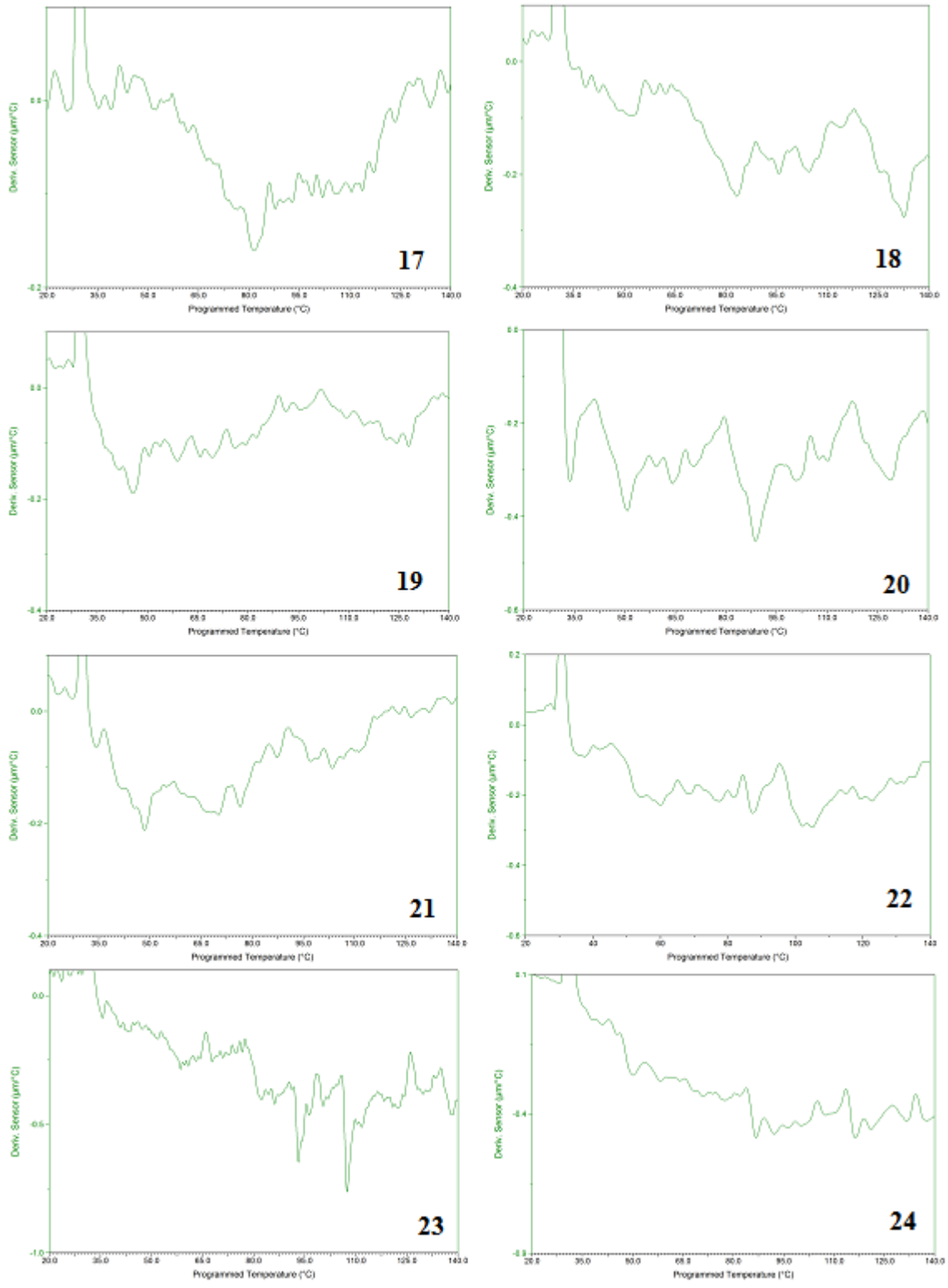

Figure 5.12 - LTA trace of dried *Vicia faba*, showing multiple transitions.

As well as the Tm peaks being showed, the double peak associated with solid-solid transitions are also present (Fagerstrom et al., 2013). These are from traces 2 and 10, with trace 2 showing two such peaks. These peaks have a relatively high transition temperature with the first transitions in trace 2 occurring at 78.12 °C with T_m at 84.89 °C, the second transition for trace 2 happened at 110.30 °C, with the Tm at 116.73 °C. This is show again with trace 10, with the solid-solid transition at 104.03 °C, with the Tm at 113.35 °C. Other traces are difficult to discern if there are transition on the profile is just the base line of the SThM, like trace 19.

Live Field Bean cuticle trace is shown in figure 5.13, 5.14 and 5.15, which show multiple transitions like the dried leaf trace, though the transitions of the live leaf are more defined and easily identifiable. There appears to be many T_m transitions, with trace 7 showing the full phase transition that can occur at the surface of the live cuticle, with the temperature of transitions shown in table 5.3. Traces 5 and 19, show melting transitions, but less defined compared to the other thermographs of the live leaf surface, this could be a consequence of SThM being unable to resolve the transitions, resulting in the grouping of the melt transition that is observed in other traces.

Table 5.3 - Table showing the values of transition seen in 5.8

Transition number	Value (°C)
1	33.9
2	40.6
3	46.7
4	57.4
5 (first peak and second peak)	62.6 and 69.8
6	79.0

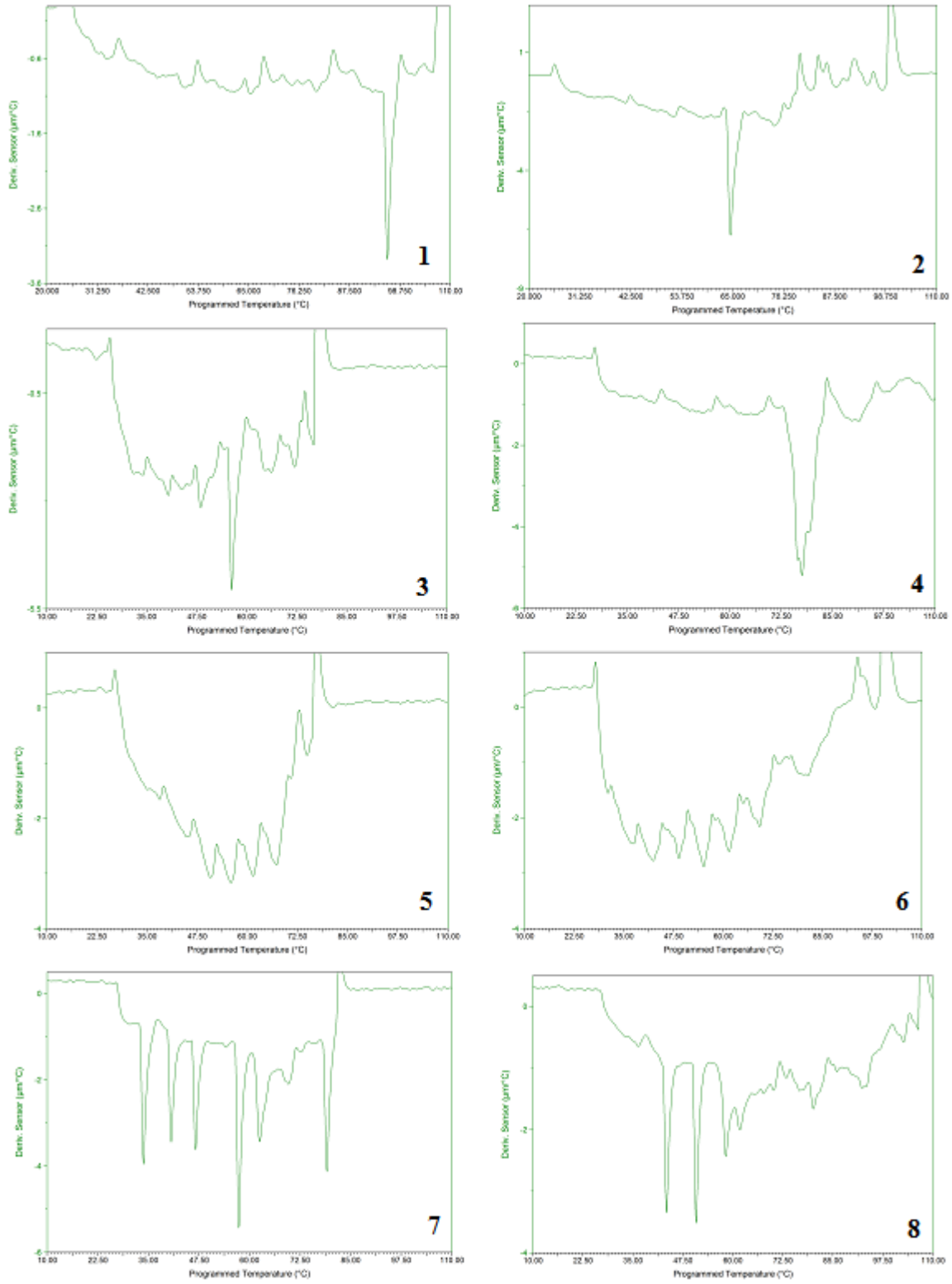

Figure 5.13 - LTA trace of live *Vicia faba* leaf surface, showing multiple transitions.

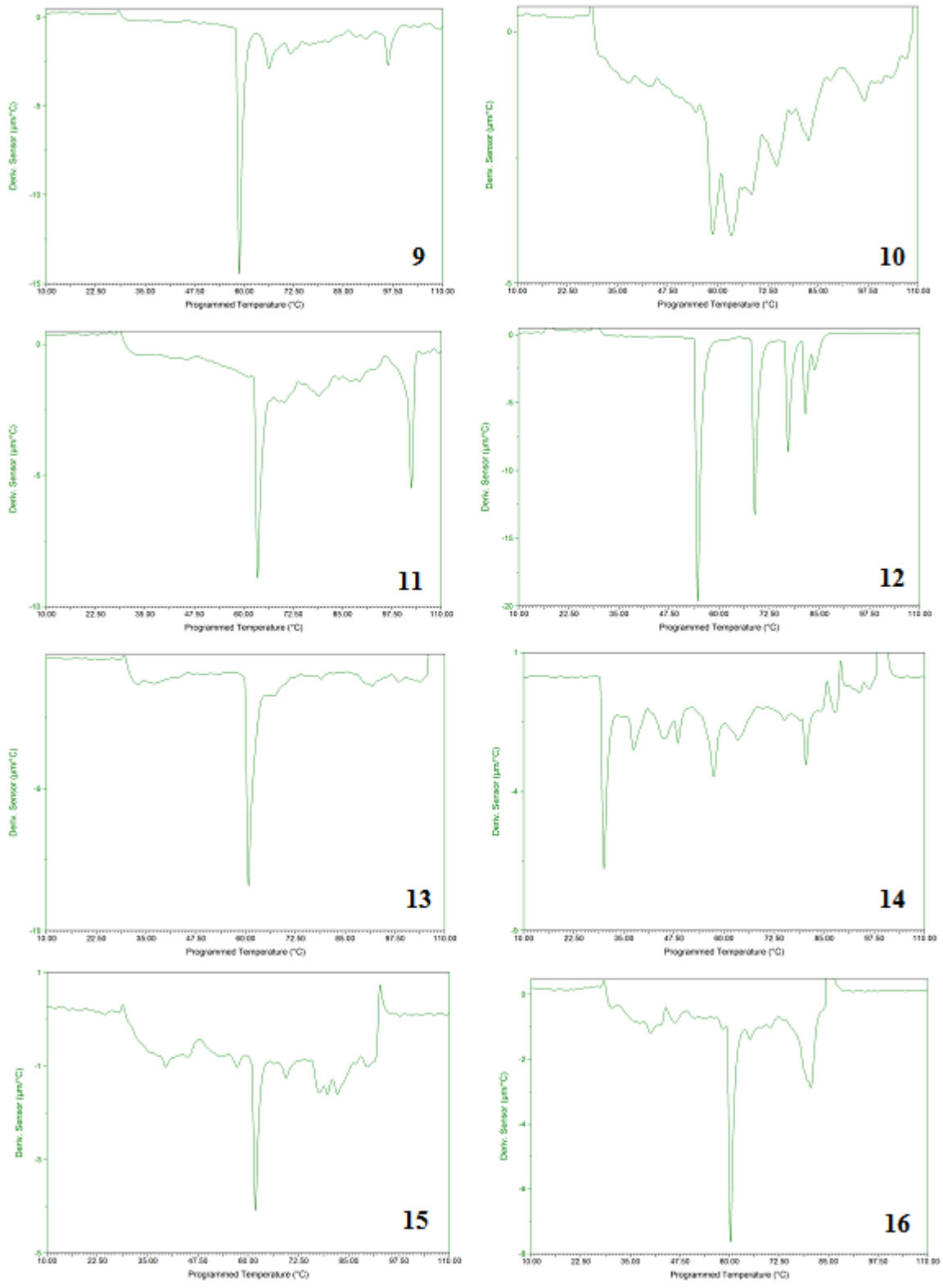

Figure 5.14 - LTA trace of live *Vicia faba* leaf surface, showing multiple transitions.

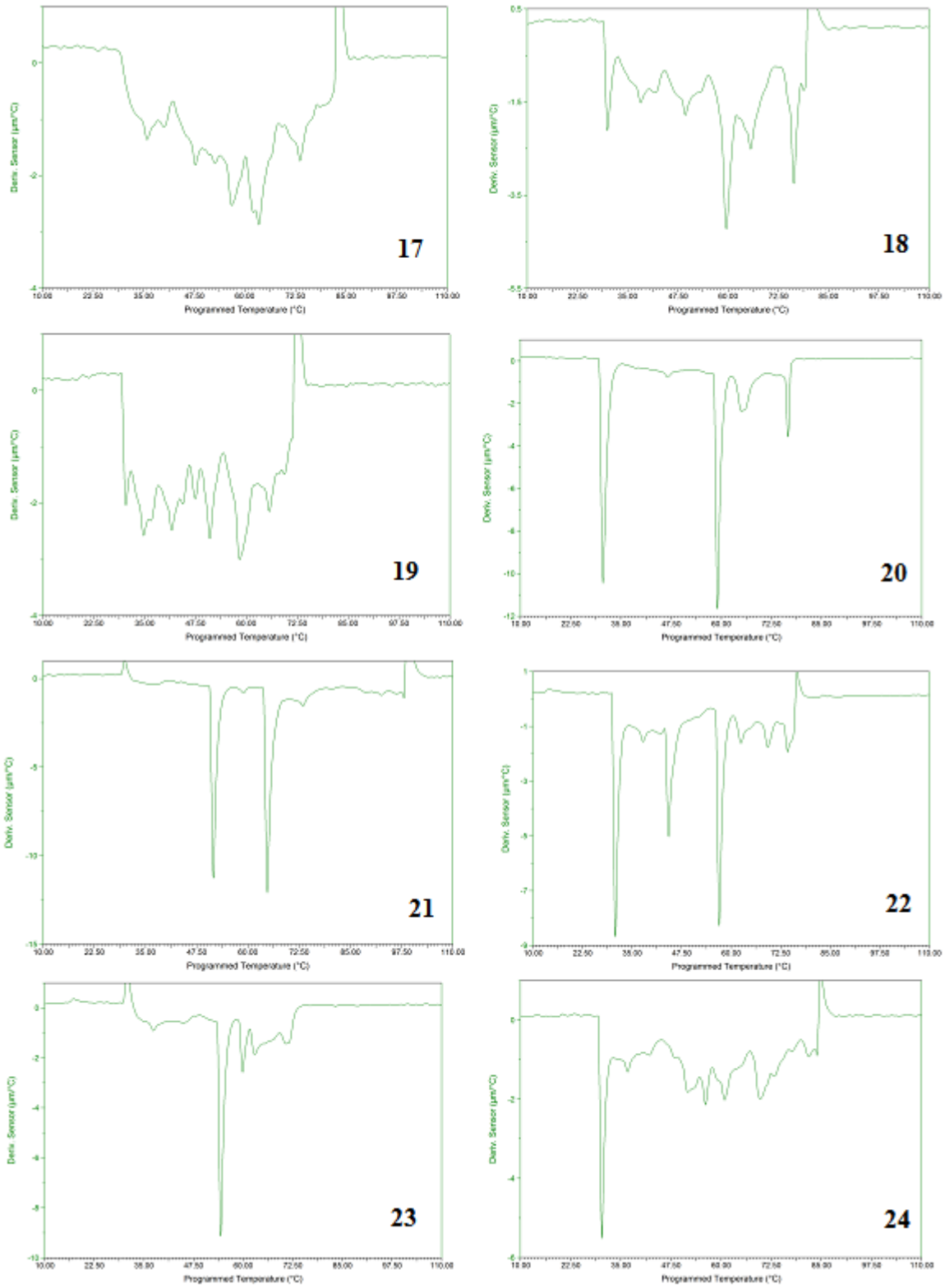

Figure 5.15 - LTA trace of live *Vicia faba* leaf surface, showing multiple transitions.

The other traces of the live leaf show similar peaks, though some have just T_m peak (or variations of different peak combinations) or just show the two-point peak. This suggests that the surface is heterogeneous in composition and structure of this leaf varies in different areas. This isn't seen with the dried leaf surface. Another observation of the live leaf surface is that all transition occur below 100 °C, while with the dried the two distinct peaks happen to be above 100 °C. This can be attributed to the plasticizing effect of water. The easily definable peaks of the live leaf surface make the live field bean a good choice for studying surfactants of live leave surfaces.

5.3.2 AFM images of live Field Bean

5.3.2.1 AFM images of live Field Bean

The Field Bean was used because of the distinct phase transitions that were observed in chapter 5, which can be compared with any effect resulting in adjuvants applied to the surface being monitored. Also, the leaf surface is relatively flat and TM-AFM imaging can be performed, with the ability to stabilise and fix without damaging the leaf itself.

The live Field Bean leaf surface was first imaged without any adjuvants present to understand the natural state of the surface. This was to allow comparison between the images from the effected leaf surfaces. These images are of the height and simultaneously recorded phase images of the live leaf cuticle. Field Bean surface shows nanoscale variations in height, shown in the height image of figure 5.16. The Field bean is considered not to have an epicuticular wax (EW) layer (Jeffree, 2006) so the variations are the result of the intracuticular waxes (IW).

The variations on the surface are the textured granular wax features which cover the entire surface of the area imaged. The simultaneously acquired phase image adds extra contrast showing the globular wax features being recognisable and showing that they are the only variations on the surface topology of the leaf, agreeing with the height image.

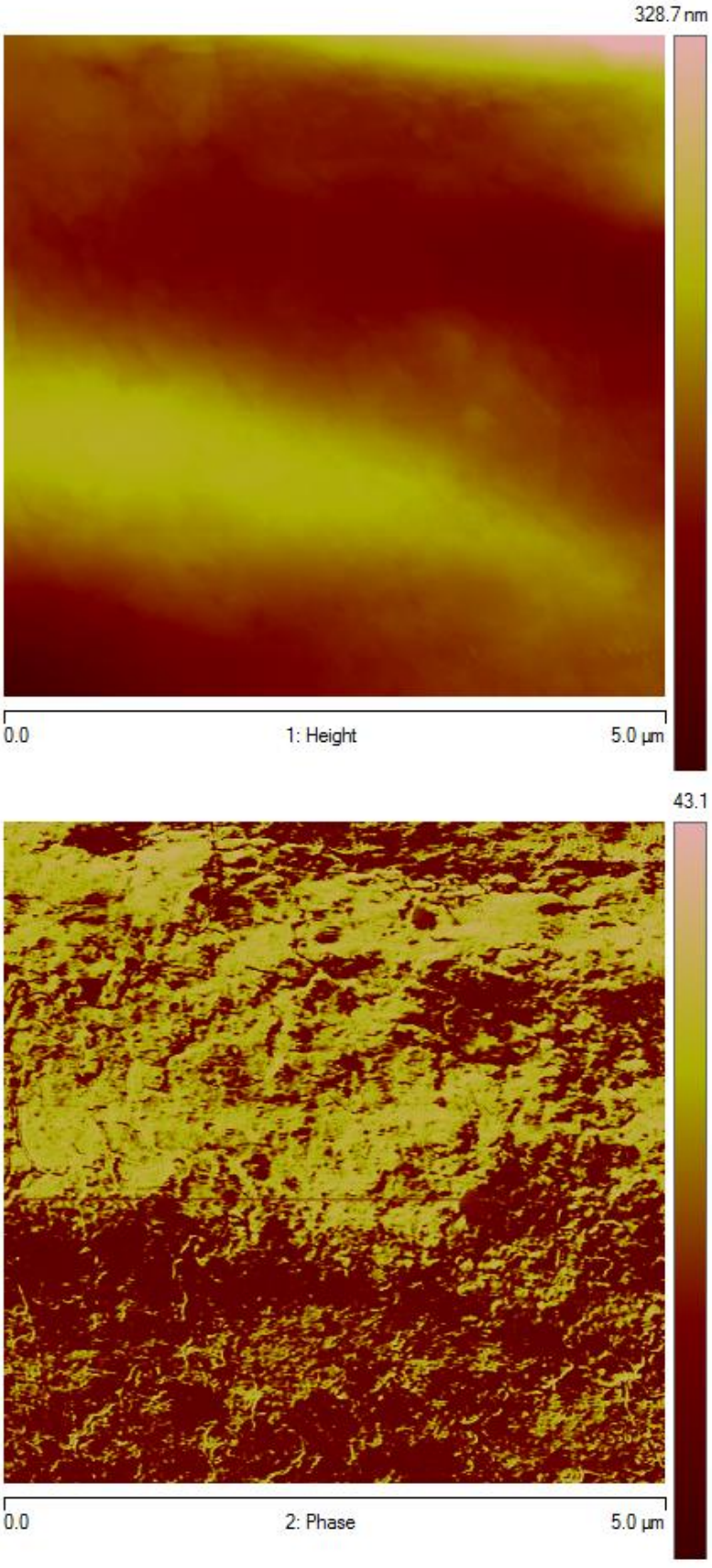

Figure 5.16 - TM-AFM height (top) and phase (Bottom) images depicting the surface of the live Field Bean leaf

TM-AFM was also used the image the impact of TEHP on the cuticle of Field Bean. The adjuvant was allowed to dry for two hours before imaging was performed, the images produced are shown in figures 5.17 and 5.18. After drying the deposit of TEHP was observed to create a spherical area, which the entire area was affected by the solution. This was observed through the CCD camera. Figure 5.17 and 5.18 shows the same area with different scan sizes, to aid in the depiction of the area inside the spherical droplet.

Figure 5.17 height image shows that there are two distinct regions associated with the surface after the droplet has dried. The first area, observed at the bottom right hand corner of the image, is relatively smooth compared with the other area in the image and figure 5.16. The smooth area does not have the globular area associated with unaffected leaf, but still shows small variations in topology. The other area appears to be less smooth, though the globular features are still not present, there are still wax constructs present. The phase imaging shows the statement to be true, with no contrast edges seen in the first area, while the edges of the wax constructs are visible. The first area possesses a different physiochemical property from that of the second area. I believe the first area is the most affected area by the TEHP and the second, though not unaffected, less affected. This is shown by the removal of the globular features.

Figure 5.18 utilised a larger scan size to depict the size of the smoother area and to see the impact of the adjuvant. The globular features are still not observed, but wax features still remain on the surface (shown by the height and phase imaging). There are two smoother regions in the image, showing as the adjuvant does not affect the whole surface. The affected areas are in close proximity to each other.

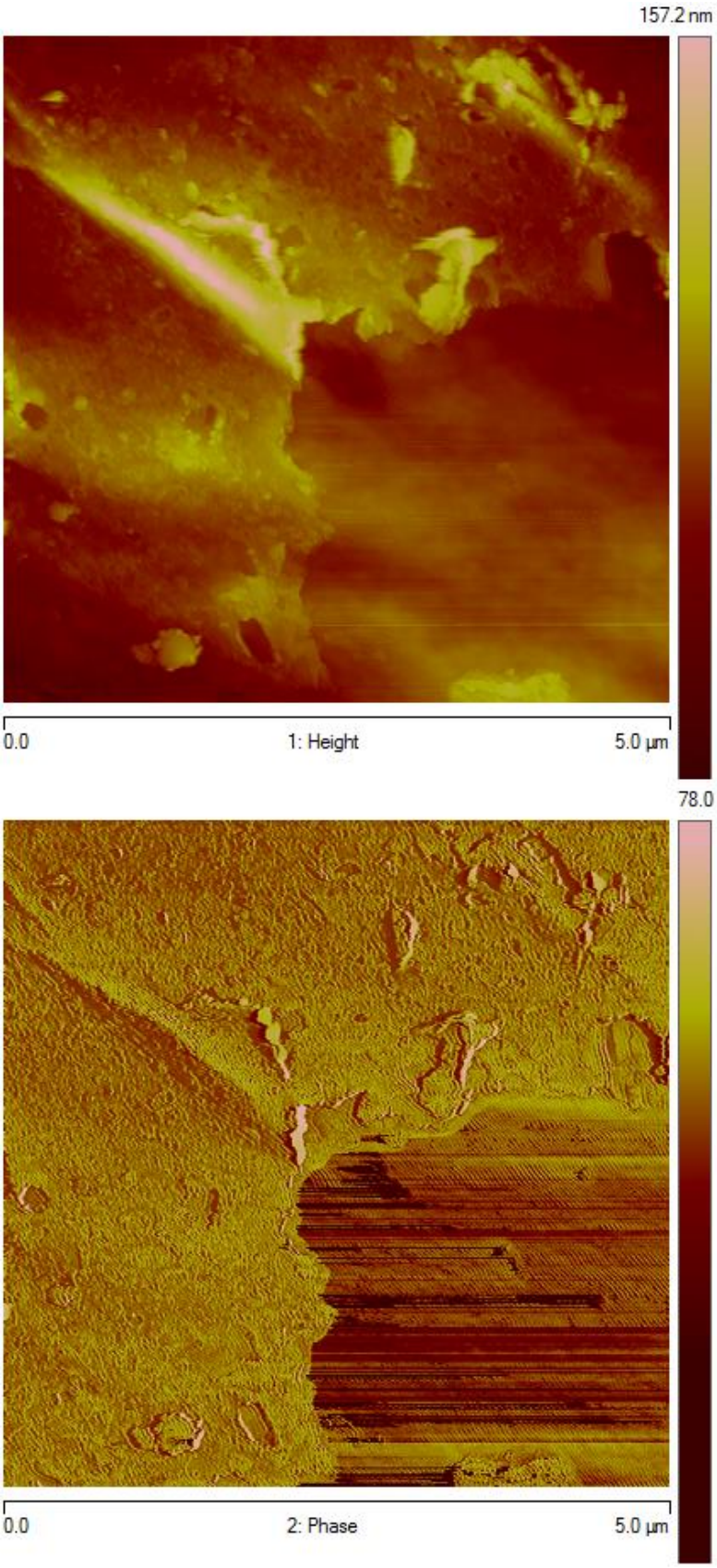

Figure 5.17 - TM-AFM height (top) and phase (Bottom) images depicting the surface of the live Field Bean leaf which has been affected with the TEHP solution 5 x 5 µm scan size.

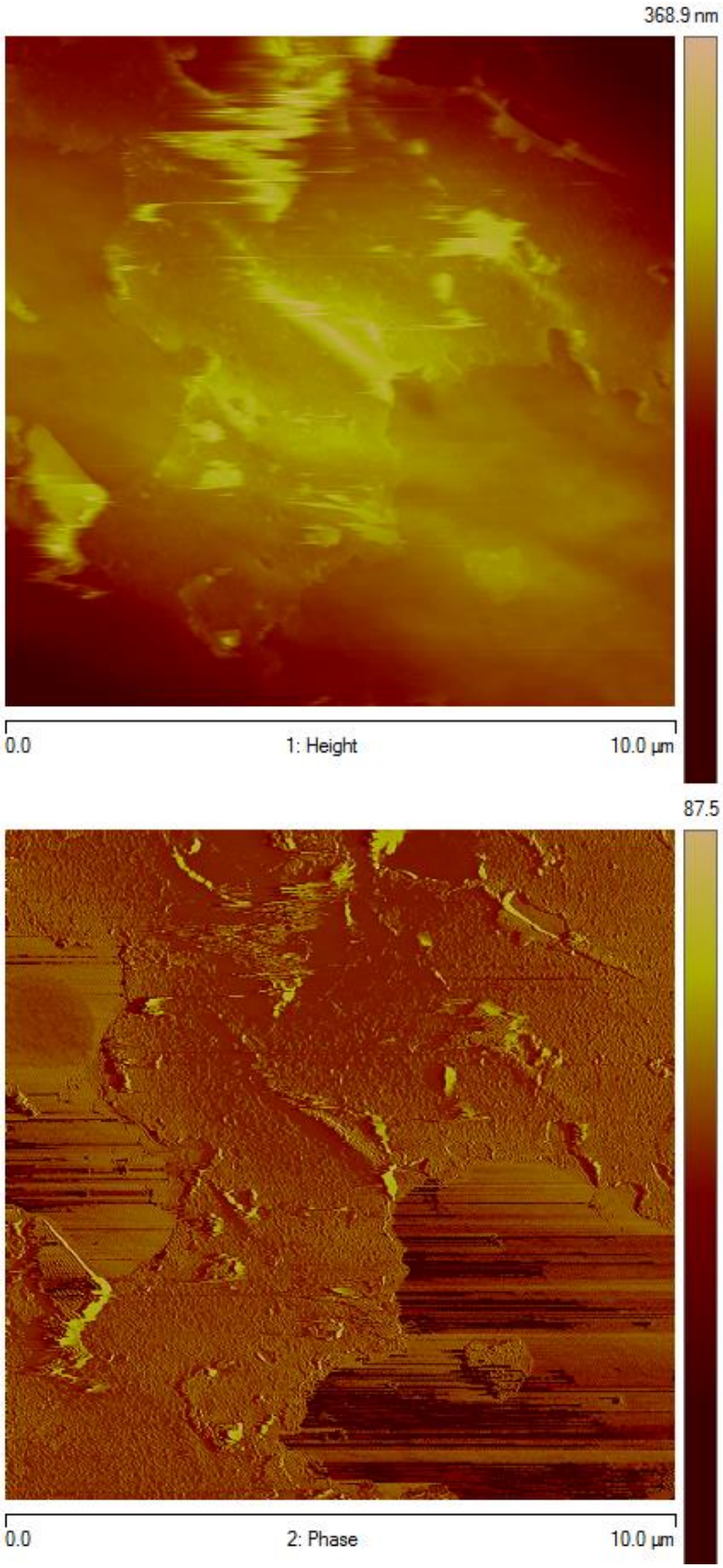

Figure 5.18 TM-AFM height (top) and phase (Bottom) images depicting the surface of the live Field Bean leaf which has been affected with the TEHP solution 10 x 10 µm scan size of the same area.

The phase imaging of figure 5.18 adds extra contrast to the scan area, showing the variations in size and shape of the wax features. Also it shows the lack of variations inside the affected areas, with few features present.

Brij 98 was also imaged after the droplet was dried, the CCD camera shows the process deposited the surfactant around the edge of the droplet in a “coffee” ring effect. This suggest that the surfactant only effects a small area of the leaf surface. TM-AFM was used to image the affected area to allow comparison with TEHP.

The height images of figure 5.19 shows the surface of the live Field Bean leaf that has been affected by Brij 98. The image shows the variations in height though the globular features of the unaffected leaf (Figure 5.16) are not shown after the deposit has dried. The height image also indicates that there are wax compositions present on the surface.

The phase imaging contrast aid in depicting the consequence of the Brij 98 surfactant. The image shows the surfactant also produced two main regions that are both smooth. The first, like with figure 5.18, is the smoother region that does not depict relatively large variations or are there any waxy contrast in the area. This can be seen in the top left hand corner of the image. The other area is rougher showing regular variations in height with waxy constructs present. The area where the surfactant had larger impacts is the first smooth area.

Comparisons between the TEHP and Brij 98 solution show that both adjuvants disperse and deposit onto the surface in different ways. With TEHP showing low density of large regions of affected areas and the Brij 98 showing high density of smaller areas.

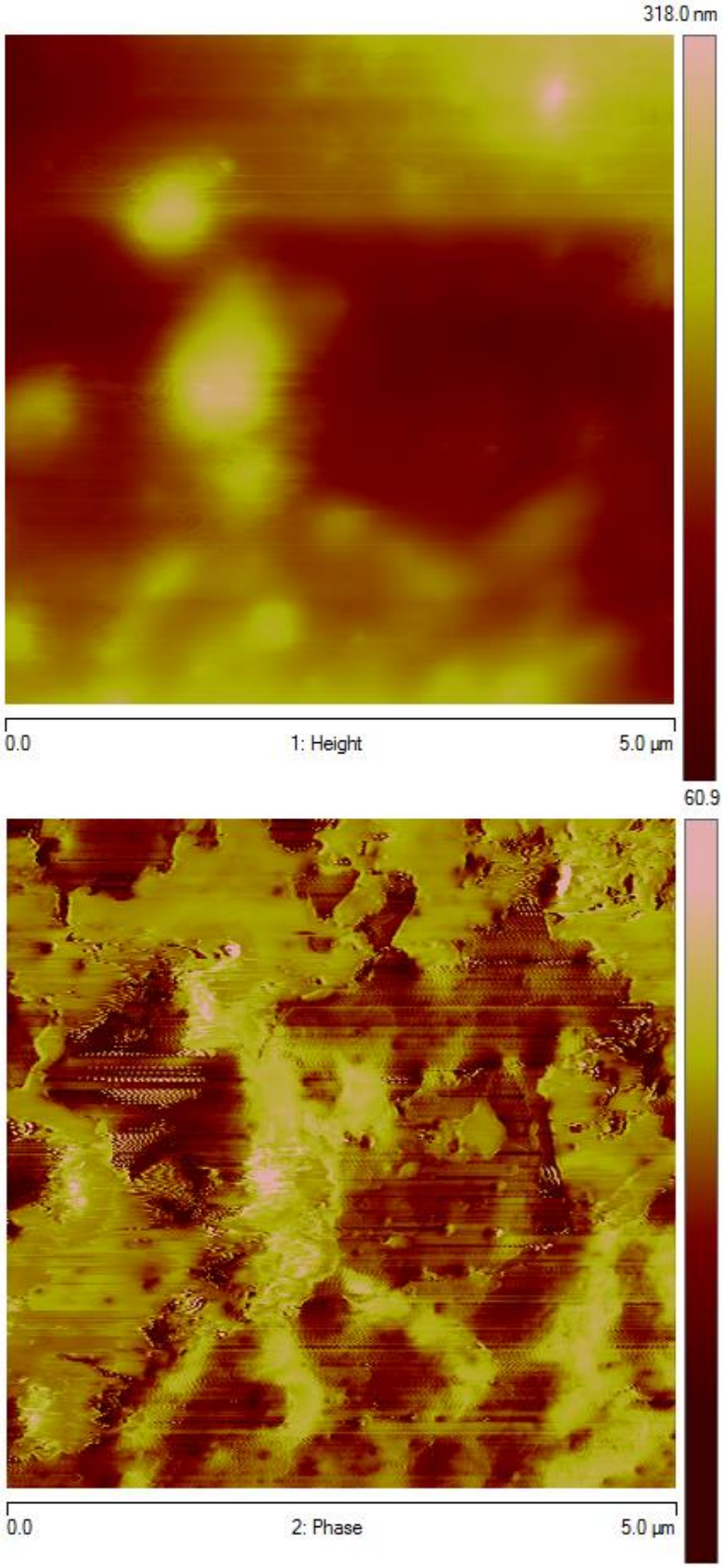

Figure 5.19- TM-AFM height (top) and phase (Bottom) images depicting the surface of the live Field Bean leaf which has been affected with the Brij 98 solution.

5.3.2.2 LTA of adjuvant affected live Field Bean

The SThM and LTA were used to understand the physical impact of the adjuvants on the leaf surface, comparing affect and unaffected areas with each other. LTA of the native live of Field Bean, shows there are many T_m transitions that occur over a range of temperatures. Since different Field Bean leaf surfaces have variations in chemistry and structure LTA where first conducted on unaffected areas before the analysis of the deposit area, for both adjuvants

Figure 5.20 shows the traces of the live Filed Bean cuticle that has been unaffected by the TEHP adjuvant. Phase transitions can be seen through a range of temperature from below 40 to 125 °C, which compares with the LTA of live field bean from the previous section. These transitions are likely to be T_m of the cuticle and show the large range in chemical and structure composition., also that there is no effect from the TEHP allowing for comparison between affected areas.

Following characterization of the leaf away from the droplet LTA was then performed on the leaf surface inside the droplet area after drying. The LTA trace are from the same leaf surface but within the droplet, the deposit was visible through the CCD camera. Since the deposit of TEHP was spherical and appeared to have saturated the area LTA measurements were performed across the deposit. The LTA traces of the affected area is shown in figure 5.21, 5.22 and 5.23,

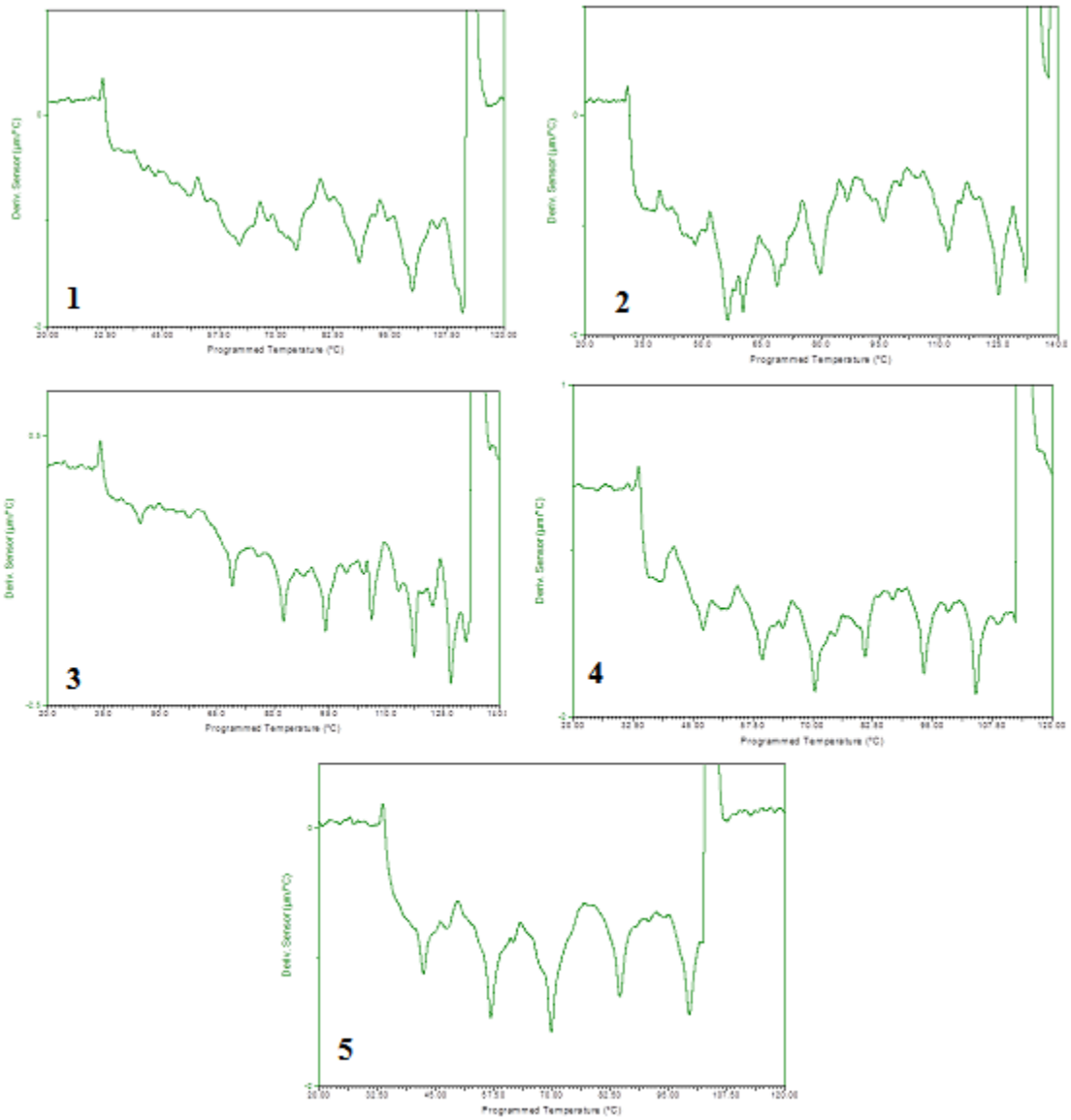

Figure 5.20 - LTA traces of unaffected areas of live Field Bean surfaces.

The affected area LTA show that there are areas that are not effected by TEHP, this is shown in traces 3, 5, 10, and 18. These thermograms are comparable to the unaffected traces shown in figure 5.20. This suggest that within the droplet there are still areas where the adjuvant has not covered and penetrated the cuticle. This seems consistent with the AFM images, figure 5.18, where areas of the scan showed no affect from TEHP.

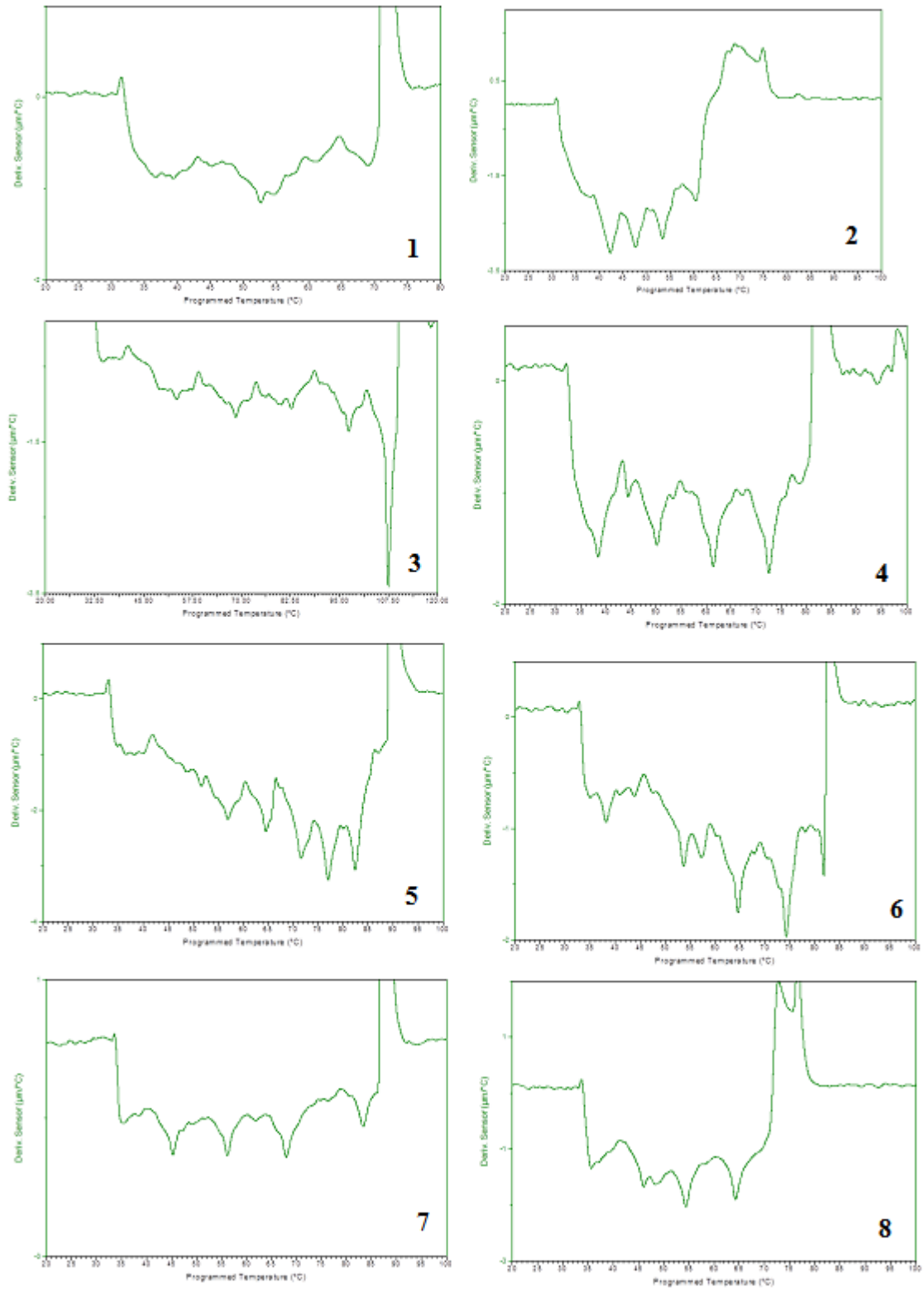

Figure 5.21 - LTA traces of affected areas of the live Field Bean leaf, affected by TEHP

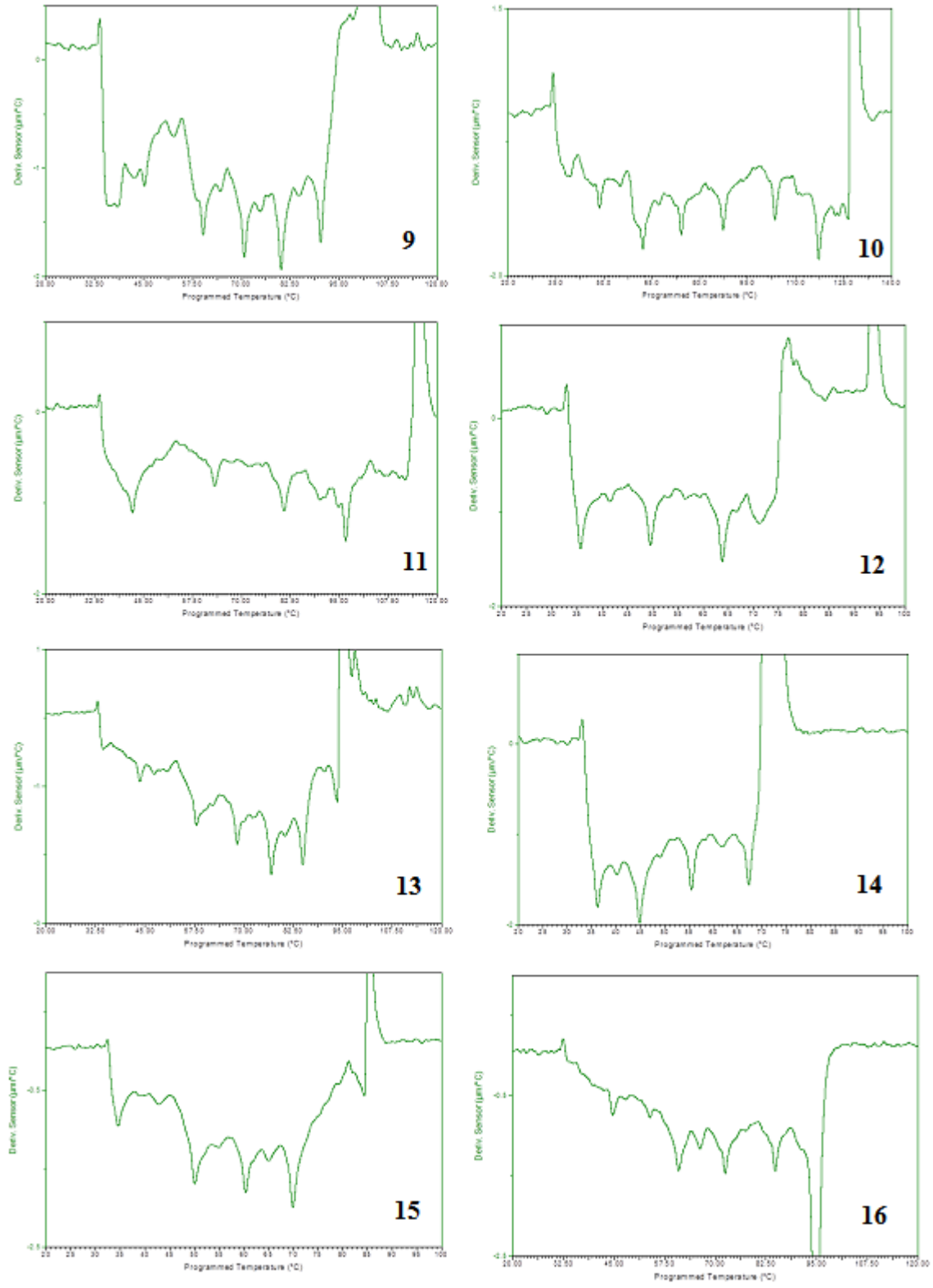

Figure 5.22 - LTA traces of affected areas of the live Field Bean leaf, affected by TEHP.

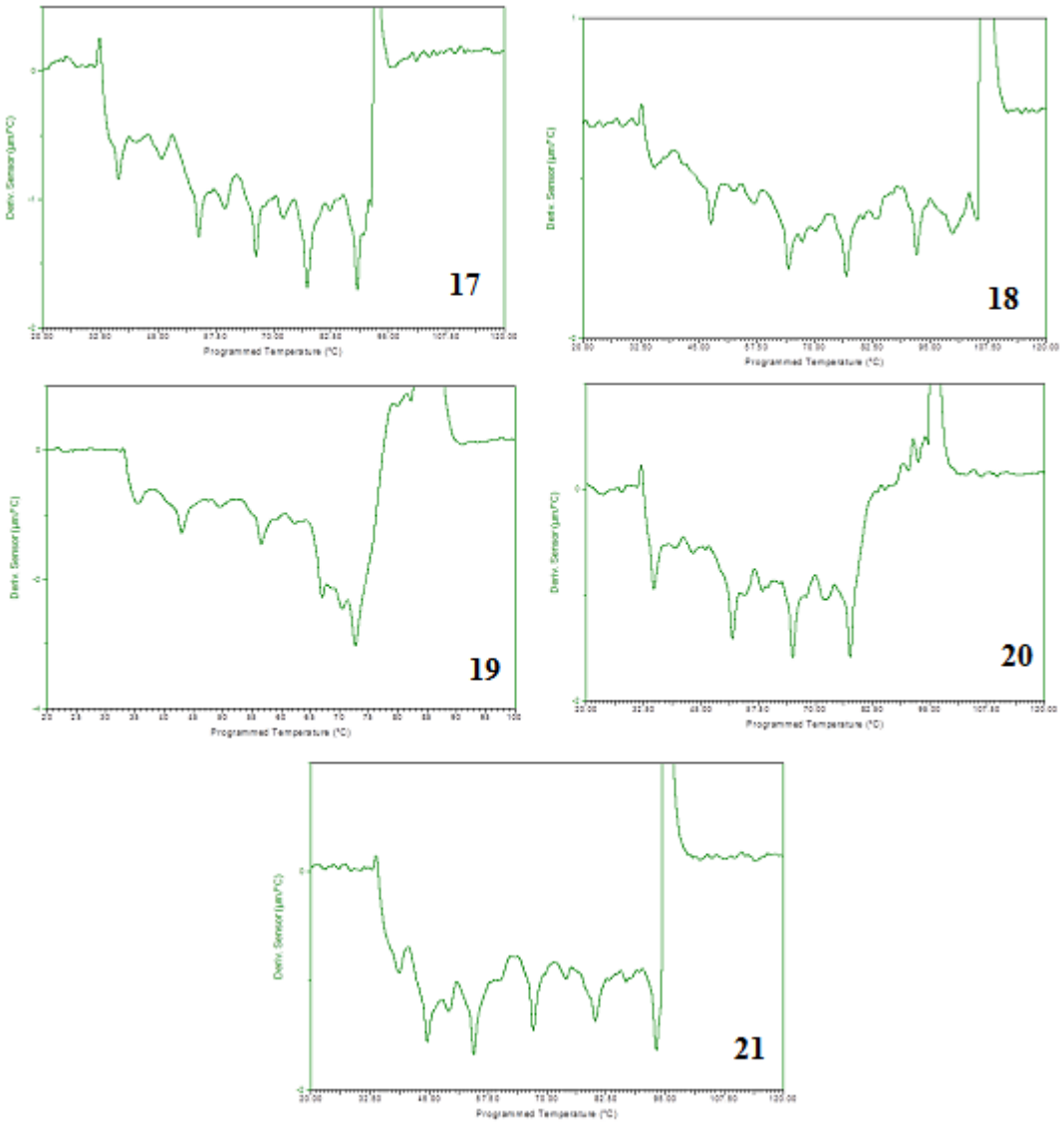

Figure 5.23 - LTA traces of affected areas of the live Field Bean leaf, affected by TEHP

LTA trace 2, figure 5.21, does show the cuticle has been affected by TEHP, showing a plasticizing effect, with the transitions occurring within 42.4 – 60.0 °C. Compared to the unaffected LTA traces, which range from 100 – 125 °C. Though, this was the only trace that should this type of result. The other thermographs so a slight decrease compared with the unaffected traces, though the thermal profiles still look similar to the unaffected.

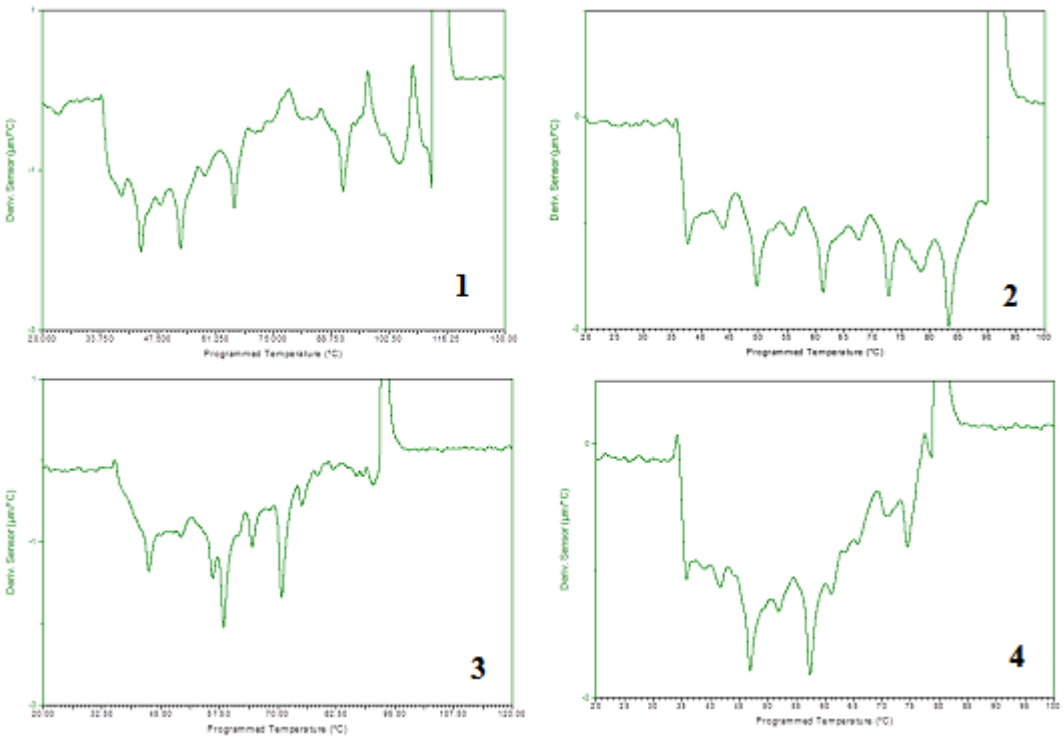

Figure 5.24 - LTA traces of unaffected live Field Bean leaf surface, for Brij 98.

Figure 5.24 shows the unaffected LTA traces for Brij 98, with characterization of the leaf away from the droplet to allow comparison to effected area traces. The traces, 1 – 4, show the end of the trace to end between 75 – 115 °C. The thermographs of the uneffaced areas show the same traces as the unaffected area for the TEHP study and the live leaf study in the previous section, though with lower end temperatures.

LTA was then performed on the leaf surface inside the droplet area after drying. The CCD camera of the SThM shows the same as previously stated, that the drying of Brij 98 solution produces a “coffee” ring effect. LTA was performed across the thin rim of the deposit, but since it was thin measurements were recorded around to rim at random distances apart to allow further comparison of traces, these are show in figure 5.25 and 5.26.

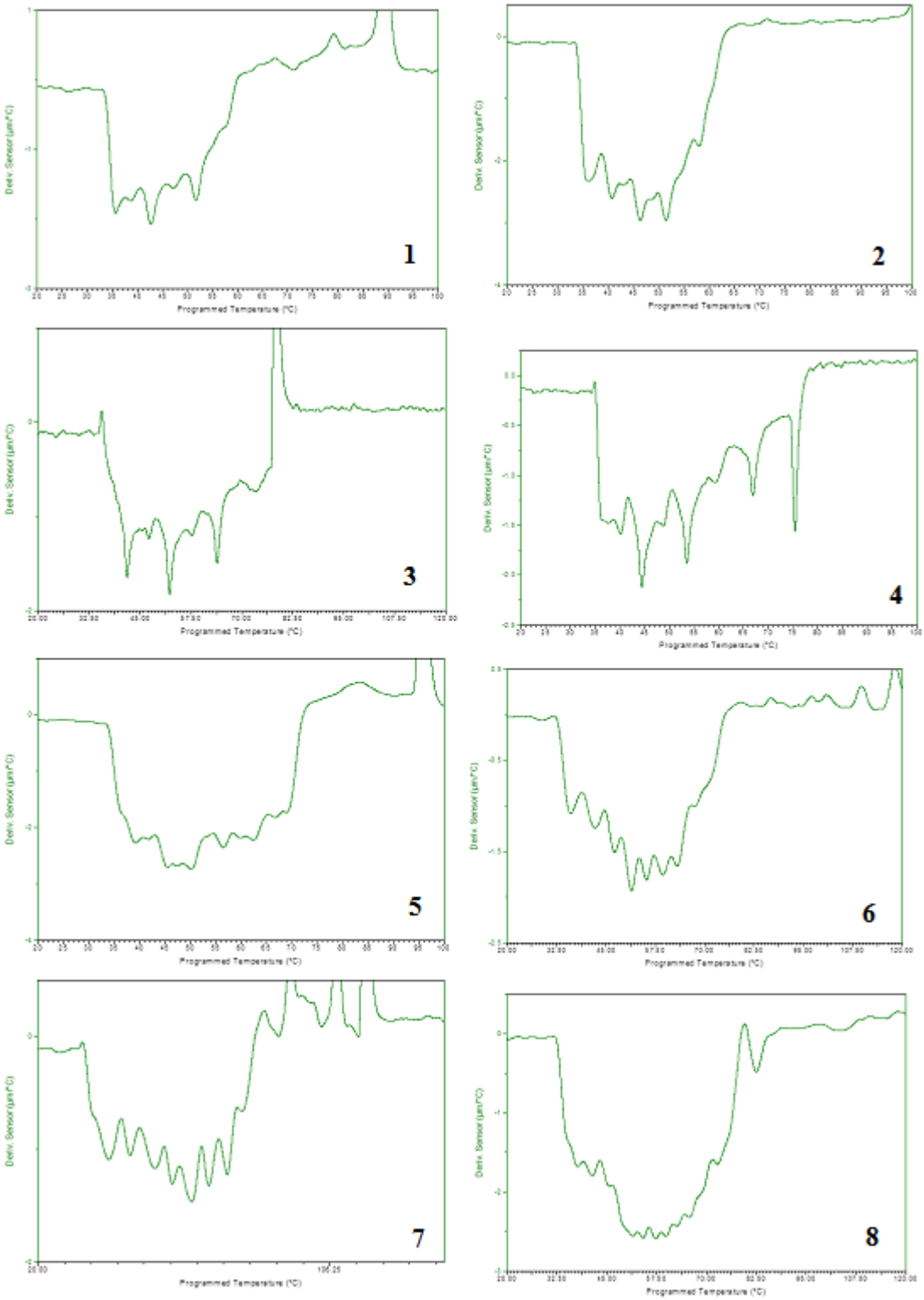

Figure 5.25 - LTA traces of affected live Field Bean leaf surface, affected by Brij 98.

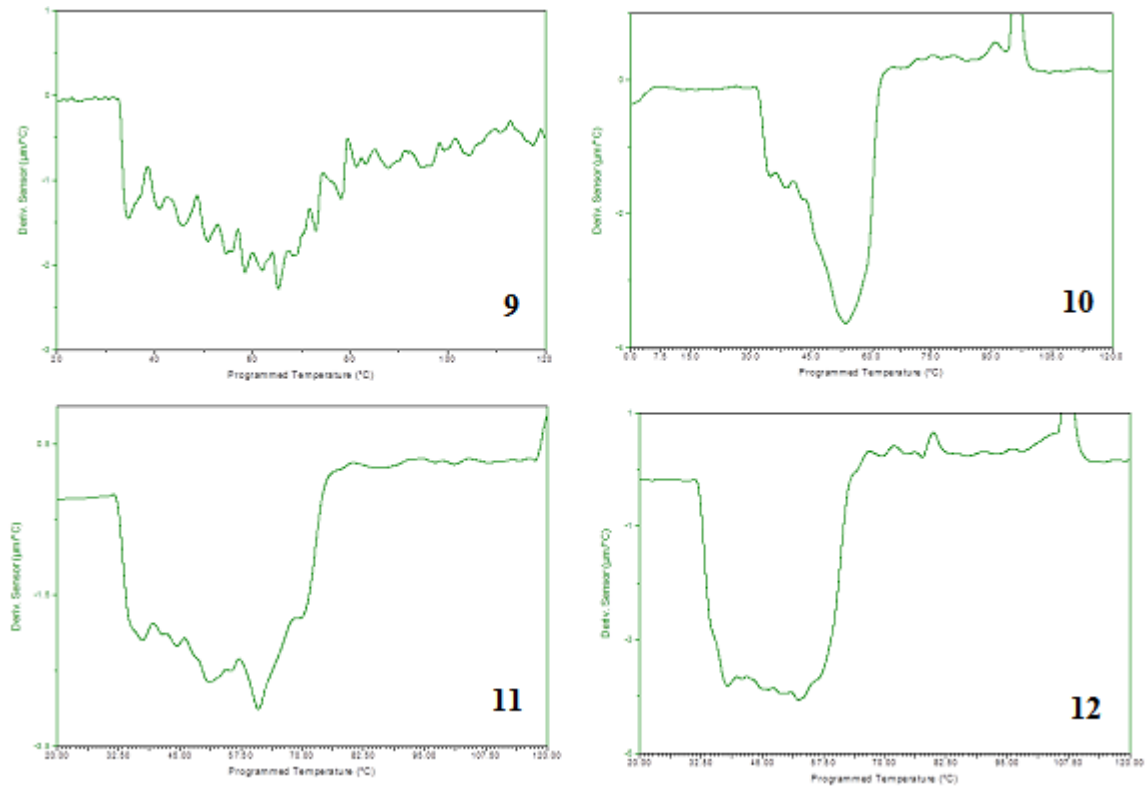

Figure 5.26 - LTA traces of affected live Field Bean leaf surface, affected by Brij 98

The LTA traces from the affected area shows the effect of the surfactant on the T_m of the cuticle. The trace shows the surfactant has produced a trace that seems to appear as one large transition, this is shown is traces 8, 10 and 12. Trace 12 transitions starts from 37.4 °C and continues to 54.5 °C. This type of thermal profile could be the result of the solubilisation of the cuticle resulting in a mixture of varying fatty acid chain lengths. The traces that don't show this type of profile still show to be affected by Brij 98, this is seen with the lowering end point temperature, compared with the unaffected areas.

5.5 Conclusion

These experiments have focused on the understanding of the phase transitions of the cuticle on living leaf organ, and for the case of English Ivy a representation of live. The phase transitions of the different leaf surfaces and leaf states do show significant differences, not just between different leaves but also different states. The difference traces observed for different leaf surface can be attributed to different chemical and structural compositions (Jeffree, 2006). The English Ivy, for example, has a crystallinity at 25 °C to be between 69 – 80 % (Merk et al., 1998).

The differences between the states measured are the result of the presence of water. Water as a plasticizing effect, which is seen in the literature and with these experiments (Dominguez et al., 2011b, Dominguez et al., 2011a). This is observed with the LTA traces between different leaf states, like Field Bean, showing T_m as high has 100 – 125 °C, being reduced to below ~ 75 °C. This is also seen with English Ivy, though when fresh more transitions are observed.

There is also, by comparison, a change in the thermal profiles of the dried and live/fresh leaf surfaces. These differences of the traces between dried to wet is not explained by the plasticizing effect. An example of this is English Ivy, when dry you observed two peaks the T_m and the solid-solid transition, when water was present multiple transitions were observed. DSC studies on isolated cuticles that were hydrated still have not shown this differences (Perkins et al., 2005a) or on wax models of the cuticle (Fagerstrom et al., 2013). This could be because of the inherent disadvantages of the models used, the simplification of binary and ternary systems of chemical compounds (Fagerstrom et al., 2014, Fagerstrom et al., 2013), resulting in only a few structures being formed. It could also be because the movement of water might play impact the structure of wax crystal formation in the cuticle. It

was shown that it was possible for the movement of water through a polymer membrane to move waxes through and allow self-assembly on the surface (Neinhuis et al., 2001). Tough if water was able to separate and accumulate waxes of similar chain lengths in the cuticle the process would be unknown.

There are two main peaks that are observed in the thermographs, these are the solid-solid interactions and T_m. The solid-solid transitions are shown throughout the literature has orthorhombic to a hexagonal crystal lattice structure (Reynhardt and Riederer, 1994, Reynhardt, 1997, Fagerstrom et al., 2013) of various waxes and mixtures of aliphatic compounds. The trace with multiple solid-solid transitions must have been the result of crystal with similar chemical makeup. Though with different temperature the crystal must have been composed of different chain lengths but compose the same crystalline structure.

The added phase transitions of the traces of the live leaves are more challenging to ascertain the type of transition, which could make characterisation of living leaf cuticle and agrochemicals difficult. Though the information gained from studying the interaction of adjuvants with a live leaf might provide further insight into the interaction of the cuticle with chemicals.

Initial experiments focused on the imaging of the live Field Bean surface, to compare the impact of different adjuvants on the surface with that of an unaffected leaf. TM-AFM showed that the unaffected live leaf had variations in height across the cuticle with the phase imaging showing these are the result of globular wax build up. These are not EW crystals because it is reported that the Field Bean has little or no EW layer (Jeffree, 2006), suggesting they are the result of the IW. It was also observed that the surface did not have any smooth regions.

The affected leaf surfaces showed that the globular wax feature were not visible and that regions of smooth topographically flat surface were seen. This suggests that the adjuvants had an effect on entire surface either by removing these features has the droplet dried. The other suggestion is that the solution with the adjuvant dissolved the waxes and redeposit them as the droplet dries as the adjuvants collected into areas.

The TM-AFM of the surface affected by TEHP and Brij 98 both show that the surface differences between each other. The smooth areas of both affected leaves are considered to show the largest impact of the adjuvants, with the majority of the adjuvant penetrating into the cuticle there. That would increase the plasticizing effect, making the area more fluidic and, by association, smoother (Riederer et al., 1995).The smooth areas of the images are different depending on the adjuvant used, TEHP solution resulted in large areas of uptake into the cuticle. While the surfactant Brij 98 resulted in frequent small areas. The reason for this might be because of the compounds partition coefficient, TEHP is not soluble is water. The adjuvant would precipitate out of solution during drying and with micelles forming (Attwood et al., 1989). Brij 98 “coffee” ring effect shows the majority of the surfactant is being carried to the edge of the droplet before the droplet fully dries. This is caused by continuous capillary flow of liquid from the centre from the centre of the droplet as it dries (Deegan et al., 1997, Nagel, 1999, Berteloot et al., 2012). This suggests the overall placement of solute onto the surface is controlled by droplet physics and solubility inside the droplet.

The thermal analysis of both adjuvants have shown that, TEHP and Brij 98, where the solution was deposited the adjuvant caused a depression in the T_m of the multiple transitions. The LTA trace of the affect TEHP area still resolves T_m on the cuticle surface. The transition temperature is still lower than what is observed for the native leaf showing it is an efficient plasticizer. The LTA measurements across the surface of the deposited area shows the same depression across the droplet area, there are some areas that show the same transition as the

native leaf. This shows the spreading ability of TEHP to also be efficient, with the LTA and TM-AFM showing the same observations, that there are some areas that are unaffected or have little effect from the TEHP plasticizer. This is good agreement with published literature on the uptake improvements of phosphoric acid ester (Shi et al., 2005, Schonherr et al., 2001)

Compared with the affected area of Brij 98, where the LTA trace shows one relatively large T_m something you would observe in an impure sample. This suggest that Brij 98 plasticizing effect is more efficient than TEHP. Studies with alcohol ethoxylates have shown uptake of lipophilic compounds are more efficient with lower levels of ethoxylation (Baur et al., 1997b, Baur et al., 1999b). Brij 98 is a large ethoxylated compound. Thought the trace suggest that plasticizing, which effects solubility and mobility, ability is efficient. The LTA measurements across the small rim and inside the rim show there are only small variations in the range of the large T_m observed. LTA measurements were also performed inside the droplet area but away from the rim, these showed no depression in T_m and no plasticizing effect. This shows the spreading ability of the Brij 98 solution to be poor, which might explain the low uptake of lipophilic compounds in other studies.

The overall aim of these experiments was to utilise TM-AFM and LTA was to investigate the possibility of live leaf imaging and characterisation. TM-AFM was able to image live leave surface, which has been achieved before (Koch et al., 2004) showing the regeneration of EW on the cuticle, these experiments were for assessing the usefulness of live leaf imaging for agrochemical studies. TM-AFM as provided insight to how spreading occurred with the two adjuvants and was able to observe the differences between them. LTA of live leaf surfaces, that the multiple transitions of the surface might be too complex to perform live studies. The LTA measurements of TEHP and Brij 98 have shown that this is not the case and it is possible, by comparison, to investigate agrochemicals on live leaf surfaces.

Chapter 6

Conclusions

6.1 Thesis conclusions

6.1.1 SICM and its uses in leaf imaging and characterisation

The main aim of this thesis was to perform imaging with the SICM and to investigate the uses of the technique to image and characterise the leaf surface. SICM was able to image a number of different leaf surfaces, including featureless surfaces like English Ivy and Sugar beet, which still have large variation in topology. It imaged the Strawberry leaf surface which AFM could not because of the trichromes would interact with the cantilever before the tip touched the surface, preventing imaging. Showing the fragile small filament features. Also, was able to image hydrophobic surfaces like *Festuca* grass, Pea and Oil Seed Rape. Showing that the gas/liquid interface could be imaged and the possible study of wetting can be performed with SICM.

The comparison of SICM with conventional techniques like SEM and AFM showed the disadvantage and advantages of all the techniques for leaf imaging. SEM with the ease of imaging and speed to investigate many surfaces in a small-time frame is ideal for complimentary imaging. The need to coat and perform imaging under vacuum precluded live leaf studies, this is why we utilised SICM and AFM. AFM compared with SICM had better lateral and vertical resolution, but the non-contact nature of SICM can image delicate features with damaging them. The SICM was able to image large variations in height, while the AFM could not. SICM disadvantage is speed of imaging being significantly slower than that of AFM. The SICM was also able to image topographical features which was not seen in corresponding AFM images, this was shown with the English Ivy stomata. The double wax chimney surrounding the stomata was resolved in SICM while absent in AFM, this is because of how the cantilever can interact with the leaf surface which produces artefacts.

SICM was also used to perform *in-situ* experiments of formulations drying to image the effect or not, in this case, this would have on the cuticle surface. This showed that the SICM could be used in a solution with large number of other compounds and still image, with few image artefacts being produced.

6.1.2 Imaging wetting

The SICM ability to image the gas/liquid interface without disruption allowed the study of wetting between a droplet and the pea leaf. The experiment showed the droplet sits on the surface between a Wenzel and a Cassie-Baxter regime. This is where the droplet has wetted between the platelet features of the pea leaf in one area and in another rests upon them. The imaging also showed that the droplet traps pockets of air between the platelet features of the Pea leaf and also the topographical variations of the cuticle. This creates two different sized bubbles; one set are very being between the features and the other being microns in size.

A surfactant, Tween 20, was used to perform an *in-situ* wetting experiment to image the effects of the surfactant and changes to the wetting regime. The SICM was able to image the transition between one wetting regimes to another. Showing a collapse of one of the micro bubbles, with the surface of the Pea leaf being imaged there after

6.1.3 Thermal profiling of live leaf cuticles

The second area of focus for this thesis was to investigate live leaf imaging and characterisation. The requirement to keep the leaf living restricts the use of certain techniques, this includes any technique that require high vacuum like SEM or time of flight

mass spectrometry. The use of SPMs can be using to image and characterise live leaf surfaces and this was shown with both AFM and SThM. SThM with LTA was performed on two states of leaves, these were dried and living/fresh. This was to compare and assess the impact that water has on the cuticle. It was shown that water had a dramatic effect on the traces observed, with depress in phase transition when water was present. There was also another observed effect, the presence of water increased the complexity of the traces.

6.1.4 Adjuvant effects on live leaf surfaces.

TM-AFM was used to image the effects of two adjuvants on the surface of the Field Bean leaf and found that both had different impacts on the cuticle. This was attributed to the solutes solubility in the droplet and the precipitation of the solute while drying. This resulted in TEHP to spread across the entire deposited area, while Brij 98 resulted in the solute concentrating at the edge of the deposit. Resulting in different spreading observed for both adjuvants.

LTA measurement were used to compare the effectiveness of the adjuvants to plasticize the cuticle. With the adjuvants showing similar results. The results from the experiments shows that live leaf imaging and characterisation can aid in the understanding of different formulation compounds. With the ability to compare and contrast between them, allowing to develop formulation according to the leaf.

6.1.5 Final comments

This thesis has shown that the SICM technique has potential to provide insight into different aspects of agrochemical studies. The wetting experiments also could be used for the

development and testing of new materials designed to have certain wetting properties and relate the surface structure to these properties. Live leaf studying has shown that the leaf cuticle is a dynamic barrier, with water playing a significant part in the structure, and therefore properties, of the cuticle.

Chapter 7

References

ATTWOOD, D., ELWORTHY, P. H. & LAWRENCE, M. J. 1989. EFFECT OF STRUCTURAL VARIATIONS OF NON-IONIC SURFACTANTS ON MICELLAR PROPERTIES AND SOLUBILIZATION - SURFACTANTS WITH SEMI-POLAR HYDROPHOBES. *Journal of Pharmacy and Pharmacology,* 41**,** 585-589.

BABAKINEJAD, B., JONSSON, P., CORDOBA, A. L., ACTIS, P., NOVAK, P., TAKAHASHI, Y., SHEVCHUK, A., ANAND, U., ANAND, P., DREWS, A., FERRER-MONTIEL, A., KLENERMAN, D. & KORCHEV, Y. E. 2013. Local Delivery of Molecules from a Nanopipette for Quantitative Receptor Mapping on Live Cells. *Analytical Chemistry,* 85**,** 9333-9342.

BARGEL, H., KOCH, K., CERMAN, Z. & NEINHUIS, C. 2006. Structure-function relationships of the plant cuticle and cuticular waxes - a smart material? *Functional Plant Biology,* 33**,** 893-910.

BARGEL, H. & NEINHUIS, C. 2005. Tomato (Lycopersicon esculentum Mill.) fruit growth and ripening as related to the biomechanical properties of fruit skin and isolated cuticle. *Journal of Experimental Botany,* 56**,** 1049-1060.

BARTHLOTT, W., NEINHUIS, C., CUTLER, D., DITSCH, F., MEUSEL, I., THEISEN, I. & WILHELMI, H. 1998. Classification and terminology of plant epicuticular waxes. *Botanical Journal of the Linnean Society,* 126**,** 237-260.

BARTHLOTT, W., SCHIMMEL, T., WIERSCH, S., KOCH, K., BREDE, M., BARCZEWSKI, M., WALHEIM, S., WEIS, A., KALTENMAIER, A., LEDER, A. & BOHN, H. F. 2010. The Salvinia Paradox: Superhydrophobic Surfaces with Hydrophilic Pins for Air Retention Under Water. *Advanced Materials,* 22**,** 2325-2328.

BAUR, P., BUCHHOLZ, A. & SCHONHERR, J. 1997a. Diffusion in plant cuticles as affected by temperature and size of organic solutes: similarity and diversity among species. *Plant Cell and Environment,* 20**,** 982-994.

BAUR, P., GRAYSON, B. T. & SCHONHERR, J. 1997b. Polydisperse ethoxylated fatty alcohol surfactants as accelerators of cuticular penetration .1. Effects of ethoxy chain length and the size of the penetrants. *Pesticide Science,* 51**,** 131-152.

BAUR, P., MARZOUK, H. & SCHONHERR, J. 1999a. Estimation of path lengths for diffusion of organic compounds through leaf cuticles. *Plant Cell and Environment,* 22**,** 291-299.

BAUR, P., MARZOUK, H., SCHONHERR, J. & BAUER, H. 1996. Mobilities of organic compounds in plant cuticles as affected by structure and molar volumes of chemicals and plant species. *Planta,* 199**,** 404-412.

BAUR, P., SCHONHERR, J. & GRAYSON, B. T. 1999b. Polydisperse ethoxylated fatty alcohol surfactants as accelerators of cuticular penetration. 2: Separation of effects on driving force and mobility and reversibility of surfactant action. *Pesticide Science,* 55**,** 831-842.

BAYLIS, A. D. 2000. Why glyphosate is a global herbicide: strengths, weaknesses and prospects. *Pest Management Science,* 56**,** 299-308.

BENSALEM-FNAYOU, A., JELLOULI, N., BOUAMAMA, B., MLIKI, A. & GHORBEL, A. 2009. Investigations on the Leaf Surface Ultrastructure in Grapevine (Vitis vinifera L.) by Scanning Microscopy. *Scanning,* 31**,** 127-131.

BERTELOOT, G., HOANG, A., DAERR, A., KAVEHPOUR, H. P., LEQUEUX, F. & LIMAT, L. 2012. Evaporation of a sessile droplet: Inside the coffee stain. *Journal of Colloid and Interface Science,* 370**,** 155-161.

BHUSHAN, B. 2005. Nanotribology and nanomechanics. *Wear,* 259**,** 1507-1531.

BHUSHAN, B. & JUNG, Y. C. 2006. Micro- and nanoscale characterization of hydrophobic and hydrophilic leaf surfaces. *Nanotechnology,* 17**,** 2758-2772.

BINNIG, G., QUATE, C. F. & GERBER, C. 1986. ATOMIC FORCE MICROSCOPE. *Physical Review Letters,* 56**,** 930-933.

BIRKS, L. S. & BROOKS, E. J. 1957. ELECTRON PROBE X-RAY MICROANALYZER. *Review of Scientific Instruments,* 28**,** 709-712.

BOOM, A., DAMSTE, J. S. S. & DE LEEUW, J. W. 2005. Cutan, a common aliphatic biopolymer in cuticles of drought-adapted plants. *Organic Geochemistry,* 36**,** 595-601.

BRUCKBAUER, A., YING, L. M., ROTHERY, A. M., ZHOU, D. J., SHEVCHUK, A. I., ABELL, C., KORCHEV, Y. E. & KLENERMAN, D. 2002. Writing with DNA and protein using a nanopipet for controlled delivery. *Journal of the American Chemical Society,* 124**,** 8810-8811.

BUCHHOLZ, A. 2006. Characterization of the diffusion of non-electrolytes across plant cuticles: properties of the lipophilic pathway. *Journal of Experimental Botany,* 57**,** 2501-2513.

BUCHHOLZ, A., BAUR, P. & SCHONHERR, J. 1998. Differences among plane species in cuticular permeabilities and solute mobilities are not caused by differential size selectivities. *Planta,* 206**,** 322-328.

BUCHHOLZ, A. & SCHONHERR, J. 2000. Thermodynamic analysis of diffusion of non-electrolytes across plant cuticles in the presence and absence of the plasticiser tributyl phosphate. *Planta,* 212**,** 103-111.

BURGHARDT, M., SCHREIBER, L. & RIEDERER, M. 1998. Enhancement of the diffusion of active ingredients in barley leaf cuticular wax by monodisperse alcohol ethoxylates. *Journal of Agricultural and Food Chemistry,* 46**,** 1593-1602.

BURTON, Z. & BHUSHAN, B. 2006. Surface characterization and adhesion and friction properties of hydrophobic leaf surfaces. *Ultramicroscopy,* 106**,** 709-719.

BUSCHHAUS, C., HERZ, H. & JETTER, R. 2007. Chemical composition of the epicuticular and intracuticular wax layers on adaxial sides of Rosa canina leaves. *Annals of Botany,* 100**,** 1557-1564.

BUSCHHAUS, C. & JETTER, R. 2011. Composition differences between epicuticular and intracuticular wax substructures: How do plants seal their epidermal surfaces? *Journal of Experimental Botany,* 62**,** 841-853.

BUSSOTTI, F. & GROSSONI, P. 1997. European and Mediterranean oaks (Quercus L; Fagaceae): SEM characterization of the micromorphology of the abaxial leaf surface. *Botanical Journal of the Linnean Society,* 124**,** 183-199.

CANET, D., ROHR, R., CHAMEL, A. & GUILLAIN, F. 1996. Atomic force microscopy study of isolated ivy leaf cuticles observed directly and after embedding in Epon(R). *New Phytologist,* 134**,** 571-577.

CASTRO, M. J. L., OJEDA, C. & CIRELLI, A. F. 2014. Advances in surfactants for agrochemicals. *Environmental Chemistry Letters,* 12**,** 85-95.

CHAMEL, A., PINERI, M. & ESCOUBES, M. 1991. QUANTITATIVE-DETERMINATION OF WATER SORPTION BY PLANT CUTICLES. *Plant Cell and Environment,* 14**,** 87-95.
CHEN, X., DAVIES, M. C., ROBERTS, C. J., TENDLER, S. J. B., WILLIAMS, P. M., DAVIES, J., DAWKES, A. C. & EDWARDS, J. C. 1998. Interpretation of tapping mode atomic force microscopy data using amplitude-phase-distance measurements. *Ultramicroscopy,* 75**,** 171-181.
DEEGAN, R. D., BAKAJIN, O., DUPONT, T. F., HUBER, G., NAGEL, S. R. & WITTEN, T. A. 1997. Capillary flow as the cause of ring stains from dried liquid drops. *Nature,* 389**,** 827-829.
DEGENNES, P. G. 1985. WETTING - STATICS AND DYNAMICS. *Reviews of Modern Physics,* 57**,** 827-863.
DEL LINZ, S., WILLMAN, E., CALDWELL, M., KLENERMAN, D., FERNANDEZ, A. & MOSS, G. 2014. Contact-Free Scanning and Imaging with the Scanning Ion Conductance Microscope. *Analytical Chemistry,* 86**,** 2353-2360.
DELCHEVA, I., RALSTON, J., BEATTIE, D. A. & KRASOWSKA, M. 2015. Static and dynamic wetting behaviour of ionic liquids. *Advances in Colloid and Interface Science,* 222**,** 162-171.
DESHMUKH, A. P., SIMPSON, A. J., HADAD, C. M. & HATCHER, P. G. 2005. Insights into the structure of cutin and cutan from Agave americana leaf cuticle using HRMAS NMR spectroscopy. *Organic Geochemistry,* 36**,** 1072-1085.
DOMINGUEZ, E., CUARTERO, J. & HEREDIA, A. 2011a. An overview on plant cuticle biomechanics. *Plant Science,* 181**,** 77-84.
DOMINGUEZ, E., ESPANA, L., LOPEZ-CASADO, G., CUARTERO, J. & HEREDIA, A. 2009. Biomechanics of isolated tomato (Solanum lycopersicum) fruit cuticles during ripening: the role of flavonoids. *Functional Plant Biology,* 36**,** 613-620.
DOMINGUEZ, E., HEREDIA-GUERRERO, J. A. & HEREDIA, A. 2011b. The biophysical design of plant cuticles: an overview. *New Phytologist,* 189**,** 938-949.
DOUBLET, J., MAMY, L. & BARRIUSO, E. 2009. Delayed degradation in soil of foliar herbicides glyphosate and sulcotrione previously absorbed by plants: Consequences on herbicide fate and risk assessment. *Chemosphere,* 77**,** 582-589.
EDWARDS, M. A., WILLIAMS, C. G., WHITWORTH, A. L. & UNWIN, P. R. 2009. Scanning Ion Conductance Microscopy: a Model for Experimentally Realistic Conditions and Image Interpretation. *Analytical Chemistry,* 81**,** 4482-4492.
EICHERT, T. & BURKHARDT, J. 2001. Quantification of stomatal uptake of ionic solutes using a new model system. *Journal of Experimental Botany,* 52**,** 771-781.
EICHERT, T. & GOLDBACH, H. E. 2008. Equivalent pore radii of hydrophilic foliar uptake routes in stomatous and astomatous leaf surfaces - further evidence for a stomatal pathway. *Physiologia Plantarum,* 132**,** 491-502.
EICHERT, T., KURTZ, A., STEINER, U. & GOLDBACH, H. E. 2008. Size exclusion limits and lateral heterogeneity of the stomatal foliar uptake pathway for aqueous solutes and water-suspended nanoparticles. *Physiologia Plantarum,* 134**,** 151-160.
ERBIL, H. Y. 2012. Evaporation of pure liquid sessile and spherical suspended drops: A review. *Advances in Colloid and Interface Science,* 170**,** 67-86.
FAGERSTROM, A., KOCHERBITOV, V., WESTBYE, P., BERGSTROM, K., ARNEBRANT, T. & ENGBLOM, J. 2014. Surfactant softening of plant leaf cuticle model wax - A Differential Scanning Calorimetry (DSC) and Quartz Crystal Microbalance with Dissipation (QCM-D) study. *Journal of Colloid and Interface Science,* 426**,** 22-30.

FAGERSTROM, A., KOCHERBITOV, V., WESTBYE, P., BERGSTROM, K., MAMONTOVA, V. & ENGBLOM, J. 2013. Characterization of a plant leaf cuticle model wax, phase behaviour of model wax-water systems. *Thermochimica Acta,* 571**,** 42-52.

FARRIS, S., INTROZZI, L., BIAGIONI, P., HOLZ, T., SCHIRALDI, A. & PIERGIOVANNI, L. 2011. Wetting of Biopolymer Coatings: Contact Angle Kinetics and Image Analysis Investigation. *Langmuir,* 27**,** 7563-7574.

FENG, L., ZHANG, Y. A., XI, J. M., ZHU, Y., WANG, N., XIA, F. & JIANG, L. 2008. Petal effect: A superhydrophobic state with high adhesive force. *Langmuir,* 24**,** 4114-4119.

FOY, C. L. 1964. FOLIAR PENETRATION - REVIEW OF HERBICIDE PENETRATION THROUGH PLANT SURFACES. *Journal of Agricultural and Food Chemistry,* 12**,** 473-&.

FRITZ, M., RADMACHER, M. & GAUB, H. E. 1993. INVITRO ACTIVATION OF HUMAN PLATELETS TRIGGERED AND PROBED BY ATOMIC FORCE MICROSCOPY. *Experimental Cell Research,* 205**,** 187-190.

GASKIN, R. E. & HOLLOWAY, P. J. 1992. SOME PHYSICOCHEMICAL FACTORS INFLUENCING FOLIAR UPTAKE ENHANCEMENT OF GLYPHOSATE-MONO(ISOPROPYLAMMONIUM) BY POLYOXYETHYLENE SURFACTANTS. *Pesticide Science,* 34**,** 195-206.

GMELIN, E., FISCHER, R. & STITZINGER, R. 1998. Sub-micrometer thermal physics - An overview on SThM techniques. *Thermochimica Acta,* 310**,** 1-17.

GNIWOTTA, F., VOGG, G., GARTMANN, V., CARVER, T. L. W., RIEDERER, M. & JETTER, R. 2005. What do microbes encounter at the plant surface ? Chemical composition of pea leaf cuticular waxes. *Plant Physiology,* 139**,** 519-530.

GOURET, E., ROHR, R. & CHAMEL, A. 1993. ULTRASTRUCTURE AND CHEMICAL-COMPOSITION OF SOME ISOLATED PLANT CUTICLES IN RELATION TO THEIR PERMEABILITY TO THE HERBICIDE, DIURON. *New Phytologist,* 124**,** 423-431.

GREEN, J. M. & BEESTMAN, G. B. 2007. Recently patented and commercialized formulation and adjuvant technology. *Crop Protection,* 26**,** 320-327.

HAMILTON, R. J. 1993. STRUCTURE AND GENERAL-PROPERTIES OF MINERAL AND VEGETABLE-OILS USED AS SPRAY ADJUVANTS. *Pesticide Science,* 37**,** 141-146.

HAMMICHE, A., HOURSTON, D. J., POLLOCK, H. M., READING, M. & SONG, M. 1996a. Scanning thermal microscopy: Subsurface imaging, thermal mapping of polymer blends, and localized calorimetry. *Journal of Vacuum Science & Technology B,* 14**,** 1486-1491.

HAMMICHE, A., READING, M., POLLOCK, H. M., SONG, M. & HOURSTON, D. J. 1996b. Localized thermal analysis using a miniaturized resistive probe. *Review of Scientific Instruments,* 67**,** 4268-4274.

HANSMA, P. K., DRAKE, B., MARTI, O., GOULD, S. A. C. & PRATER, C. B. 1989. THE SCANNING ION-CONDUCTANCE MICROSCOPE. *Science,* 243**,** 641-643.

HEREDIA, A. 2003. Biophysical and biochemical characteristics of cutin, a plant barrier biopolymer. *Biochimica Et Biophysica Acta-General Subjects,* 1620**,** 1-7.

HOLLOWAY, P. J. 1969. EFFECTS OF SUPERFICIAL WAX ON LEAF WETTABILITY. *Annals of Applied Biology,* 63**,** 145-&.

HOLLOWAY, P. J. 1993. Structure and chemistry of plant cuticles. *Pesticide Science,* 37**,** 203-206.

JEFFREE, C. E. 1996. Structure and ontogeny of plant cuticles. *In:* KERSTIENS, G. (ed.) *Environmental Plant Biology Series; Plant cuticles: An integrated functional approach.* BIOS Scientific Publishers Ltd., St. Thomas House, Becket Street, Oxford OX1 ISJ, England; BIOS Scientific Publishers, P. O. Box 605, Herndon, Virginia 20172-0605.

JEFFREE, C. E. 2006. The fine structure of the plant cuticle. *In:* RIEDERER, M. & MULLER, C. (eds.) *Biology of the Plant Cuticle.* Blackwell Publishing.

JEFFREE, C. E., BAKER, E. A. & HOLLOWAY, P. J. 1975. ULTRASTRUCTURE AND RECRYSTALLIZATION OF PLANT EPICUTICULAR WAXES. *New Phytologist,* 75**,** 539-+.

JETTER, R., KUNST, L. & SAMUELS, A. L. 2006. Composition of plant cuticular waxes. *In:* RIEDERER, M. & MULLER, C. (eds.) *Biology of the Plant Cuticle.* Blackwell Publishing.

JETTER, R. & SCHAFFER, S. 2001. Chemical composition of the Prunus laurocerasus leaf surface. Dynamic changes of the epicuticular wax film during leaf development. *Plant Physiology,* 126**,** 1725-1737.

JETTER, R., SCHAFFER, S. & RIEDERER, M. 2000. Leaf cuticular waxes are arranged in chemically and mechanically distinct layers: evidence from Prunus laurocerasus L. *Plant Cell and Environment,* 23**,** 619-628.

JUNG, Y. C. & BHUSHAN, B. 2007. Wetting transition of water droplets on superhydrophobic patterned surfaces. *Scripta Materialia,* 57**,** 1057-1060.

KASAS, S., THOMSON, N. H., SMITH, B. L., HANSMA, P. K., MIKLOSSY, J. & HANSMA, H. G. 1997. Biological applications of the AFM: From single molecules to organs. *International Journal of Imaging Systems and Technology,* 8**,** 151-161.

KERSTIENS, G. 2006. Water transport in plant cuticles: an update. *Journal of Experimental Botany,* 57**,** 2493-2499.

KIM, K. W., AHN, J. J. & LEE, J. H. 2009. Micromorphology of epicuticular wax structures of the garden strawberry leaves by electron microscopy: Syntopism and polymorphism. *Micron,* 40**,** 327-334.

KINOSHITA, T., DOI, M., SUETSUGU, N., KAGAWA, T., WADA, M. & SHIMAZAKI, K. 2001. phot1 and phot2 mediate blue light regulation of stomatal opening. *Nature,* 414**,** 656-660.

KIRKWOOD, R. C. 1999. Recent developments in our understanding of the plant cuticle as a barrier to the foliar uptake of pesticides. *Pesticide Science,* 55**,** 69-77.

KOCH, K. & BARTHLOTT, W. 2009. Superhydrophobic and superhydrophilic plant surfaces: an inspiration for biomimetic materials. *Philosophical Transactions of the Royal Society a-Mathematical Physical and Engineering Sciences,* 367**,** 1487-1509.

KOCH, K., BARTHLOTT, W., KOCH, S., HOMMES, A., WANDELT, K., MAMDOUH, W., DE-FEYTER, S. & BROEKMANN, P. 2006. Structural analysis of wheat wax (Triticum aestivum, c.v. 'Naturastar' L.): from the molecular level to three dimensional crystals. *Planta,* 223**,** 258-270.

KOCH, K., BHUSHAN, B. & BARTHLOTT, W. 2008. Diversity of structure, morphology and wetting of plant surfaces. *Soft Matter,* 4**,** 1943-1963.

KOCH, K., BHUSHAN, B., ENSIKAT, H. J. & BARTHLOTT, W. 2009a. Self-healing of voids in the wax coating on plant surfaces. *Philosophical Transactions of the Royal Society a-Mathematical Physical and Engineering Sciences,* 367**,** 1673-1688.

KOCH, K., DOMMISSE, A., NIEMIETZ, A., BARTHLOTT, W. & WANDELT, K. 2009b. Nanostructure of epicuticular plant waxes: Self-assembly of wax tubules. *Surface Science,* 603**,** 1961-1968.

KOCH, K. & ENSIKAT, H. J. 2008. The hydrophobic coatings of plant surfaces: Epicuticular wax crystals and their morphologies, crystallinity and molecular self-assembly. *Micron,* 39**,** 759-772.
KOCH, K., NEINHUIS, C., ENSIKAT, H. J. & BARTHLOTT, W. 2004. Self assembly of epicuticular waxes on living plant surfaces imaged by atomic force microscopy (AFM). *Journal of Experimental Botany,* 55**,** 711-718.
KOLATTUKUDY, P. E. 1981. STRUCTURE, BIOSYNTHESIS, AND BIODEGRADATION OF CUTIN AND SUBERIN. *Annual Review of Plant Physiology and Plant Molecular Biology,* 32**,** 539-567.
KORCHEV, Y. E., BASHFORD, C. L., MILOVANOVIC, M., VODYANOY, I. & LAB, M. J. 1997. Scanning ion conductance microscopy of living cells. *Biophysical Journal,* 73**,** 653-658.
LEE, K. S., IVANOVA, N., STAROV, V. M., HILAL, N. & DUTSCHK, V. 2008. Kinetics of wetting and spreading by aqueous surfactant solutions. *Advances in Colloid and Interface Science,* 144**,** 54-65.
LI, M., TANK, H., KENNEDY, A., ZHANG, H., DOWNER, B., OUSE, D. & LIU, L. 2013. Enlist Duo Herbicide: A Novel 2,4-D Plus Glyphosate Premix Formulation with Low Potential for Off-target Movement. *Pesticide Formulations and Delivery Systems: Innovating Legacy Products for New Uses, 32nd Volume,* 1558**,** 3-14.
LIU, X., YANG, X., ZHANG, B., ZHANG, X. F., LU, H. J., ZHANG, J. N. & ZHANG, Y. J. 2011. High-resolution morphological identification and characterization of living neuroblastoma SK-N-SH cells by hopping probe ion conductance microscopy. *Brain Research,* 1386**,** 35-40.
LUQUE, P., GAVARA, R. & HEREDIA, A. 1995. A STUDY OF THE HYDRATION PROCESS OF ISOLATED CUTICULAR MEMBRANES. *New Phytologist,* 129**,** 283-288.
MACEY, M. J. K. & BARBER, H. N. 1970. CHEMICAL GENETICS OF WAX FORMATION ON LEAVES OF PISUM-SATIVUM. *Phytochemistry,* 9**,** 5-&.
MACKERRON, D. K. L. 1976. WIND DAMAGE TO SURFACE OF STRAWBERRY LEAVES. *Annals of Botany,* 40**,** 351-&.
MANHEIM, B. S. & MULROY, T. W. 1978. TRITERPENOIDS IN EPICUTICULAR WAXES OF DUDLEYA SPECIES. *Phytochemistry,* 17**,** 1799-1800.
MARKSTADTER, C., FEDERLE, W., JETTER, R., RIEDERER, M. & HOLLDOBLER, B. 2000. Chemical composition of the slippery epicuticular wax blooms on Macaranga (Euphorbiaceae) ant-plants. *Chemoecology,* 10**,** 33-40.
MARMUR, A. 2003. Wetting on hydrophobic rough surfaces: To be heterogeneous or not to be? *Langmuir,* 19**,** 8343-8348.
MARMUR, A. 2004. The lotus effect: Superhydrophobicity and metastability. *Langmuir,* 20**,** 3517-3519.
MCKINNEY, D. E., BORTIATYNSKI, J. M., CARSON, D. M., CLIFFORD, D. J., DELEEUW, J. W. & HATCHER, P. G. 1996. Tetramethylammonium hydroxide (TMAH) thermochemolysis of the aliphatic biopolymer cutan: Insights into the chemical structure. *Organic Geochemistry,* 24**,** 641-650.
MCLELLAN, T. 2005. Correlated evolution of leaf shape and trichomes in Begonia dregei (Begoniaceae). *American Journal of Botany,* 92**,** 1616-1623.
MCMULLAN, D. 1995. SCANNING ELECTRON-MICROSCOPY 1928-1965. *Scanning,* 17**,** 175-185.
MERK, S., BLUME, A. & RIEDERER, M. 1998. Phase behaviour and crystallinity of plant cuticular waxes studied by Fourier transform infrared spectroscopy. *Planta,* 204**,** 44-53.

MOULINET, S. & BARTOLO, D. 2007. Life and death of a fakir droplet: Impalement transitions on superhydrophobic surfaces. *European Physical Journal E,* 24**,** 251-260.
NAGEL, S. R. 1999. Klopsteg Memorial Lecture (August, 1998): Physics at the breakfast table - or waking up to physics. *American Journal of Physics,* 67**,** 17-25.
NAIR, R., VARGHESE, S. H., NAIR, B. G., MAEKAWA, T., YOSHIDA, Y. & KUMAR, D. S. 2010. Nanoparticulate material delivery to plants. *Plant Science,* 179**,** 154-163.
NAIRN, J. J., FORSTER, W. A. & VAN LEEUWEN, R. M. 2011. Quantification of physical (roughness) and chemical (dielectric constant) leaf surface properties relevant to wettability and adhesion. *Pest Management Science,* 67**,** 1562-1570.
NAWRATH, C. 2006. Unraveling the complex network of cuticular structure and function. *Current Opinion in Plant Biology,* 9**,** 281-287.
NEINHUIS, C. & BARTHLOTT, W. 1997. Characterization and distribution of water-repellent, self-cleaning plant surfaces. *Annals of Botany,* 79**,** 667-677.
NEINHUIS, C., KOCH, K. & BARTHLOTT, W. 2001. Movement and regeneration of epicuticular waxes through plant cuticles. *Planta,* 213**,** 427-434.
NIEDERL, S., KIRSCH, T., RIEDERER, M. & SCHREIBER, L. 1998. Co-permeability of H-3-labeled water and C-14-labeled organic acids across isolated plant cuticles - Investigating cuticular paths of diffusion and predicting cuticular transpiration. *Plant Physiology,* 116**,** 117-123.
NOVAK, P., LI, C., SHEVCHUK, A. I., STEPANYAN, R., CALDWELL, M., HUGHES, S., SMART, T. G., GORELIK, J., OSTANIN, V. P., LAB, M. J., MOSS, G. W. J., FROLENKOV, G. I., KLENERMAN, D. & KORCHEV, Y. E. 2009. Nanoscale live-cell imaging using hopping probe ion conductance microscopy. *Nature Methods,* 6**,** 279-281.
ORBOVIC, V., JIFON, J. L. & SYVERTSEN, J. P. 2001. Foliar-applied surfactants and urea temporarily reduced carbon assimilation of grapefruit leaves. *Journal of the American Society for Horticultural Science,* 126**,** 486-490.
PASTRE, D., IWAMOTO, H., LIU, J., SZABO, G. & SHAO, Z. F. 2001. Characterization of AC mode scanning ion-conductance microscopy. *Ultramicroscopy,* 90**,** 13-19.
PATHAN, A. K., BOND, J. & GASKIN, R. E. 2008. Sample preparation for scanning electron microscopy of plant surfaces-Horses for courses. *Micron,* 39**,** 1049-1061.
PERKINS, M. C., BELL, G., BRIGGS, D., DAVIES, M. C., FRIEDMAN, A., HART, C. A., ROBERTS, C. J. & RUTTEN, F. J. M. 2008. The application of ToF-SIMS to the analysis of herbicide formulation penetration into and through leaf cuticles. *Colloids and Surfaces B-Biointerfaces,* 67**,** 1-13.
PERKINS, M. C., ROBERTS, C. J., BRIGGS, D., DAVIES, M. C., FRIEDMANN, A., HART, C. & BELL, G. 2005a. Macro and microthermal analysis of plant wax/surfactant interactions: plasticizing effects of two alcohol ethoxylated surfactants on an isolated cuticular wax and leaf model. *Applied Surface Science,* 243**,** 158-165.
PERKINS, M. C., ROBERTS, C. J., BRIGGS, D., DAVIES, M. C., FRIEDMANN, A., HART, C. A. & BELL, G. A. 2005b. Surface morphology and chemistry of Prunus laurocerasus L. leaves: a study using X-ray photoelectron spectroscopy, time-of-flight secondary-ion mass spectrometry, atomic-force microscopy and scanning-electron microscopy. *Planta,* 221**,** 123-134.
PIMENTEL, D. 1995. AMOUNTS OF PESTICIDES REACHING TARGET PESTS - ENVIRONMENTAL IMPACTS AND ETHICS. *Journal of Agricultural & Environmental Ethics,* 8**,** 17-29.
POLLARD, M., BEISSON, F., LI, Y. H. & OHLROGGE, J. B. 2008. Building lipid barriers: biosynthesis of cutin and suberin. *Trends in Plant Science,* 13**,** 236-246.

POPP, C., BURGHARDT, M., FRIEDMANN, A. & RIEDERER, M. 2005. Characterization of hydrophilic and lipophilic pathways of Hedera helix L. cuticular membranes: permeation of water and uncharged organic compounds. *Journal of Experimental Botany,* 56**,** 2797-2806.

PRICE, D. M., READING, M., HAMMICHE, A. & POLLOCK, H. M. 1999. Micro-thermal analysis: scanning thermal microscopy and localised thermal analysis. *International Journal of Pharmaceutics,* 192**,** 85-96.

PRICE, D. M., READING, M., HAMMICHE, A. & POLLOCK, H. M. 2000. New adventures in thermal analysis. *Journal of Thermal Analysis and Calorimetry,* 60**,** 723-733.

REYNHARDT, E. C. 1997. The role of hydrogen bonding in the cuticular wax of Hordeum vulgare L. *European Biophysics Journal with Biophysics Letters,* 26**,** 195-201.

REYNHARDT, E. C. & RIEDERER, M. 1994. STRUCTURES AND MOLECULAR-DYNAMICS OF PLANT WAXES .2. CUTICULAR WAXES FROM LEAVES OF FAGUS-SYLVATICA L AND HORDEUM-VULGARE L. *European Biophysics Journal with Biophysics Letters,* 23**,** 59-70.

RHEE, Y., HLOUSEK-RADOJCIC, A., PONSAMUEL, J., LIU, D. H. & POST-BEITTENMILLER, D. 1998. Epicuticular wax accumulation and fatty acid elongation activities are induced during leaf development of leeks. *Plant Physiology,* 116**,** 901-911.

RHEINLAENDER, J., GEISSE, N. A., PROKSCH, R. & SCHAFFER, T. E. 2011. Comparison of Scanning Ion Conductance Microscopy with Atomic Force Microscopy for Cell Imaging. *Langmuir,* 27**,** 697-704.

RHEINLAENDER, J. & SCHAFFER, T. E. 2009. Image formation, resolution, and height measurement in scanning ion conductance microscopy. *Journal of Applied Physics,* 105**,** 9.

RIEDERER, M., BURGHARDT, M., MAYER, S., OBERMEIER, H. & SCHONHERR, J. 1995. SORPTION OF MONODISPERSE ALCOHOL ETHOXYLATES AND THEIR EFFECTS ON THE MOBILITY OF 2,4-D IN ISOLATED PLANT CUTICLES. *Journal of Agricultural and Food Chemistry,* 43**,** 1067-1075.

RIEDERER, M. & FRIEDMANN, A. 2006a. Transport of lipophilic non-electrolytes across the cuticle. *In:* RIEDERER, M. & MULLER, C. (eds.) *Biology of the Plant Cuticle.* Blackwell Publishing.

RIEDERER, M. & FRIEDMANN, A. 2006b. Transport of lipophilic non-electrolytes across the cuticle. *Biology of the Plant Cuticle,* 23**,** 250-279.

RIEDERER, M. & SCHREIBER, L. 2001. Protecting against water loss: analysis of the barrier properties of plant cuticles. *Journal of Experimental Botany,* 52**,** 2023-2032.

RIEDERER, M. S., LUKAS 1995. Waxes - the transport barriers of plant cuticles. *RJ Hamilton, ed, Waxes: Chemistry, Molecular Biology and Functions, The Oily Press, West Ferry, Dundee, Scotland,* 6**,** 26.

ROUND, A. N., YAN, B., DANG, S., ESTEPHAN, R., STARK, R. E. & BATTEAS, J. D. 2000. The influence of water on the nanomechanical behavior of the plant biopolyester cutin as studied by AFM and solid-state NMR. *Biophysical Journal,* 79**,** 2761-2767.

SACK, L. & HOLBROOK, N. M. 2006. Leaf hydraulics. *Annual Review of Plant Biology,* 57**,** 361-381.

SANDERS, G. H. W., ROBERTS, C. J., DANESH, A., MURRAY, A. J., PRICE, D. M., DAVIES, M. C., TENDLER, S. J. B. & WILKINS, M. J. 2000. Discrimination of polymorphic forms of a drug product by localized thermal analysis. *Journal of Microscopy-Oxford,* 198**,** 77-81.

SANTIER, S. & CHAMEL, A. 1996. Penetration of triolein and methyl oleate through isolated plant cuticles and their effect on penetration of C-14 quizalofop-ethyl and C-14 fenoxaprop-ethyl. *Weed Research,* 36**,** 167-174.
SCHONHERR, J. 2002. A mechanistic analysis of penetration of glyphosate salts across astomatous cuticular membranes. *Pest Management Science,* 58**,** 343-351.
SCHONHERR, J. 2006. Characterization of aqueous pores in plant cuticles and permeation of ionic solutes. *Journal of Experimental Botany,* 57**,** 2471-2491.
SCHONHERR, J. & RIEDERER, M. 1989. FOLIAR PENETRATION AND ACCUMULATION OF ORGANIC-CHEMICALS IN PLANT CUTICLES. *Reviews of Environmental Contamination and Toxicology,* 108**,** 1-70.
SCHONHERR, J., SCHREIBER, L. & BUCHHOLZ, A. 2001. Effects of temperature and concentration of the accelerators ethoxylated alcohols, diethyl suberate and tributyl phosphate on the mobility of (14)C 2,4-dichlorophenoxy butyric acid in plant cuticles. *Pest Management Science,* 57**,** 17-24.
SCHREIBER, L. 2002. Co-permeability of H-3-labelled water and C-14-labelled organic acids across isolated Prunus laurocerasus cuticles: effect of temperature on cuticular paths of diffusion. *Plant Cell and Environment,* 25**,** 1087-1094.
SCHREIBER, L. 2005. Polar paths of diffusion across plant cuticles: New evidence for an old hypothesis. *Annals of Botany,* 95**,** 1069-1073.
SCHREIBER, L. 2006. Review of sorption and diffusion of lipophilic molecules in cuticular waxes and the effects of accelerators on solute mobilities. *Journal of Experimental Botany,* 57**,** 2515-2523.
SCHREIBER, L., ELSHATSHAT, S., KOCH, K., LIN, J. X. & SANTRUCEK, J. 2006. AgCl precipitates in isolated cuticular membranes reduce rates of cuticular transpiration. *Planta,* 223**,** 283-290.
SCHREIBER, L. & RIEDERER, M. 1996. Determination of diffusion coefficients of octadecanoic acid in isolated cuticular waxes and their relationship to cuticular water permeabilities. *Plant Cell and Environment,* 19**,** 1075-1082.
SCHREIBER, L. & SCHONHERR, J. 1993. UPTAKE OF 2 CHLORINATED CHEMICALS IN CONIFER NEEDLES - REVERSIBILITY AND COMPARTMENTAL ANALYSIS. *New Phytologist,* 123**,** 547-554.
SCHREIBER, L., SCHORN, K. & HEIMBURG, T. 1997. H-2 NMR study of cuticular wax isolated from Hordeum vulgare L. leaves: identification of amorphous and crystalline wax phases. *European Biophysics Journal with Biophysics Letters,* 26**,** 371-380.
SCHÖNHERR, J. 1982. Resistance of plant surfaces to water loss: transport properties of cutin, suberin and associated lipids. *Physiological plant ecology II.* <span style="font-size:10.0pt;line-height:200%;

font-family:"Arial",sans-serif;mso-fareast-font-family:Calibri;mso-fareast-theme-font:

minor-latin;background:white;mso-ansi-language:EN-GB;mso-fareast-language:EN-US;

mso-bidi-language:AR-SA">Springer Berlin Heidelberg.
SHAO, Z. F., YANG, J. & SOMLYO, A. P. 1995. Biological atomic force microscopy: From microns to nanometers and beyond. *Annual Review of Cell and Developmental Biology,* 11**,** 241-265.
SHECHTER, M. & CHEFETZ, B. 2008. Insights into the sorption properties of cutin and cutan biopolymers. *Environmental Science & Technology,* 42**,** 1165-1171.
SHECHTER, M., XING, B. S. & CHEFETZ, B. 2010. Cutin and Cutan Biopolymers: Their Role as Natural Sorbents. *Soil Science Society of America Journal,* 74**,** 1139-1146.

SHEVCHUIK, A. I., FROLENKOV, G. I., SANCHEZ, D., JAMES, P. S., FREEDMAN, N., LAB, M. J., JONES, R., KLENERMAN, D. & KORCHEV, Y. E. 2006. Imaging proteins in membranes of living cells by high-resolution scanning ion conductance microscopy. *Angewandte Chemie-International Edition,* 45**,** 2212-2216.

SHEVCHUK, A. I., NOVAK, P., TAKAHASHI, Y., CLARKE, R., MIRAGOLI, M., BABAKINEJAD, B., GORELIK, J., KORCHEV, Y. E. & KLENERMAN, D. 2011. Realizing the biological and biomedical potential of nanoscale imaging using a pipette probe. *Nanomedicine,* 6**,** 565-575.

SHEVCHUK, A. I., NOVAK, P., VELAZQUEZ, M. A., FLEMING, T. P. & KORCHEV, Y. E. 2013. Combined ion conductance and fluorescence confocal microscopy for biological cell membrane transport studies. *Journal of Optics,* 15**,** 10.

SHI, T. S., SIMANOVA, E., SCHONHERR, J. & SCHREIBER, L. 2005. Effects of accelerators on mobility of C-14-2,4-dichlorophenoxy butyric acid in plant cuticles depends on type and concentration of accelerator. *Journal of Agricultural and Food Chemistry,* 53**,** 2207-2212.

SINHA, N. 1999. Leaf development in angiosperms. *Annual Review of Plant Physiology and Plant Molecular Biology,* 50**,** 419-446.

SNOWDEN, M. E., GUELL, A. G., LAI, S. C. S., MCKELVEY, K., EBEJER, N., O'CONNELL, M. A., COLBURN, A. W. & UNWIN, P. R. 2012. Scanning Electrochemical Cell Microscopy: Theory and Experiment for Quantitative High Resolution Spatially-Resolved Voltammetry and Simultaneous Ion-Conductance Measurements. *Analytical Chemistry,* 84**,** 2483-2491.

STABENTHEINER, E., ZANKEL, A. & POLT, P. 2010. Environmental scanning electron microscopy (ESEM)-a versatile tool in studying plants. *Protoplasma,* 246**,** 89-99.

STEVENS, P. J. G. & BUKOVAC, M. J. 1987. STUDIES ON OCTYLPHENOXY SURFACTANTS .1. EFFECTS OF OXYETHYLENE CONTENT ON PROPERTIES OF POTENTIAL RELEVANCE TO FOLIAR ABSORPTION. *Pesticide Science,* 20**,** 19-35.

STOCK, D. & HOLLOWAY, P. J. 1993. POSSIBLE MECHANISMS FOR SURFACTANT-INDUCED FOLIAR UPTAKE OF AGROCHEMICALS. *Pesticide Science,* 38**,** 165-177.

STOKES, D. 2008. *Principles and practice of variable pressure/environmental scanning electron microscopy (VP-ESEM),* Chincester, UK, John Wiley and Sons Ltd.

TALBOT, M. J. & WHITE, R. G. 2013. Cell surface and cell outline imaging in plant tissues using the backscattered electron detector in a variable pressure scanning electron microscope. *Plant Methods,* 9**,** 16.

TSUJI, K. 2001. Microencapsulation of pesticides and their improved handling safety. *Journal of Microencapsulation,* 18**,** 137-147.

USHIKI, T., NAKAJIMA, M., CHOI, M., CHO, S. J. & IWATA, F. 2012. Scanning ion conductance microscopy for imaging biological samples in liquid: A comparative study with atomic force microscopy and scanning electron microscopy. *Micron,* 43**,** 1390-1398.

UZU, G., SOBANSKA, S., SARRET, G., MUNOZ, M. & DUMAT, C. 2010. Foliar Lead Uptake by Lettuce Exposed to Atmospheric Fallouts. *Environmental Science & Technology,* 44**,** 1036-1042.

VOEGLER, W. & EULER, J. P. 2004. MON 78294 - a novel glyphosate herbicide formulation. *Zeitschrift Fur Pflanzenkrankheiten Und Pflanzenschutz-Journal of Plant Diseases and Protection***,** 685-689.

WALKER, T. S., BAIS, H. P., DEZIEL, E., SCHWEIZER, H. P., RAHME, L. G., FALL, R. & VIVANCO, J. M. 2004. Pseudomonas aeruginosa-plant root interactions. Pathogenicity, biofilm formation, and root exudation. *Plant Physiology,* 134**,** 320-331.

WANG, C. J. & LIU, Z. Q. 2007. Foliar uptake of pesticides - Present status and future challenge. *Pesticide Biochemistry and Physiology,* 87**,** 1-8.

WHITESIDES, G. M. & LAIBINIS, P. E. 1990. WET CHEMICAL APPROACHES TO THE CHARACTERIZATION OF ORGANIC-SURFACES - SELF-ASSEMBLED MONOLAYERS, WETTING, AND THE PHYSICAL ORGANIC-CHEMISTRY OF THE SOLID LIQUID INTERFACE. *Langmuir,* 6**,** 87-96.

WHYMAN, G., BORMASHENKO, E. & STEIN, T. 2008. The rigorous derivation of Young, Cassie-Baxter and Wenzel equations and the analysis of the contact angle hysteresis phenomenon. *Chemical Physics Letters,* 450**,** 355-359.

WIJMANS, J. G. & BAKER, R. W. 1995. THE SOLUTION-DIFFUSION MODEL - A REVIEW. *Journal of Membrane Science,* 107**,** 1-21.

WOODBURN, A. T. 2000. Glyphosate: production, pricing and use worldwide. *Pest Management Science,* 56**,** 309-312.

YANG, X., LIU, X., ZHANG, X. F., LU, H. J., ZHANG, J. N. & ZHANG, Y. J. 2011. Investigation of morphological and functional changes during neuronal differentiation of PC12 cells by combined Hopping Probe Ion Conductance Microscopy and patch-clamp technique. *Ultramicroscopy,* 111**,** 1417-1422.

YING, L. M., BRUCKBAUER, A., ROTHERY, A. M., KORCHEV, Y. E. & KLENERMAN, D. 2002. Programmable delivery of DNA through a nanopipet. *Analytical Chemistry,* 74**,** 1380-1385.

YING, L. M., BRUCKBAUER, A., ZHOU, D. J., GORELIK, J., SHEVEHUK, A., LAB, M., KORCHEV, Y. & KLENERMAN, D. 2005. The scanned nanopipette: A new tool for high resolution bioimaging and controlled deposition of biomolecules. *Physical Chemistry Chemical Physics,* 7**,** 2859-2866.

ZHANG, J. X., BUNKER, M., CHEN, X. Y., PARKER, A. P., PATEL, N. & ROBERTS, C. J. 2009. Nanoscale thermal analysis of pharmaceutical solid dispersions. *International Journal of Pharmaceutics,* 380**,** 170-173.

ZHANG, J. X., BUNKER, M., PARKER, A., MADDEN-SMITH, C. E., PATEL, N. & ROBERTS, C. J. 2011. The stability of solid dispersions of felodipine in polyvinylpyrrolidone characterized by nanothermal analysis. *International Journal of Pharmaceutics,* 414**,** 210-217.

ZHANG, J. X., ROBERTS, C. J., SHAKESHEFF, K. M., DAVIES, M. C. & TENDLER, S. J. B. 2003. Micro- and macrothermal analysis of a bioactive surface-engineered polymer formed by physical entrapment of poly(ethylene glycol) into poly(lactic acid). *Macromolecules,* 36**,** 1215-1221.

ZHANG, X. G. & BASARAN, O. A. 1997. Dynamic surface tension effects in impact of a drop with a solid surface. *Journal of Colloid and Interface Science,* 187**,** 166-178.

ZHENG, T., WALDRON, K. W. & DONALD, A. M. 2009. Investigation of viability of plant tissue in the environmental scanning electron microscopy. *Planta,* 230**,** 1105-1113.

ZWIENIECKI, M. A., BOYCE, C. K. & HOLBROOK, N. M. 2004. Functional design space of single-veined leaves: Role of tissue hydraulic properties in constraining leaf size and shape. *Annals of Botany,* 94**,** 507-513.

Acknowledgements

I would like to thank my academic supervisors, Prof. Clive Roberts and Prof. Stephanie Allen for their guidance and support over the past four years. Also for aiding in increasing my understanding of the SPMs and techniques I have used. I would also like to thank my industrial supervisor Dr Gordon Bell, for his advice in everything plant surface related and agrochemical. I also would like to acknowledge BBRSC and Syngenta for the funding provided for this research and time spent at Jealott's hill.

Throughout my PhD I was encourage and helped by many people during experiments and writing up. I would like to thank Dr Giovanna De Filippi for the invaluable help provided toward the SICM instrument, for teaching me to use the technique effectively and support when it was broken. I would also like to thank Prof. Xinyong Chem for traning me on the AFM and SThM, also for helping to improve my images and knowledge of the techniques.

I would also like to thank my family for pretending to understand what I was doing during my PhD. Their continued support though the hard times when techniques refused to work and reassurance. I would like to especially thank my Grandparents Ted and Pat Jones, for the countless support when I had completely given up.

I would like to thank my best friend Sarah Chappelle for her constant support and encouragement throughout the PhD. I would also like to thank Steve tickle and Peter Abell, for both of them allowing me stay at their houses over many weekends just to relax.

Appendix

Published works